

DO NOT REMOVE FROM
THE RESEARCH OFFICE

Development of Maintenance-Free Highway Safety Appurtenances

WA-RD 308.1

Final Report
November 1992



Washington State Department of Transportation
Washington State Transportation Commission
Transit, Research, and Intermodal Planning (TRIP) Division

in cooperation with the
Strategic Highway Research Program

WASHINGTON STATE DEPARTMENT OF TRANSPORTATION
TECHNICAL REPORT STANDARD TITLE PAGE

1. REPORT NO. WA-RD 308.1	2. GOVERNMENT ACCESSION NO.	3. RECIPIENT'S CATALOG NO.
4. TITLE AND SUBTITLE Development of Maintenance-Free Highway Safety Appurtenances	5. REPORT DATE November 1992	
	6. PERFORMING ORGANIZATION CODE	
7. AUTHOR(S) John F. Carney III	8. PERFORMING ORGANIZATION REPORT NO. VUWASHS	
9. PERFORMING ORGANIZATION NAME AND ADDRESS Vanderbilt University Box 18, Station B Nashville, TN 37235	10. WORK UNIT NO.	
	11. CONTRACT OR GRANT NO. WSDOT-G-C9309	
	13. TYPE OF REPORT AND PERIOD COVERED Final Report, 9/1/91-11/30/92	
12. SPONSORING AGENCY NAME AND ADDRESS Washington State Department of Transportation Transportation Building Olympia, WA 98504	14. SPONSORING AGENCY CODE	
15. SUPPLEMENTARY NOTES This project was co-sponsored by the Strategic Highway Research Program		
16. ABSTRACT This final report demonstrates the feasibility of employing high molecular weight/high density polyethylene cylinders as the energy dissipating medium in highway safety appurtenances. It is shown that this polymer can dissipate large amounts of kinetic energy, undergo large deformations and strains without fracturing, and essentially restore itself to its original size, shape, and energy dissipation potential when the forcing function is removed. This research involves a quasi-static and impact loading experimental investigation to determine the energy dissipation characteristics of HMW HDPE tubes as functions of temperature, radius to wall thickness ratio, strain, strain-rate, deformation, and repeated and cyclic loading. The results of this experimental program are analyzed to develop analytic energy dissipation expressions which are then employed in the design of truck mounted attenuators (TMA). Finally, an expert system computer program, CADS, is modified to use HMW HDPE tubes in the generalized design of crash cushions. The potential financial, legal, and safety payoffs for highway operations associated with developing highway safety devices which are essentially maintenance free are significant. Maintenance costs associated with the repair of impacted safety devices would be greatly reduced or eliminated. Tort liability exposure related to damaged or collapsed hardware would be significantly decreased. Finally, the safety of the motoring public and the maintenance personnel involved in maintaining and repairing damaged hardware would be enhanced.		
17. KEY WORDS Highway safety, impact attenuation devices, maintenance free, reusable, polyethylene, self-restoration	18. DISTRIBUTION STATEMENT No restrictions. This document is available to the public through the National Technical Information Service, Springfield, VA 22616	
19. SECURITY CLASSIF. (of this report) None	20. SECURITY CLASSIF. (of this page) None	21. NO. OF PAGES 93
		22. PRICE

Final Report
for
Research Project WSDOT-G-C9309
"Development of Maintenance-Free Highway Safety Appurtenances"

**DEVELOPMENT OF MAINTENANCE - FREE
HIGHWAY SAFETY APPURTENANCES**

by

John F. Carney III
Department of Civil and Environmental Engineering
Vanderbilt University
Box 18, Station B
Nashville, Tennessee 37235

Technical Monitor
Don J. Gripne
Washington State Department of Transportation

Prepared for

Washington State Transportation Commission
Department of Transportation
and in cooperation with the
Strategic Highway Research Program

November 1992

DISCLAIMER

The contents of this report reflect the views of the author, who is responsible for the facts and the accuracy of the data presented herein. The contents do not necessarily reflect the official views or policies of the Washington State Department of Transportation or the Strategic Highway Research Program. This report does not constitute a standard, specification or regulation.

TABLE OF CONTENTS

<u>Section</u>	<u>Page</u>
SUMMARY	1
CONCLUSIONS AND RECOMMENDATIONS	2
INTRODUCTION	3
OBJECTIVE	4
SCOPE	6
REVIEW OF PREVIOUS WORK	7
ENERGY DISSIPATION IN HIGHWAY SAFETY APPURTENANCES	8
PROCEDURES AND DISCUSSION	15
PHASE I	15
QUASI - STATIC TESTS	16
REPEATED LOADING TESTS	18
EXPERIMENTS WITH LARGE DIAMETER TUBES	22
SIGNIFICANT FINDINGS FROM QUASI-STATIC TESTS	22
IMPACT TESTS	25
SIGNIFICANT FINDINGS FROM IMPACT TESTS	27
MATHEMATICAL MODELING OF ENERGY DISSIPATION	
CHARACTERISTICS OF HMW HDPE TUBES	27
IMPACT MODEL FOR LARGE DIAMETER TUBES	29

PHASE II	31
TRUCK MOUNTED ATTENUATOR DESIGNS	31
Design Procedure	35
GENERALIZED CRASH CUSHION DESIGN	38
Design Strategy	41
APPLICATIONS	43
REFERENCES	44
APPENDIX	46

LIST OF TABLES

<u>Table</u>	<u>Page</u>
Table 1. Specimens in First Quasi-Static Test Series	19
Table 2. Quasi-Static Loading to Complete Collapse	20
Table 3. Quasi-Static Loading to Half Original Diameter	21
Table 4. Large Quasi-Static Test Specimens	23

LIST OF FIGURES

<u>Figure</u>	<u>Page</u>
Figure 1. Truck Mounted Attenuator (TMA)	11
Figure 2. The Connecticut Impact Attenuation System (CIAS)	12
Figure 3. The Narrow Connecticut Impact Attenuation System (NCIAS)	14
Figure 4. Typical Quasi-Static Test	17
Figure 5. Loading of Larger Samples	24
Figure 6. Predicted vs Actual Energy Dissipation in 4.5- and 6.625-in Diameter Tubes Under Quasi-Static Loading	28
Figure 7. Predicted vs Actual Energy Dissipation in Large Diameter Tubes Under Quasi-Static Loading	30
Figure 8. Energy Dissipation Sensitivity to Radius of Tube	32
Figure 9. Energy Dissipation Sensitivity to Wall Thickness of Tube	33
Figure 10. Temperature Effects Under Quasi-Static and Impact Loading Conditions	34
Figure 11. Truck Mounted Attenuator Designs	37
Figure A1. Quasi-static Load vs. Displacement for IPS 4 SDR 17	47
Figure A2. Quasi-static Load vs. Displacement for IPS 4 SDR 26	48
Figure A3. Quasi-static Load vs. Displacement for IPS 4 SDR 32.5	49
Figure A4. Quasi-static Load vs. Displacement for IPS 6 SDR 17	50
Figure A5. Quasi-static Load vs. Displacement for IPS 6 SDR 21	51

Figure A6. Quasi-static Load vs. Displacement for IPS 6 SDR 26	52
Figure A7. Quasi-static Load vs. Displacement for IPS 6 SDR 32.5	53
Figure A8. Load vs. Displacement Histories for IPS 4 SDR 17	54
Figure A9. Load vs. Displacement Histories for IPS 4 SDR 26	55
Figure A10. Load vs. Displacement Histories for IPS 4 SDR 32.5	56
Figure A11. Load vs. Displacement Histories for IPS 6 SDR 17	57
Figure A12. Load vs. Displacement Histories for IPS 6 SDR 21	58
Figure A13. Load vs. Displacement Histories for IPS 6 SDR 26	59
Figure A14. Load vs. Displacement Histories for IPS 6 SDR 32.5	60
Figure A15. Quasi-static Load vs. Displacement for IPS 24 SDR 17	61
Figure A16. Quasi-static Load vs. Displacement for IPS 24 SDR 32.5	62
Figure A17. Quasi-static Load vs. Displacement for IPS 32 SDR 32.5	63
Figure A18. Quasi-static Load vs. Displacement for IPS 36 SDR 32.5	64
Figure A19. 8.5 mph Impact Test for IPS 4 SDR 17	65
Figure A20. 8.5 mph Impact Test for IPS 4 SDR 26	66
Figure A21. 8.5 mph Impact Test for IPS 4 SDR 32.5	67
Figure A22. 8.5 mph Impact Test for IPS 6 SDR 17	68
Figure A23. 8.5 mph Impact Test for IPS 6 SDR 21	69
Figure A24. 8.5 mph Impact Test for IPS 6 SDR 26	70
Figure A25. 8.5 mph Impact Test for IPS 6 SDR 32.5	71
Figure A26. 22 mph Impact Test for IPS 4 SDR 17	72
Figure A27. 22 mph Impact Test for IPS 4 SDR 26	73

Figure A28. 22 mph Impact Test for IPS 4 SDR 32.5	74
Figure A29. 22 mph Impact Test for IPS 6 SDR 17	75
Figure A30. 22 mph Impact Test for IPS 6 SDR 21	76
Figure A31. 22 mph Impact Test for IPS 6 SDR 26	77
Figure A32. 22 mph Impact Test for IPS 6 SDR 32.5	78
Figure A33. Strain Rate Sensitivity Factors for IPS 4 SDR 17	79
Figure A34. Strain Rate Sensitivity Factors for IPS 4 SDR 26	80
Figure A35. Strain Rate Sensitivity Factors for IPS 4 SDR 32.5	81
Figure A36. Strain Rate Sensitivity Factors for IPS 6 SDR 17	82
Figure A37. Strain Rate Sensitivity Factors for IPS 6 SDR 21	83
Figure A38. Strain Rate Sensitivity Factors for IPS 6 SDR 26	84
Figure A39. Strain Rate Sensitivity Factors for IPS 6 SDR 32.5	85

SUMMARY

Highway safety appurtenances such as truck mounted attenuators, crash cushions, terminals, and longitudinal barriers are widely used and very effective. The employment of these devices has resulted in thousands of lives saved and serious injuries avoided over the last 25 years. Although a strong case can be made for the cost-effectiveness of highway safety appurtenances, the fact remains that their life cycle costs are high. A significant percentage of this total cost typically is associated with maintenance activities following vehicular impacts. This is the case because the vast majority of highway safety hardware dissipate energy through the use of sacrificial elements which must be discarded and replaced after an impact event.

Phase I of this project demonstrated the feasibility of employing a unique energy dissipating medium in these highway safety appurtenances: *high molecular weight/high density polyethylene*. The investigation of the material and energy dissipation properties of this thermoplastic material indicated that it possesses ideal energy dissipating characteristics. It can dissipate large amounts of kinetic energy, undergo large deformations and strains without fracturing, and restore itself to its original size, shape, and energy dissipation potential when the forcing function is removed.

Phase II involved the design of one 45 mi/h and two 60 mi/h Truck Mounted Attenuators which employ HMW HDPE cylinders to dissipate kinetic energy. In addition, a generalized HMW HDPE crash cushion design procedure was developed for 40-60 mi/h impact speeds and a wide range of hazard widths.

The potential financial, legal, and safety payoffs for highway operations associated with developing highway safety devices which are essentially maintenance free are significant. Maintenance costs associated with the repair of impacted safety devices

would be greatly reduced or eliminated. Tort liability exposure related to damaged or collapsed hardware would be significantly decreased. Finally, the safety of the motoring public and the maintenance personnel involved in maintaining and repairing damaged hardware would be enhanced.

CONCLUSIONS AND RECOMMENDATIONS

This research has documented the energy dissipative characteristics of high molecular weight/high density polyethylene (HMW HDPE), a "smart" thermoplastic which possesses the unique properties of self-restoration and reusability.

Quasi-static and impact experiments have shown that this material has a memory and restores itself over time to 90 percent of its original shape following extensive deformation and associated energy dissipation. The material properties are only moderately affected by temperature. Furthermore, HMW HDPE is quite ductile. Polyethylene tubes have been loaded laterally to complete collapse without fracture, and the self-restoring tubes can be reloaded repeatedly.

It is recommended that HMW HDPE tubes be employed in the design of maintenance free crash cushions and longitudinal barriers. These new devices should be crash tested according to the requirements of NCHRP guidelines. In addition to the obvious increased safety benefits, the development of impact attenuation devices which will automatically restore themselves to their original shapes and require little or no maintenance could save State DOT's millions of dollars in maintenance, repair, and litigation costs over the lives of these safety systems.

INTRODUCTION

Motor vehicle related accidents are a major, worldwide health problem and constitute a great economic loss to society. For example, vehicular crashes kill more Americans between the ages of 1 and 34 than any other source of injury or disease. Put another way, for almost half the average life span, people are at greater risk of dying in a roadway crash than in any other way. In the U.S., more than 95 percent of all transportation deaths are motorway related, compared to 2 percent for rail and 2 percent for air. The yearly world wide societal costs of motorway deaths and injuries runs in the hundreds of billions of dollars. Indeed, the productive or potential years of life that are lost prior to age 65 as a result of motor vehicle related injuries or death are greater than those lost to cancer or heart disease.

Measures are being taken to reduce the billions of dollars lost in medical expenses, earnings, insurance claims, and litigation, as well as the intangible costs associated with human suffering. One important contribution to improved highway safety has been the development of impact attenuation devices which prevent errant vehicles from crashing into fixed object hazards that cannot be removed, relocated, or made breakaway. These devices have existed since the 1960's, and many technical improvements and innovative designs have been developed in the intervening years.

Today, such highway safety appurtenances as truck mounted attenuators, crash cushions, terminals, and longitudinal barriers are widely used and very effective. The employment of these devices has resulted in thousands of lives saved and serious injuries avoided over the last 25 years. Although a strong case can be made for the cost-

effectiveness of highway safety appurtenances, the fact remains that their life cycle costs are high. A significant percentage of this total cost typically is associated with maintenance activities following vehicular impacts. This is the case because the vast majority of highway safety hardware dissipate energy through the use of sacrificial elements which must be discarded and replaced after an impact event.

In many instances, the initial installed cost of such hardware is small compared with recurring maintenance and refurbishment costs. Truck mounted attenuators, crash cushions, and terminals usually employ energy dissipating components which have almost no post-impact value and must be replaced at great expense. Similar problems with flexible longitudinal barriers have led to the increased use of the concrete safety shape barrier even though its installation cost per foot is significantly higher than beam-post systems.

There is another serious problem associated with damaged roadside hardware. In an alarming number of cases, the incapacitated safety device sits for days, weeks, or months before repairs are made. The potential safety and tort liability ramifications also translate into millions of dollars of lost revenue. It is clear that this money could be saved if all or most of our highway safety hardware were as maintenance-free as the concrete safety shape barrier. Obviously, impact attenuation devices cannot be composed of rigid concrete components. In fact, significant deformations are usually required of such devices.

OBJECTIVE

The objective of this investigation is to determine the feasibility of employing high molecular weight/high density polyethylene (HMW HDPE) tubes in highway safety appurtenances, resulting in the development of families of maintenance-free impact

attenuation devices. There is a high potential that maintenance and repair costs can be virtually eliminated in such devices after a vehicular impact if HMW HDPE is a "smart" material, possessing the unique ability to first dissipate large amounts of energy, and then restore itself to approximately 90 percent of its original shape. If the stated research objective can be achieved, the employment of this new technology could lead to millions of dollars of savings in maintenance, repair, and litigation costs. Furthermore, the safety of the motoring public will be enhanced and the exposure to danger of DOT personnel will be reduced.

Polyethylene is not a new material. In fact, polyethylenes are the most widely used plastic in the United States. High density polyethylene is a thermoplastic material which is solid in its natural state. This polymer is characterized by its opacity, chemical inertness, toughness at both low and high temperatures, and chemical and moisture resistance. High density can be achieved because of the linear polymer shape which permits the tight packing of polymer chains. The physical properties of high density polyethylene are also affected by the weight-average molecular weight of the polymer. When this high density polymer is used with a high molecular weight resin in the 200,000 - 500,000 range, a high molecular weight/high density polyethylene is produced which exhibits the following favorable material characteristics:

- High stiffness
- High abrasion resistance
- High chemical corrosion resistance
- High moisture resistance
- High ductility
- High toughness
- High tensile strength
- High impact resistance over a wide temperature range

Because of these valuable properties, HMW HDPE has been employed in several high performance market areas, including film, piping, blow molding, and sheet production.

All of the properties mentioned above are crucially important in an impact attenuation device application. Mild steel, which is currently being used in many such devices, also exhibits most of these favorable characteristics. What was discovered in this research work which distinguishes HMW HDPE from mild steel is its ability to remember and almost return to its original configuration after loading. A HMW HDPE tube, for example, when crushed laterally between two plates to complete collapse, will restore itself to approximately 90 percent of its original shape upon removal of the load. It can be reloaded and unloaded repeatedly, exhibiting almost identical load-deformation / energy dissipation characteristics. It remains ductile at temperatures well below 0° F, and its energy dissipation potential is still significant at temperatures above 100° F.

The production of HMW HDPE piping over a wide range of diameters and wall thicknesses has gone on for years. The primary pipe applications have been in oil and gas recovery, water supply systems, sewer and sewer rehabilitation linings, and in other industrial and mining uses. Tubing made of HMW HDPE is, therefore, readily available and relatively inexpensive. Its self-restorative properties were heretofore unknown and have never been exploited.

SCOPE

This research involves a quasi-static and impact loading experimental investigation to determine the energy dissipation characteristics of HMW HDPE tubes as functions of temperature, radius to wall thickness ratio, strain, strain-rate, deformation, and repeated and cyclic loading. The results of this experimental program are analyzed to develop

analytic energy dissipation expressions which are then employed in the design of truck mounted attenuators (TMA). Finally, an expert system computer program, CADS, is modified to use HMW HDPE tubes in the generalized design of crash cushions.

REVIEW OF PREVIOUS WORK

In the 1960's the reality of traffic fatalities occurring at a rate of 1,000 per week prompted the U.S. Federal Highway Administration to initiate a research and development program to provide rapid improvement in highway safety. The development of roadside safety appurtenances was an important part of this highway safety program and a variety of devices have evolved during the last 25 years. The installation of these devices on the roadway system of the United States has substantially reduced the severity of many accidents.

The first recommended procedures for performing full-scale crash tests were contained in the single page *Highway Research Board Circular 482* published in 1962 (1). This document specified a 4000-lb test vehicle, two impact angles (7 and 25 degrees), and an impact velocity of 60 mi/h for testing guardrails. In 1974, an expanded set of procedures and guidelines were published as *NCHRP Report 153* (2). This report was the first comprehensive specification which addressed a broad range of roadside hardware including longitudinal barriers, terminals, transitions, crash cushions, and breakaway supports. Specific evaluation criteria were presented as were specific procedures for performing tests and reducing test data. In the years following the publication of *Report 153*, a wealth of additional information regarding crash testing procedures and evaluation criteria became available, and in 1976 Transportation Research Board Committee A2A04

was given the task of reviewing *Report 153* and providing recommendations. The result of this effort was *Transportation Research Circular No. 191 (3)*. As *TRC 191* was being published, a new NCHRP project was initiated to update and revise *Report 153*. The result of this NCHRP project was *Report 230 (4)*, published in 1981. In many ways *Report 153* was the first draft of *Report 230*; six years of discussion, dissension, and clarification were required before the highway safety community reached the consensus represented by *Report 230*.

Report 230 specifies the test procedures and evaluation criteria to be followed in evaluating the effectiveness of roadside safety hardware. Appurtenances are grouped into three general categories: (1) longitudinal barriers, (2) crash cushions and (3) breakaway and yielding supports. Longitudinal barriers redirect errant vehicles away from roadside hazards and include devices such as guard rails, median barriers, and bridge railings. Terminals and transitions are particular types of longitudinal barriers designed to safely end a barrier or provide a transition between two different barrier systems. Crash cushions are designed to safely bring an errant vehicle to a controlled stop under head-on impact conditions and may or may not redirect when struck along the side. Breakaway and yielding supports are devices used for roadway signs and luminaires that are designed to disengage, fracture, or bend away under impact conditions.

ENERGY DISSIPATION IN HIGHWAY SAFETY APPURTENANCES

Currently available highway safety hardware dissipate energy in a variety of ways (5). Examples include:

- Crushing of cartridges filled with polyurethane foam enclosed in a hex-shaped cardboard honeycomb matrix.
- An extrusion process in which a W-beam guardrail is permanently deformed and deflected.
- A cable/brake assembly which does work by developing friction forces between brakes and a wire rope cable.
- Shearing off a multitude of steel band sections between slots in a W-beam guardrail.
- Transferring the momentum of an errant vehicle into sand particles contained in frangible plastic barrels.

The P.I. has developed and crash tested several different types of impact attenuators which dissipate the kinetic energy associated with a high speed vehicular collision by plastically deforming mild steel cylinders. These laterally loaded cylinders are either formed from flat plate stock or cut from pipe sections and possess some attractive energy dissipation characteristics. These include the ability to achieve deformations approaching 95 percent of their original diameters, a stable load-deformation behavior, an insensitivity to the direction of loading, and a high energy dissipation capability per unit mass. The systems will now be described in some detail because of the potential of easily replacing their existing mild steel cylindrical energy dissipators with HMW HDPE cylinders.

The specific appurtenances developed include:

1. A portable truck mounted attenuator (TMA), which is employed in slow-moving maintenance operations (e.g., line-stripping, pavement overlay) to provide protec-

tion for both the errant motorist and maintenance personnel (6–9). This TMA, which uses four 2-ft diameter steel pipe sections to dissipate energy, is shown in Figure 1. It has been employed by many State Departments of Transportation since the 1970's and its use has been credited with saving lives and reducing accident injury severities.

2. The Connecticut Impact Attenuation System (CIAS), an *operational* crash cushion composed of 14 mild steel cylinders of 3- or 4-ft diameters (10,11). This crash cushion is unique in that it is designed to trap the errant vehicle when it impacts the unit on the side unless the area of the impact on the device is so close to the back of the system that significant energy dissipation and acceptable deceleration responses are unobtainable because of the proximity of the hazard. Only in this situation will the impact attenuation device redirect the vehicle back into the traffic flow direction.

This redirective capability is achieved through the use of steel "tension" straps (ineffective under compressive loading) and "compression" pipes (ineffective in tension). This bracing system ensures that the crash cushion will respond in a stiff manner when subjected to an oblique impact near the rear of the unit, providing the necessary lateral force to redirect the errant vehicle. On the other hand, the braced tubes retain their unstiffened response when the attenuation system is crushed by impacts away from the back of the device.

The CIAS, shown in Figure 2, uses 4 ft high cylinders with the individual wall thicknesses varying from cylinder to cylinder.

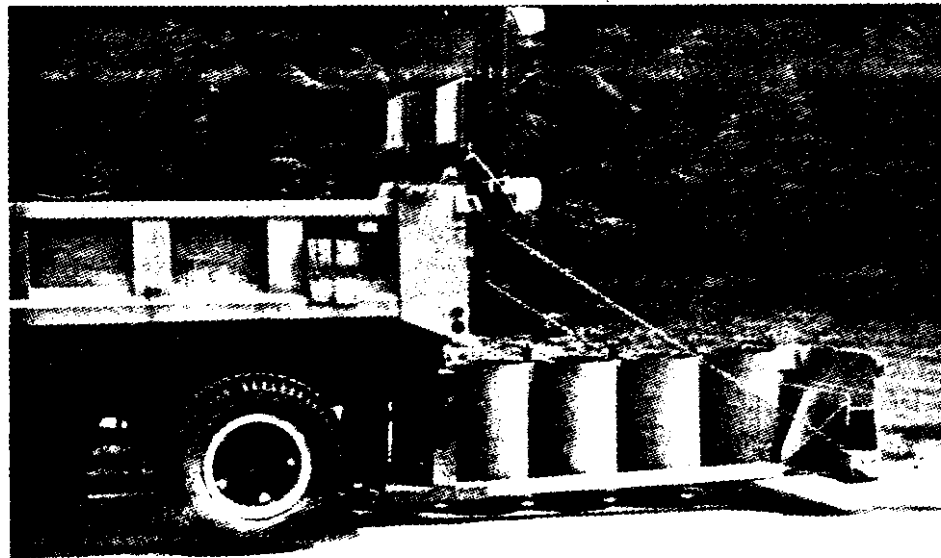
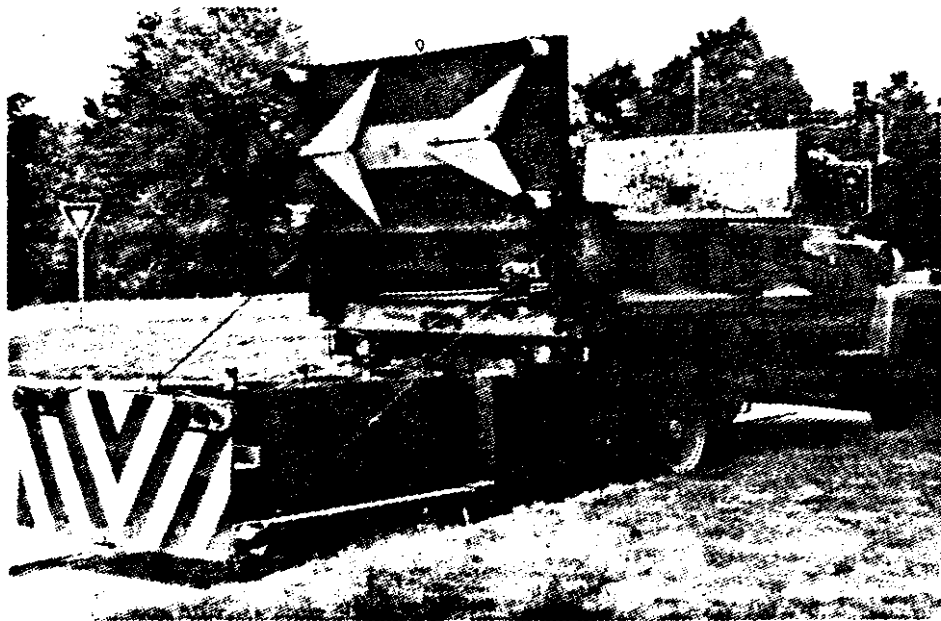


Figure 1. Truck Mounted Attenuator (TMA).

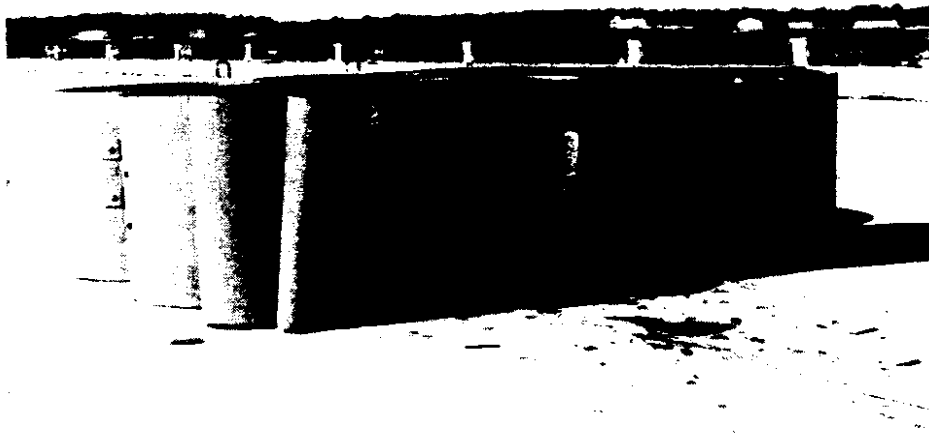
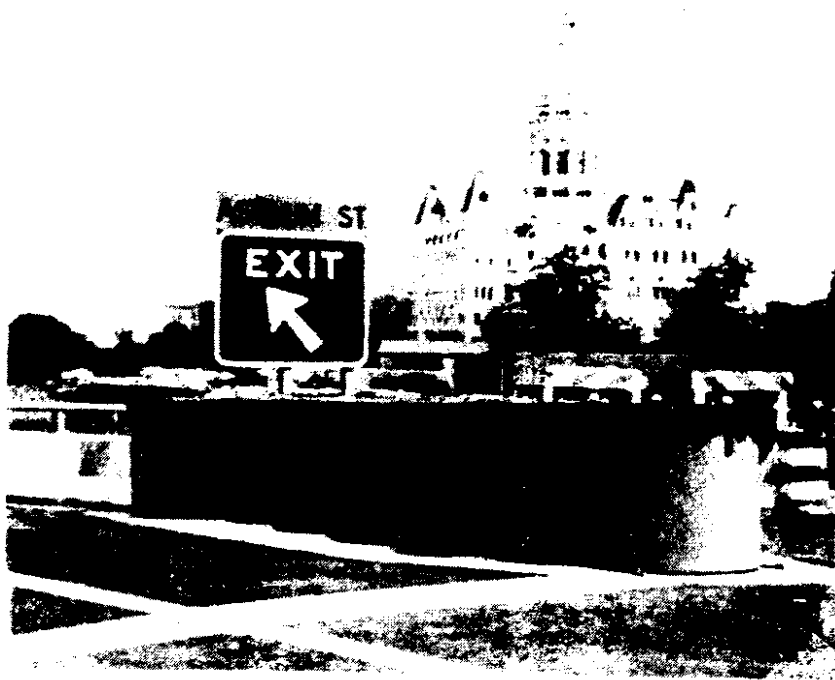


Figure 2. The Connecticut Impact Attenuation System (CIAS).

3. A new narrow hazard system, known as the Connecticut Narrow Hazard Crash Cushion (12), and shown in Figure 3. The system is composed of a single row of eight 3-ft diameter mild steel cylinders of different thicknesses (see Figure 3a). All cylinders are 4 ft high, and a total of four 1-in diameter cables (two on each side of the system) provide lateral stability and assist in redirecting errant vehicles under side impact conditions. The 24 ft length of the crash cushion was chosen as the probable minimum acceptable length for the crash cushion if occupant risk crash test requirements are to be met. The 3 ft width was selected because most narrow highway hazards are approximately 2 ft wide and the crash cushion should be slightly wider than this dimension.

The Connecticut Narrow Hazard Crash Cushion has also been granted operational status by the Federal Highway Administration and there are several installations in Connecticut and Tennessee.

4. A generalized CIAS design (13), which employs an Expert System computer program to optimize the design of the crash cushion when given the unique characteristics of a proposed site. These conditions include the available site dimensions and the speed limit. This Expert System (called CADS) can be used to optimally design crash cushions in multiple service level applications. CADS employs the guidelines of *NCHRP Report 230* (4) to ensure that performance requirements relating to occupant risk are met. The individual cylindrical wall thicknesses are determined so that the occupant impact velocities and ridedown accelerations are minimized, subject to the dual constraints of system length and the required energy dissipation capability. This computer based design system allows the non-expert to optimally design site-specific versions of the Connecticut Impact-Attenuation System.

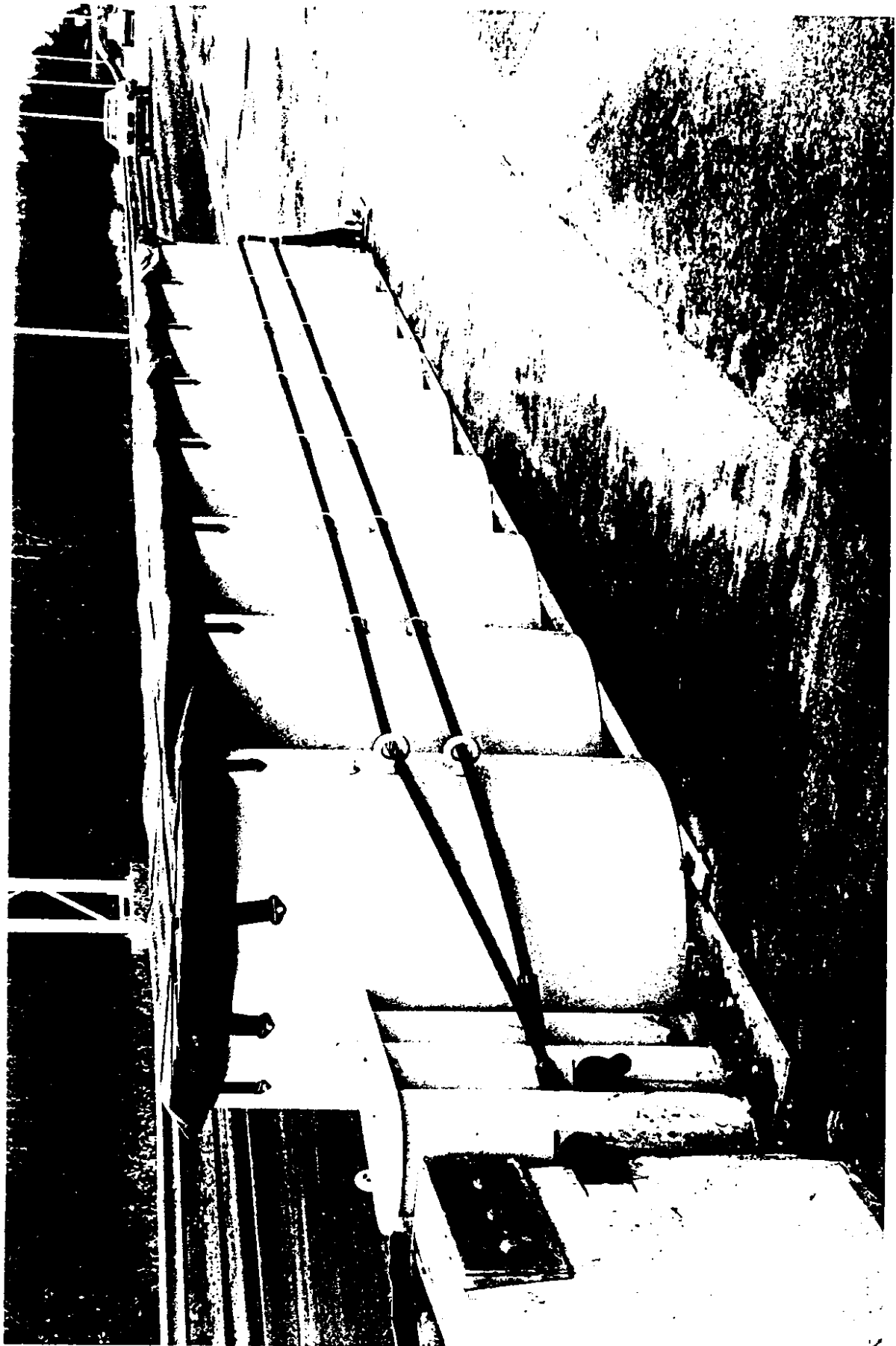


Figure 3. The Narrow Connecticut Impact Attenuation System (NCIAS).

PROCEDURES

This project was divided into two phases. In phase I, an extensive experimental program was conducted to determine the energy dissipation and self restoration characteristics of HMW HDPE tubes as functions of:

- Loading rate
- Temperature
- Diameter/thickness (R/t) ratio
- Strain
- Deformation level
- Repeated loading

Phase II involved the designs of 45 and 60 mi/h TMA's and the development of a generalized crash cushion design computer software tool.

PHASE I

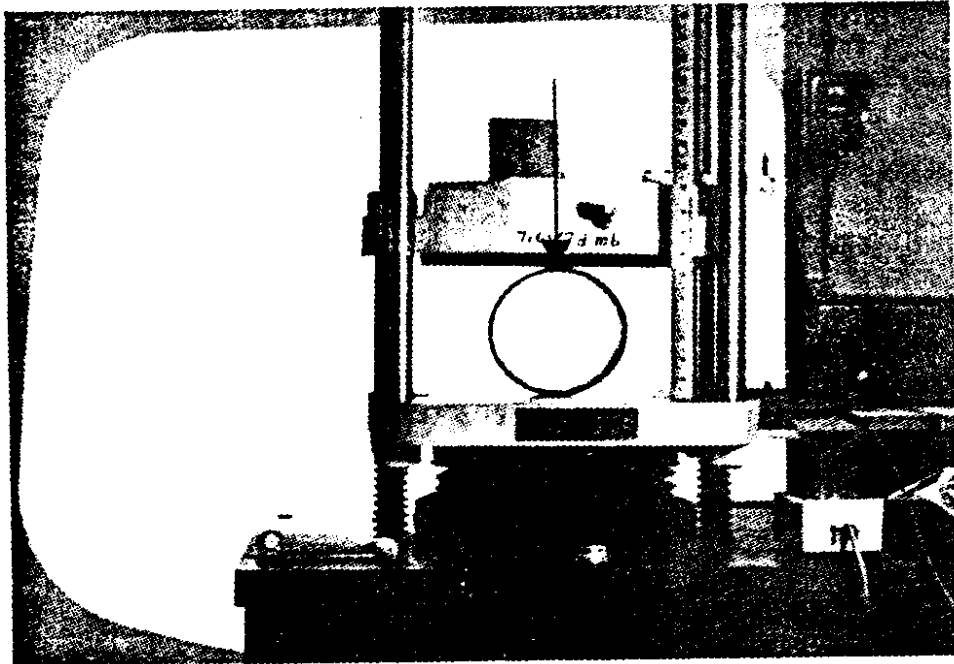
The experiments were performed over a temperature range of 0°F to 100°F. Four different D/t ratios were considered, corresponding to the plastic pipe industry standard dimension ratios (SDR = outside diameter/wall thickness = D/t) of 17, 21, 26, and 32.5. Restoration characteristics for different deformation levels and temperatures were determined. Repeated cyclic loading/deformation tests were performed to establish the ability of HMW HDPE to undergo repeated cycles of deformation while providing the same level of energy dissipation.

QUASI - STATIC TESTS

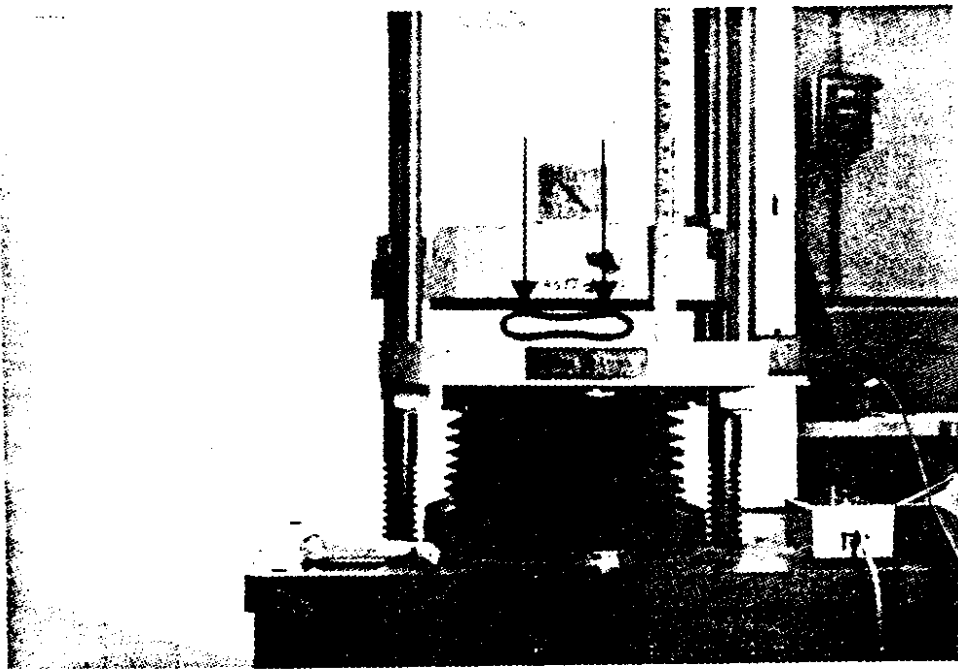
An extensive series of quasi-static tests were conducted with HMW HDPE tubes for a variety of tube diameters, thicknesses, deformation levels, loading cycles, and temperatures. A typical test setup is shown in Figure 4. The tube is loaded between two plates and load vs. deflection data recorded. The applied loads at the top and bottom of the specimen are line loads during the early stages of the collapse process. However, it is of interest and importance to note that these individual line loads bifurcate into two loads during the latter stages of deformation and travel toward the sides of the test specimen. This phenomenon has a significant effect on the character of the typical load-deflection response, tending to increase the load required for a given deflection over that which would exist if the initial line load did not bifurcate. The result is an increased area under the load-deflection curve, and this area is the energy that can be dissipated during the collapse process.

The first quasi-static test series was performed on 4.5- and 6.625-in outside diameter tubes which were 2 inches in length. A total of seven different specimens were selected, as shown in Table 1. In the table, IPS (industrial piping system) is the nominal diameter of the tube, and SDR (standard dimension ratio) has been previously defined as the ratio of the outside diameter of the tube to its minimum wall thickness.

All seven specimens were tested at temperatures of 0°, 35°, 70°, and 100°F. The results are presented in the Appendix in Figures A1-A7. The areas under each load-displacement curve, A , are given in in-lbs on the graphs. As expected, the areas tend to decrease when the temperature increases under quasi-static conditions.



(a)



(b)

Figure 4. Typical Quasi-Static Test.

REPEATED LOADING TESTS

This test series was conducted to determine if the self-restoration capabilities of HMW HDPE tubing and to investigate the ability of such tubes to retain their load-displacement characteristics under repeated loadings. The seven tube sizes given in Table 1 were subjected to load-displacement tests on five consecutive days. Two different test series were performed. In the first series, the seven tubes were loaded to complete collapse. The second test series involved tube displacements to 50 percent of their original diameters.

The self-restoration results are presented in Tables 2 and 3. Table 2 contains the complete collapse data and shows that the HMW HDPE tubes restore themselves to approximately 90 percent of their original diameter when loaded to complete collapse the first time. Further loading cycles to complete collapse results in restorations of 96-99 percent of the previous shapes. After five loadings to complete collapse, all seven tubes retained approximately 86 percent of their original collapsing strokes. The load-displacement histories for this test series are shown in Figures A8-A14. Note that the load-displacement and energy dissipation responses are only slightly affected by repeated loadings to complete collapse. Furthermore, all tubes retained their ductility and no stress fractures occurred.

This test series was then repeated under 50 percent collapse loading conditions. Such a situation is a normal occurrence in actual impact attenuation devices. Table 3 shows that restoration approaches 96 percent after the first loading and 94 percent after five loading cycles. The load-displacement characteristics were essentially unaffected by these loading cycles.

Table 1. Specimens in First Quasi-Static Test Series.

IPS (inches)	SDR
4	17
4	26
4	32.5
6	17
6	21
6	26
6	32.5

Table 2. Quasi-Static Loading to Complete Collapse.

LOADING	SAMPLE	% ORIG. DIA.	% PREV. DIA.
1	4" SDR 17	-	-
	26	-	-
	32.5	-	-
	6" SDR 17	-	-
	21	-	-
	26	-	-
	32.5	-	-
2	4" SDR 17	91.3	91.3
	26	91.1	91.1
	32.5	89.0	89.0
	6" SDR 17	90.8	90.8
	21	90.0	90.9
	26	91.3	91.3
	32.5	90.5	90.5
3	4" SDR 17	88.5	96.8
	26	88.0	96.6
	32.5	87.9	98.7
	6" SDR 17	87.7	96.5
	21	87.5	96.2
	26	88.3	96.7
	32.5	87.9	97.1
4	4" SDR 17	87.3	98.7
	26	86.7	98.5
	32.5	86.1	98.0
	6" SDR 17	86.3	98.5
	21	86.1	98.4
	26	86.9	98.4
	32.5	87.3	99.3
5	4" SDR 17	86.2	98.8
	26	86.0	99.3
	32.5	85.2	99.0
	6" SDR 17	85.5	99.1
	21	85.5	99.3
	26	86.2	99.1
	32.5	86.4	99.0

Table 3. Quasi-Static Loading to Half Original Diameter.

LOADING	SAMPLE	% ORIG.DIA.	% PREV.DIA.
1	4" SDR 17	-	-
	26	-	-
	32.5	-	-
	6" SDR 17	-	-
	21	-	-
	26	-	-
2	32.5	-	-
	4" SDR 17	95.4	95.4
	26	95.8	95.8
	32.5	96.3	96.3
	6" SDR 17	95.2	95.2
	21	95.9	95.9
3	26	96.2	96.2
	32.5	96.4	96.4
	4" SDR 17	94.0	98.5
	26	94.6	98.7
	32.5	95.2	98.9
	6" SDR 17	93.8	98.6
4	21	94.6	98.6
	26	95.1	98.9
	32.5	95.5	99.1
	4" SDR 17	93.2	99.2
	26	94.1	99.5
	32.5	94.5	99.3
5	6" SDR 17	93.1	99.2
	21	93.7	99.0
	26	94.4	99.3
	32.5	94.9	99.4
	4" SDR 17	92.5	99.2
	26	93.6	99.5
6	32.5	94.1	99.6
	6" SDR 17	92.6	99.5
	21	93.3	99.6
	26	94.2	99.8
	32.5	94.6	99.6

EXPERIMENTS WITH LARGE DIAMETER TUBES

A limited testing program was conducted with the larger diameter samples listed in Table 4.

The test specimens were all 8 in in length and loaded as shown in Figure 5. True plate loading was obtained by inserting two steel box beams in the testing machine. The load-displacement curves for these four tests are shown in Figures A15-A18.

SIGNIFICANT FINDINGS FROM QUASI-STATIC TESTS

- Loads bifurcate into two loads during collapse process, resulting in increased energy dissipation.
- Energy dissipation decreases with increase in test temperature.
- Cylinders retain their ductility under large deformations — no stress fractures occurred.
- Cylinders restore themselves to approximately 90% of their original shapes upon removal of load.
- Load-deformation characteristics are essentially unaffected by repeated loadings.

Table 4. Large Quasi-Static Test Specimens.

IPS (inches)	SDR
24	17
24	32.5
32	32.5
36	32.5

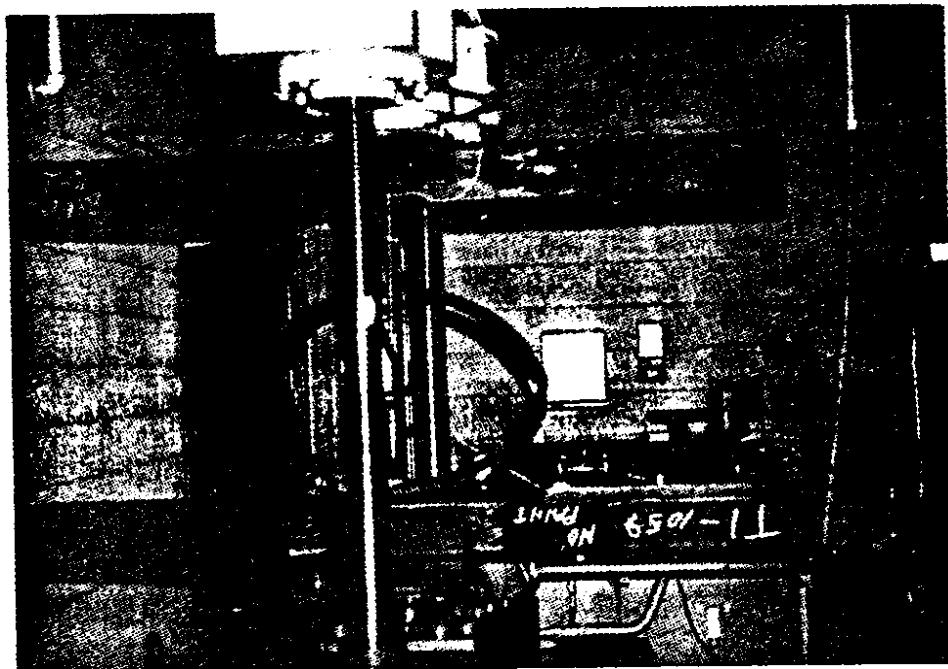
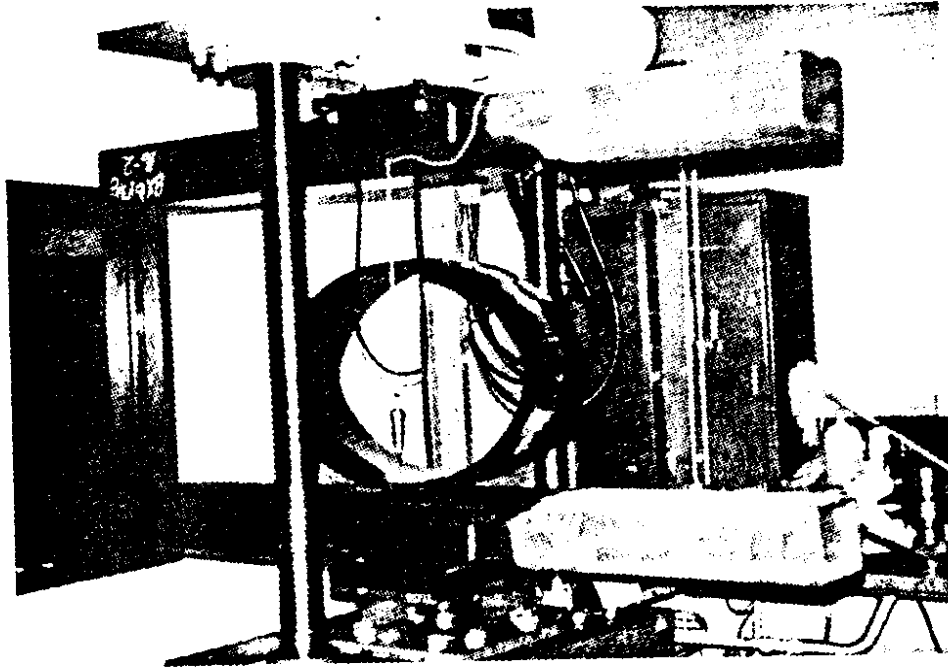


Figure 5. Loading of Larger Samples.

IMPACT TESTS

The impact loading tests were conducted in a MTS 312-31 servo-hydraulic testing machine under closed loop control. This machine is capable of applying a maximum static load of $P_{\max} = 7$ klb. The actuator was allowed to reach maximum velocity prior to impact by retracting it by approximately 10 in. The stroke (actuator's displacement) was calibrated at different scales, i.e., 2.0, 5.0, and 10.0 in., prior to testing in order to obtain accurate impact velocity measurements. The impact velocity was varied by modifying the aperture of the servo-hydraulic valve.

The impact load absorbed by the specimen was measured with a Kistler quartz force link Type 9342A installed in the cross head. This sensor is capable of gauging loads in the order of ± 7.0 klb under short term static or dynamic modes. The high rigidity of the force link, combined with its high resolution, resulted in an extremely high resonant frequency of the measuring arrangement, thus eliminating the risk of "ringing."

Data acquisition was accomplished by means of a DT2821 high speed single-board analog/digital data acquisition system (from Data Translation, Inc.) installed in an IBM AT386 clone. The software used for the A/D conversion was Global Lab from the same company. The load and stroke channels were configured in a differential mode in order to keep the electrical noise to a minimum.

The seven tube sizes given in Table 1 were each tested at two different impact velocity values, 8.5 and 22 mi/h, and four different temperatures, 0°, 35°, 70°, and 100°F. The results are presented in Figures A19-A32.

It is of interest to compare the corresponding areas under the load vs displacement curves under quasi-static and impact loading conditions. The area under each curve represents the energy dissipated during the deformation process. Note that under quasi-

static loading conditions, these areas are sensitive functions of temperature. Consider, for example, the ratio of areas for the IPS = 6, SDR = 17 specimen size at two temperature extremes (see Figure A4):

$$(A_{0^{\circ}} / A_{100^{\circ}})_{STATIC} = 4166 / 1549 = 2.69 \quad (1)$$

The impact loading program, in contrast, demonstrates that this temperature sensitivity which is present under quasi-static conditions is much reduced under impact conditions. This very significant and here-to-fore unknown fact is made clear by comparing the specific impact test results of Figures A19-A32, with the corresponding quasi-static responses of Figures A1-A7. It is of particular interest to note that:

- At 0°F, the energy dissipation capacity is largely unaffected by the rate of loading.
- At 100°F, the energy dissipation capacity is significantly influenced by the rate of loading.

The consequence of this experimental fact is that the sensitivity of the energy dissipation potential of a HMW HDPE tube to temperature under impact loading conditions is significantly less than under quasi-static ones. Consider, for example, the result from Figure A22:

$$(A_{0^{\circ}} / A_{100^{\circ}})_{IMPACT} = 4644 / 2702 = 1.72 \quad (2)$$

The strain rate sensitivity factor (SRS) is defined as the ratio of the impact to quasi-static energy dissipation capacities of a tube. Strain rate sensitivity factors are presented in Figures A33-A39 for the seven tube sizes under consideration for two sets of impact velocities. Note that the rate of loading is of little import at low temperatures and very significant at high temperatures.

SIGNIFICANT FINDINGS FROM IMPACT TESTS

- Sensitivity of energy dissipation potential of HMW HDPE to temperature under impact loading conditions is significantly less than under quasi-static ones.
- Strain rate sensitivity increases with temperature.
- Fracture under impact loading did not occur, even at low test temperature.

MATHEMATICAL MODELING OF ENERGY DISSIPATION CHARACTERISTICS OF HMW HDPE TUBES

The quasi-static and impact experimental results presented in the previous section were analyzed using Statistical Analysis Software (14) to determine the influence of the various independent parameters on the energy dissipation capacity of HMW HDPE tubes. These parameters include tube thickness, radius, and length, the test temperature, and the impact speed.

The first modeling phase involved the quasi-static data obtained for the small diameter (4.5- and 6.625-in) tubes presented in Figures A1-A7. This effort included 7 different tube sizes and 4 different test temperatures, a total of 28 experiments. The statistical analysis of this data yielded the following expression for dissipated energy:

$$\text{Energy} = \beta_0 L R^{\beta_1} t^{\beta_2} F(T) \quad (3)$$

where	L	=	length of tube in inches
	R	=	radius of tube in inches
	t	=	wall thickness of tube in inches
	T	=	test temperature in °F
	β_0	=	102.051
	β_1	=	4.315×10^{-2}
	β_2	=	2.444
	$F(T)$	=	$199.870 - 1.012T - 9.356 \times 10^{-3}T^2 + 6.840 \times 10^{-5}T^3$

This expression for quasi-static energy dissipation in small diameter tubes yields quite accurate results, as illustrated in Figure 6.

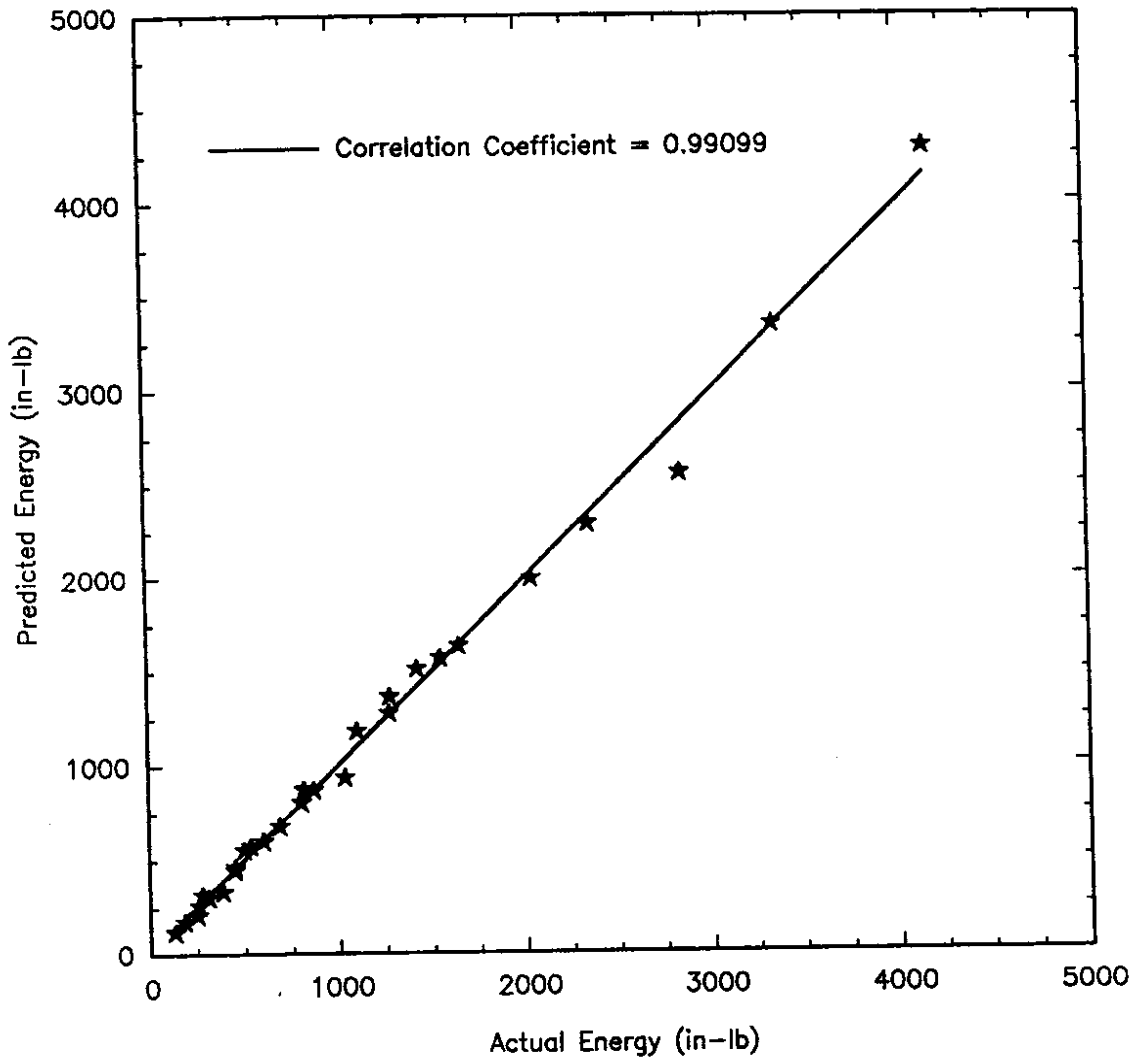


Figure 6. Predicted vs Actual Energy Dissipation in 4.5- and 6.625-in Diameter Tubes Under Quasi-Static Loading.

The second modeling phase dealt with the determination of the strain rate sensitivity (SRS) of HMW HDPE. The test results presented in Figures A33-A39 were employed to determine the increase in energy dissipation capacity of a HMW HDPE tube under impact loading conditions. A statistical analysis of the results of these 56 experiments resulted in the determination of the SRS in the form:

$$\text{SRS} = 1.106 + 6.660 \times 10^{-3}T - 7.650 \times 10^{-5}T^2 + 8.340 \times 10^{-7}T^3 \quad (4)$$

The third modeling phase involved the analysis of the quasi-static tests conducted on the four tubes of large diameter. The test results were presented in Figures A15-A18. Many real world applications would involve HMW HDPE tubes of this size or larger. The large diameter tests were conducted to avoid having to extrapolate small diameter test results into the large diameter regime. In modeling the large diameter test results, the temperature variable effect determined in the earlier tests was employed in the statistical analysis, and the following quasi-static energy dissipation predictor (EDC) was obtained:

$$\text{EDC} = \alpha_0 L R^{\alpha_1} t^{\alpha_2} F(T) \quad (5)$$

where

α_0	=	302.732
α_1	=	-0.409
α_2	=	2.356

Equation 5 yields excellent results, as can be seen in Figure 7.

IMPACT MODEL FOR LARGE DIAMETER TUBES

The results of the three modeling efforts described above yield the following expression for the dynamic energy dissipation capacity (DEDC) of a large diameter HMW HDPE tube under impact loading:

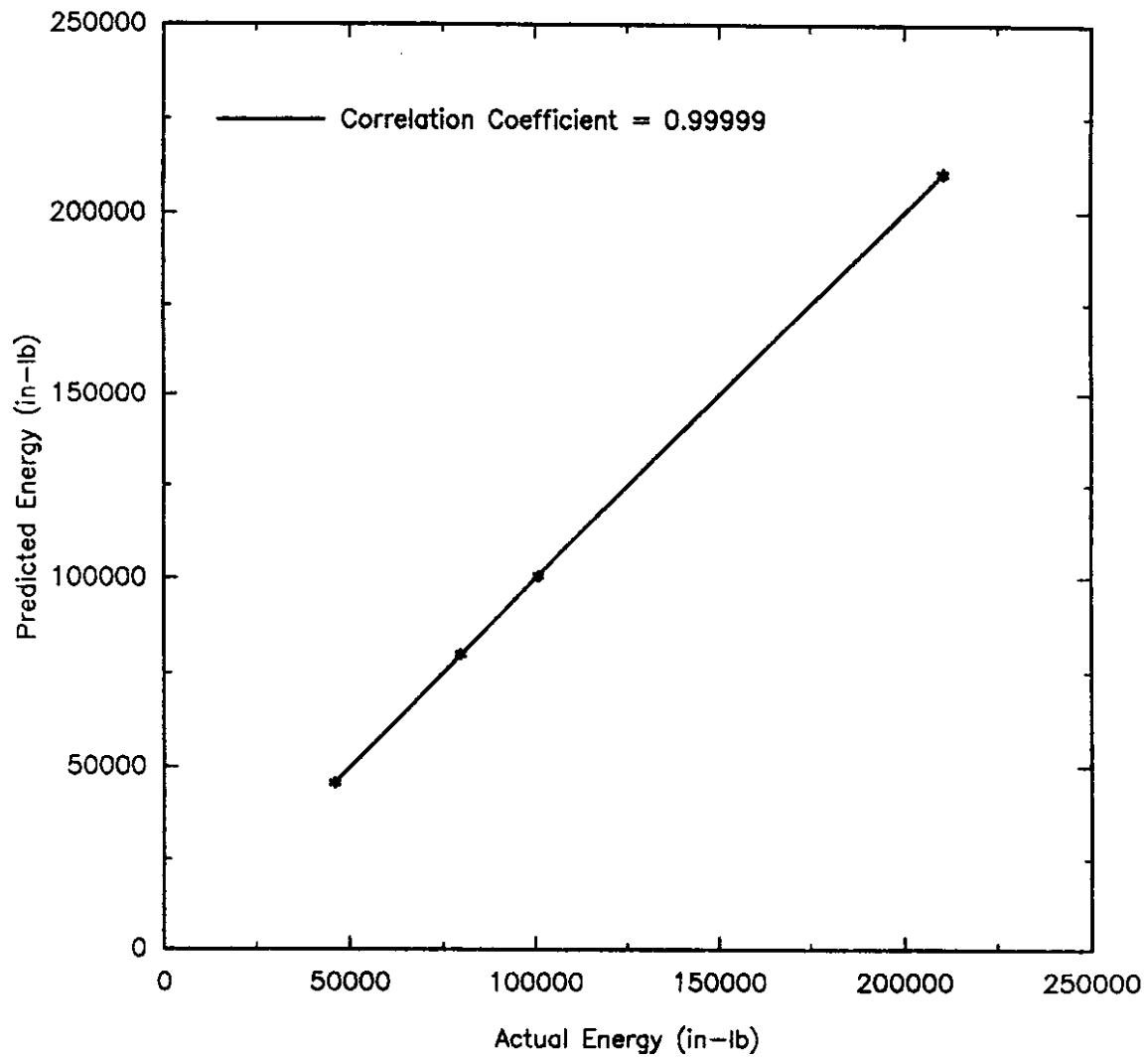


Figure 7. Predicted vs Actual Energy Dissipation in Large Diameter Tubes Under Quasi-Static Loading.

$$\text{DEDC} = (\text{EDC}) (\text{SRS}) \quad (6)$$

where SRS and EDC are given by Equations 4 and 5, respectively. It is of interest to investigate the sensitivity of the individual component variables in this energy expression. In Figure 8, R^{α_1} is plotted versus R , illustrating that the energy is relatively insensitive to a change in radius of the tube. On the other hand, the energy dissipation is a very sensitive function of tube thickness, as shown in Figure 9. The effects of temperature change under quasi-static and impact loading conditions are shown in Figure 10. $F(T)$ is the variable which captures the very significant dependence of energy dissipation on temperature under quasi-static conditions. However, note how this undesirable effect is cancelled out in large measure by the strain rate sensitivity (SRS) characteristics of HMW HDPE. The result is that the energy dissipation characteristics of HMW HDPE are not severely affected by temperature changes under *impact loading conditions*.

PHASE II

Phase II involved the designs of 45 and 60 mi/h TMA's and the development of a generalized crash cushion design computer software tool.

TRUCK MOUNTED ATTENUATOR DESIGNS

The employment of truck mounted attenuators (TMA) has more than doubled in the last eight years. This trend will certainly continue as there is no longer any question that the use of TMA's in connection with maintenance, repair, and construction projects provides badly needed protection for both the motoring public and the work crews on our country's highways and streets.

The time is right to develop a new generation TMA for the following reasons:

- All existing TMA's are expensive to purchase and repair.

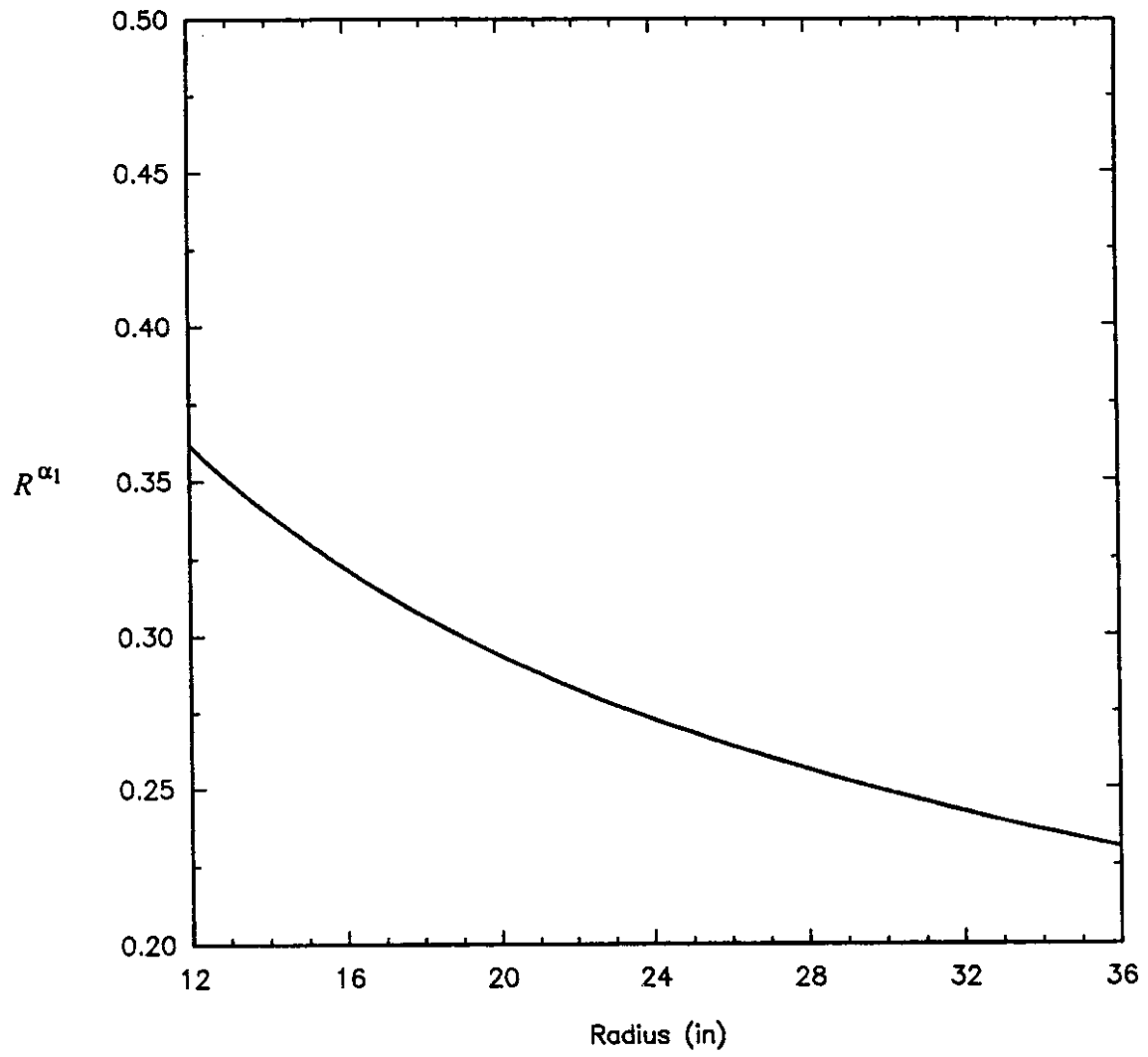


Figure 8. Energy Dissipation Sensitivity to Radius of Tube.

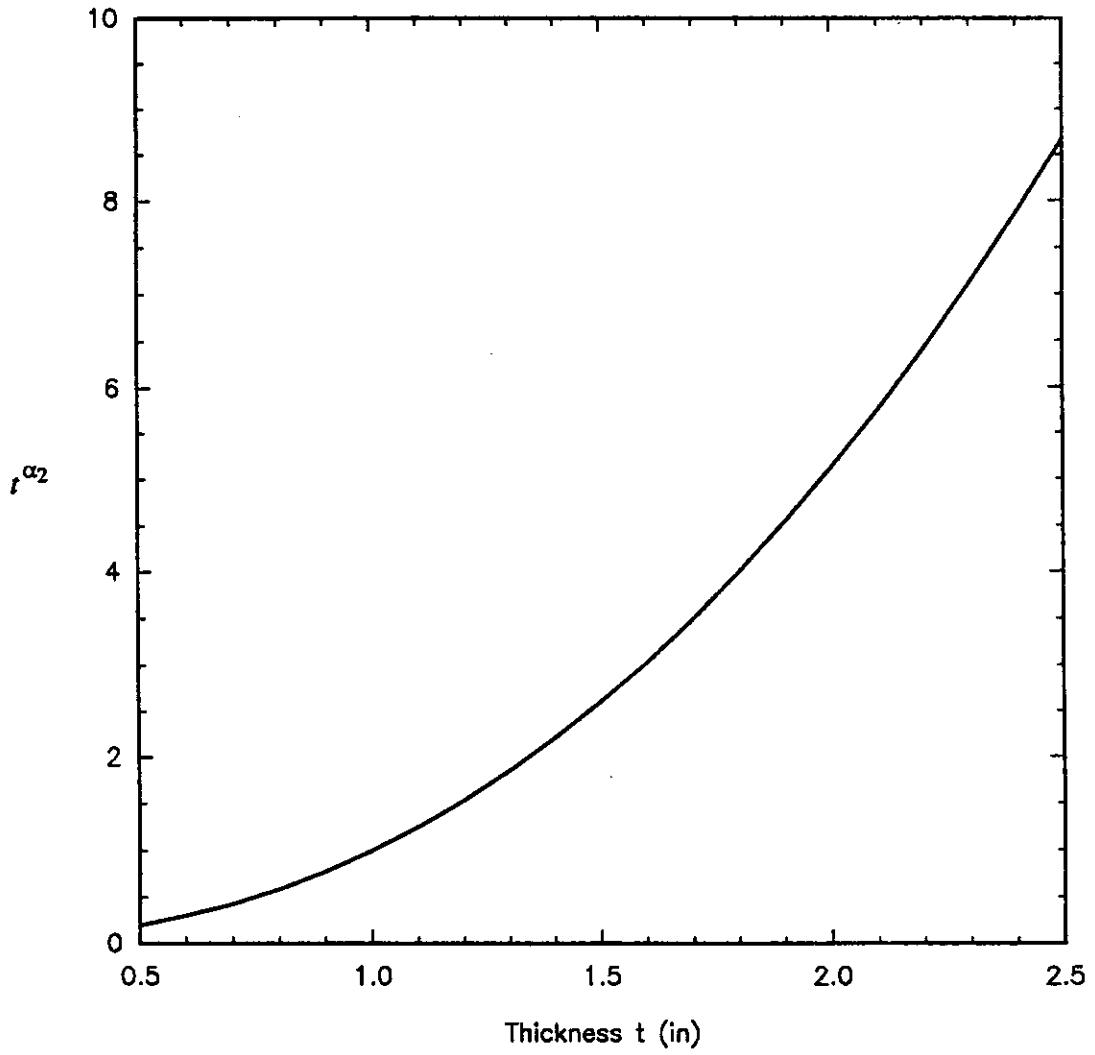


Figure 9. Energy Dissipation Sensitivity to Wall Thickness of Tube.

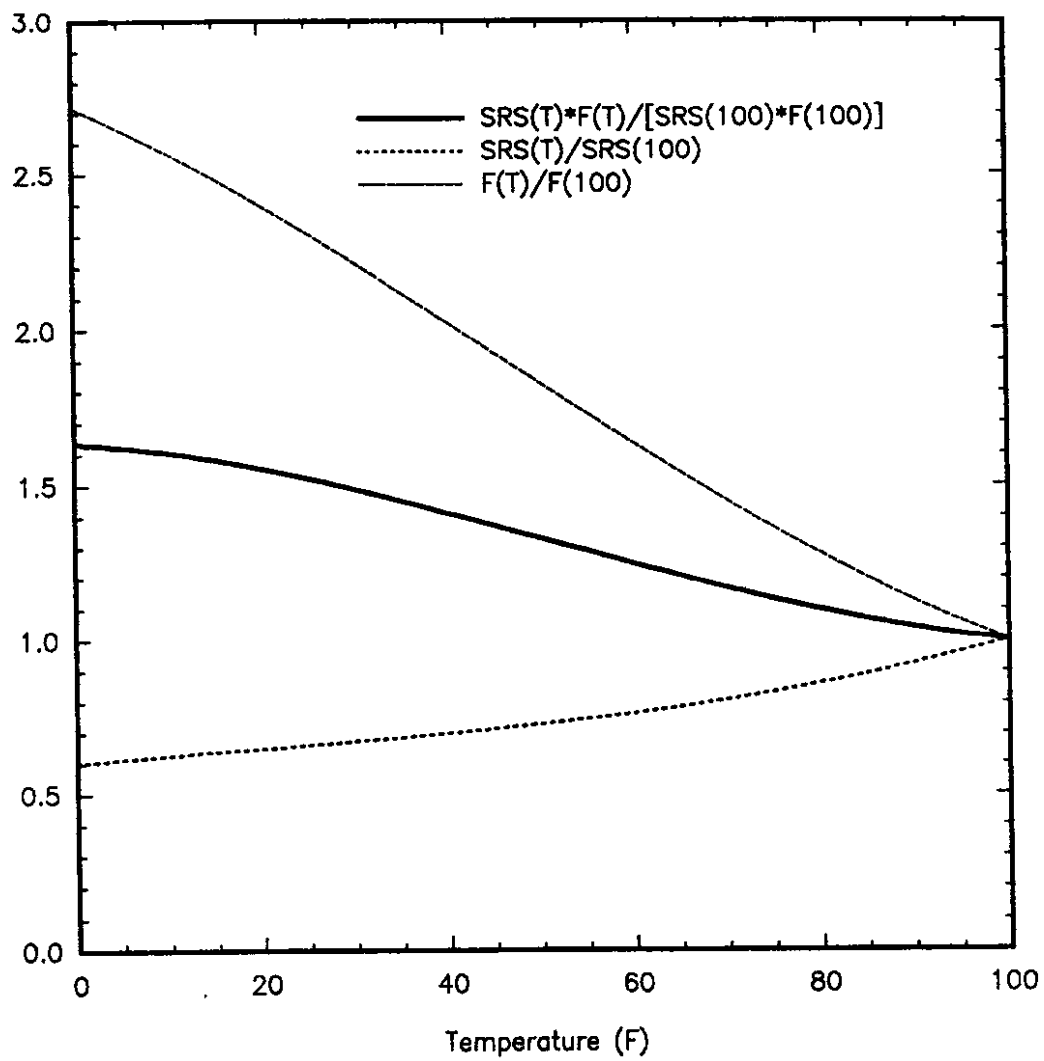


Figure 10. Temperature Effects Under Quasi-Static and Impact Loading Conditions.

- The revision of *NCHRP Report 230 (4)*, scheduled to be completed soon under NCHRP Project 22-7, will require (for the first time) that TMA's be crash tested in accordance with a specific test matrix. The current version of *NCHRP Report 230* does *not* specifically address the crash testing of TMA's.
- The revision of *NCHRP Report 230* will explicitly call for the testing of both 45 mi/h and 60 mi/h capacity TMA's. No 60 mi/h capacity TMA exists at the present time.

The Principal Investigator developed a TMA for the State of Connecticut DOT in the early 1970's which is still in use today. It dissipates energy by plastically deforming mild steel cylinders during the impact event. This TMA, called the Connecticut Crash Cushion, contains a single row of four 2 ft diameter cylinders, an aluminum impacting plate, and a steel guidance frame located underneath the truck (see Figure 1). The impacting plate and guidance frame are eliminated from the designs developed in this section.

Design Procedure

Accepted occupant risk guidelines concerning occupant impact velocity with the vehicle interior and the subsequent maximum 10 ms average ridedown deceleration combine to set a minimum acceptable collapsing stroke for the 45 mi/h design of approximately 7 ft. This is the case because crash tests must be performed using both light (1,800 lb) and heavy (4,500 lb) vehicles. The TMA is designed to collapse completely under impact at 45 mi/h with the heavy vehicle. At the same impact speed, the 1,800 lb vehicle possesses only 40% of the kinetic energy of the 4,500 lb one. The resulting col-

lapsing stroke will therefore be significantly less than that of the full capacity of the device.

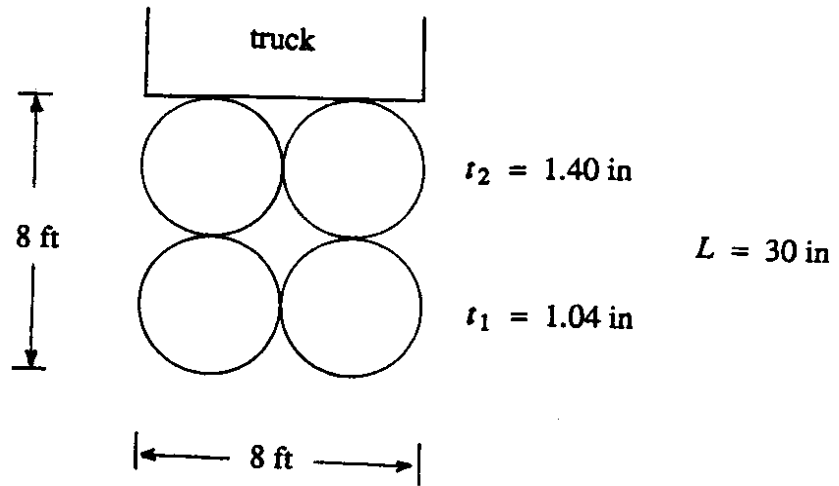
The kinetic energy of the heavy vehicle at impact is:

$$\text{K.E.}_{45} = 1/2 mv^2 = 304 \text{ k-ft} \quad (7)$$

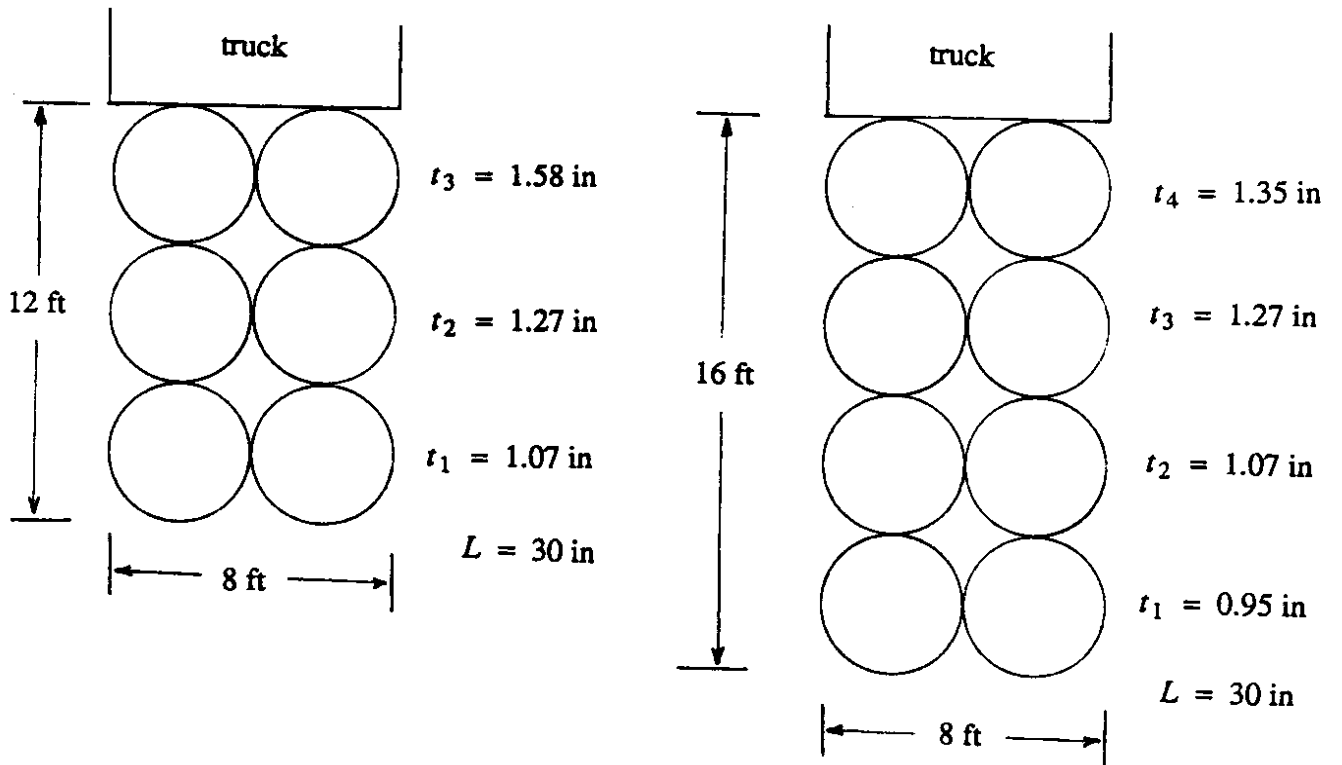
Some of this kinetic energy will be transferred to the service vehicle carrying the TMA. Assuming a service vehicle weight of 15,000 lb, it follows from the principal of conservation of momentum and the definition of kinetic energy that the service vehicle is approximately 91 k-ft. The front end of the impacting vehicle can be expected to dissipate approximately 30 k-ft of energy. The required energy dissipation capacity of the 45 mi/h TMA is, therefore,

$$\text{K.E.} = 304 - 91 - 30 = 183 \text{ k-ft} \quad (8)$$

The plan view of the 45 mi/h TMA design is shown in Figure 11(a). Note that the energy dissipating medium is 8 ft wide and 8 ft long and composed of four 4 ft diameter HMW HDPE tubes. These tubes are connected to a frame at the rear of the service vehicle and to each other wherever two tubes come in contact with each other. For reasons of vertical stability, the depth of each tube is 30 in. In order to achieve an acceptable occupant risk response under impact with a light vehicle, the TMA is designed such that the back row of tubes (nearest the service vehicle) will dissipate twice as much energy at the front row. Such a design will significantly lengthen the collapsing stroke of the light car when compared to the corresponding stroke of a TMA with equal energy dissipation in each row.



(a) 45 mph Design



(b) 60 mph Designs

Figure 11. Truck Mounted Attenuator Designs.

The energy dissipation in each tube is controlled by the proper selection of the wall thickness dimension. If $T = 100^{\circ}\text{F}$, it follows from Equation 6 that:

$$t_1 = 1.04 \text{ inches}$$

$$t_2 = 1.40 \text{ inches}$$

The 60 mi/h TMA design follows the same approach outlined above for the 45 mi/h TMA. Occupant risk considerations require a longer length for the 60 mi/h system. Two designs are presented in Figure 11(b). In the 12 ft long, 60 mi/h TMA, the energy dissipation capacity breakdown is:

Row 1 — 20%

Row 2 — 30%

Row 3 — 50%

The 16 ft long 60 mi/h TMA possesses the following energy dissipation characteristics:

Row 1 — 15%

Row 2 — 20%

Row 3 — 25%

Row 4 — 40%

GENERALIZED CRASH CUSHION DESIGN

A design procedure to generalize the Connecticut Impact Attenuation System (CIAS) has previously been developed (13). The generalized CIAS (GCIAS), like the CIAS, employs clusters of steel cylinders to dissipate kinetic energy. Computer software, called CADS, was produced which optimizes the design of a site specific crash cushion. The required input is the hazard width and the design or operating speed of the

particular roadway.

CADS has been modified, with the steel energy dissipating cylinders being replaced with HMW HDPE ones.

The basic organization of CADS is made up of four main modules:

- Data acquisition,
- Design,
- Output, and
- Explanation.

Before the design process can begin, the engineer must provide the specific characteristics of the intended attenuator site. The data acquisition module of CADS gathers such information as the required width of the rear of the system and the design speed. Any conflict between this information and the limits set for a CIAS application is checked at this point. This module also contains error-handling routines and functions performing standard calculations, such as total length of the CIAS or the weight of an individual cylinder.

The design module comprises the bulk of CADS. It is made up of subblocks corresponding to the various steps in the design, which are discussed later in detail. In short, there are four steps in the design:

1. Configuration of cylinder diameters.
2. Satisfaction of energy dissipation criteria.
3. Selection of the braced components, and
4. Installation details.

First, the configuration step involves specifying the diameters of the cylinders so the plan view of the CIAS maintains a triangular shape. Next, cylinder thicknesses are chosen based on the occupant safety criteria of *NCHRP Report 230*. Once designed for the zero-degree impact, the CIAS is fitted with the proper bracing system so the system has the stiffness for redirection capabilities. The final step consists of providing design details such as the cylinder connections, backup structure, and base pad.

The output module contains the procedures for graphical displays and output file creation. Details of the design are presented in tabular form on the display as the design progresses, and a drawing of the completed CIAS design is displayed. The design can be documented in permanent disk file storage. This documentation is sufficiently detailed that the attenuator can be manufactured by a third-party vendor.

The explanation block can be employed whenever the user is prompted. At selected stopping points, information relevant to that stage of the design is available. These points include the beginning of the program, when the user is prompted for data, the beginning and end of subblocks of the design module, and the completion of the design. For instance, if a design speed of 60 mi/h were input in the data-acquisition module, a minimum of approximately 25 ft of length would be required for installation. If the user indicated this length was not available, an explanation stating the conflict would be activated. Also, during the design the user may access material containing more specific information about a step. The user is informed in situations when the CIAS is not the definitive choice for a given site.

Design Strategy

The CIAS design process can be divided into several well-defined steps. The first is to obtain the correct width and length for the given site conditions. The width at the rear of the attenuator is based on the width of the backup structure, which is given the same width as the hazard. In order for the attenuator to redirect vehicles impacting near the rear of the device, it must be slightly wider than the backup structure. Testing has shown that the attenuator-backup connection must be offset from the edge of the backup by 6 in to prevent a failure of the connection. This offset is shown in an example system later in this paper. Imposing this constraint, the width of the CIAS is:

$$WA = 3(WB - 1)/2 \quad (9)$$

where WA and WB are the widths of the attenuator and backup in feet, respectively.

The factors used to determine the necessary length are much less concrete. A rough estimate of the distance required to stop a vehicle can be calculated when the design speed and a maximum average deceleration are given. For example, a 60 mi/h design speed and a 5-g maximum deceleration (one-third the maximum for the 10-ms window) gives a required stopping distance of 24 ft. Since the light and heavy cars cannot both use the entire length of the attenuator, their differing energies must be taken into account. Also, there is an upper bound on the attenuator length beyond which the device becomes impractical. By weighing these factors and drawing on experience, a length on the order of 25 ft was chosen for the 60 mi/h case. Lengths for other design speeds are chosen proportionally to this standard.

The next step is to choose the proper configuration for the cylinders. Given that the back row has three cylinders and the front row a single cylinder, diameters of the cylinders are chosen from back to front. The back row, by default, has a diameter equal

to one-third of the width. The two variables available are the number of rows and the increment in which adjacent rows differ in diameter. Initial values are chosen and then adjusted until the length constraint is satisfied. A minimum constraint of 2 ft is also imposed on the cylinder diameter. Using this process, the plan view of the attenuator attains a triangular shape. This triangular shape is desired for the stability and stiffness of the system during impacts other than head-on.

After the configuration of the system has been determined, the designer module can specify the thickness of each cylinder such that the kinetic energy of the vehicle is dissipated in an acceptable manner. Ten standard cylinder thicknesses are available to CADS ranging from 1/8 to 3/8 in. A preliminary design is developed by setting all thicknesses to the 1/8 in minimum. This ensures that the occupant impact velocity criteria is initially satisfied. The task, then, is to dissipate the energies of the light and heavy vehicles while not violating this safety constraint. Each change to the design must be tested with the mathematical model simulating the crash event.

Complications arise when considering both the 1,800 lb car and 4,500 lb car cases and the safety of passengers in each case. The attenuator must possess the energy dissipation capacity to stop the large car (structural adequacy criteria) while remaining flexible enough to ensure the safety of the light car's occupant (occupant risk criteria). To solve this problem, CADS must dissipate as much energy at the front of the system as possible; therefore, the impact velocity of the occupant of the light car will be as close to the maximum as possible. Later, after designing for the dissipation of the heavy car's energy, the impact velocities of the passengers are reduced if possible.

APPLICATIONS

The feasibility of employing high molecular weight/high density polyethylene as a reusable energy dissipation medium in highway safety appurtenances has been demonstrated. This polymer in tubular form can dissipate large amounts of kinetic energy, undergo large deformations and strains without fracturing, and essentially restore itself to its original size, shape, and energy dissipation potential when the forcing function is removed.

It is recommended that potentially maintenance-free HMW HDPE impact attenuation devices be designed and crash tested. One 45-mph and two 60-mph truck mounted attenuator designs have already been developed as part of this project. Similar designs for both narrow and wide stationary crash cushions should be developed. In addition, HMW HDPE applications with longitudinal barriers should be explored.

Some currently available impact attenuation devices have purchase prices in excess of \$30,000 per installation. In addition, replacement costs for impacted systems can run into thousands of dollars per system. It is projected that HMW HDPE impact attenuation devices could be constructed for less than \$10,000 each, with little or no associated repair costs. Since there are thousands of impact attenuation devices in existence, the potential future savings could run into the millions of dollars if inexpensive, reusable devices could be produced.

The potential financial, legal, and safety payoffs for highway operations associated with developing highway safety devices which are essentially maintenance free are significant. Maintenance costs associated with the repair of impacted safety devices would be greatly reduced or eliminated. Tort liability exposure related to damaged or collapsed hardware would be significantly decreased. Finally, the safety of the motoring public and the maintenance personnel involved in maintaining and repairing damaged hardware would be enhanced.

REFERENCES

1. "Full-Scale Testing Procedures for Guardrails and Guide Posts," *Highway Research Board Circular No. 482*, Highway Research Board Committee on Guardrails and Guide Posts, 1962.
2. Michie, J.D. and Bronstad, M.E., "Recommended Procedures for Vehicle Crash Testing of Highway Appurtenances," *NCHRP Report 153*, National Cooperative Highway Research Program, 1974.
3. "Recommended Procedures for Vehicle Crash Testing of Highway Appurtenances," *Transportation Research Circular No. 191*, Committee A2A04, 1978.
4. Michie, J.D., "Recommended Procedures for Safety Performance Evaluation of Highway Appurtenances," *NCHRP Report 230*, National Cooperative Highway Research Program, 1981.
5. Carney, J.F., III, "Motorway Impact Attenuation Devices: Past, Present, and Future," *Structural Crashworthiness and Failure*, Chapter 11, 1993.
6. Carney, J.F., III, "A Portable Energy Absorbing System for Highway Service Vehicles," JHRAC Project, 73-4, JHR 74-83, Final Report, 1974.
7. Carney, J.F., III and R.J. Sazinski, "A Portable Energy-Absorbing System for Highway Services Vehicles," *Transportation Engineering Journal*, ASCE, Vol. 104, No. TE4, pp. 407-421, 1978.

8. Carney, J.F., III, "Experimental Evaluation of a Portable Energy-Absorbing System for Highway Service Vehicles," TRB Transportation Research Record 679, pp. 16-18, 1978.
9. Carney, J.F., III and D.A. Larsen, "Accident Experience with the Connecticut Crash Cushion: 1977-1980," R.R. 343-16-80-19, 1980.
10. Carney, J.F., III and C.E. Dougan, "Summary of the Results of Crash Tests Performed on the Connecticut Impact-Attenuation System (CIAS)," FHWA-CT-RD-876-1-83-13, 1983.
11. Carney, J.F., III, C.E. Dougan and M.W. Hargrave, "The Connecticut Impact-Attenuation System," *Application of Safety Appurtenances*, TRB Transportation Research Record 1024, pp. 41-50, 1985.
12. Carney, J.F., III, "The Connecticut Narrow Hazard Crash Cushion," *Design and Testing of Roadside Safety Devices*, TRB Transportation Research Record 1233, pp. 43-50, 1989.
13. Carney, J.F., III, "A Generalized Design for the Connecticut Impact Attenuation System," FHWA-CT-RD-HPR-1222-F-88-15, Final Report, 1988.
14. SAS Institute, Inc. *SAS/STAT User's Guide*, 1991. Version 6.03, Fourth Edition.

APPENDIX

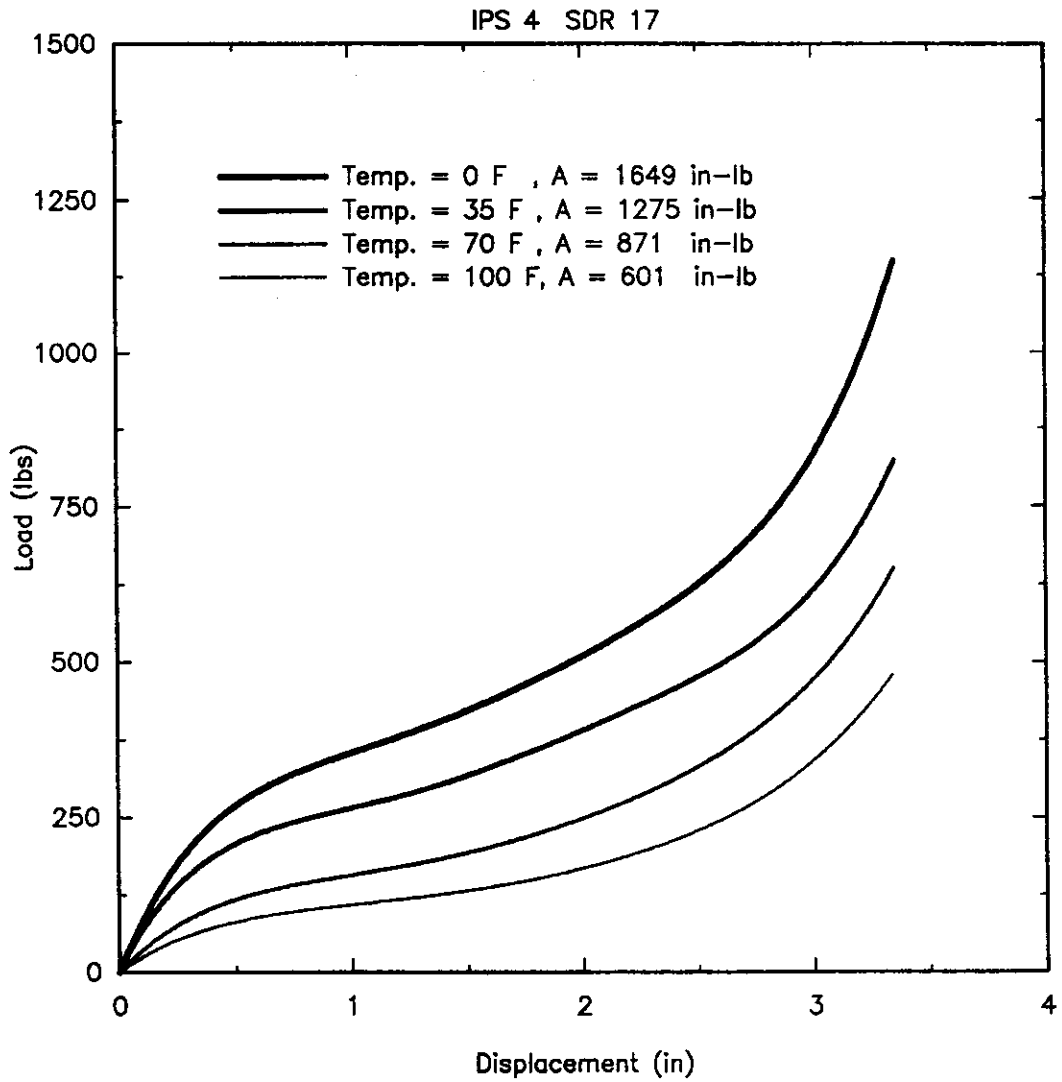


Figure A1. Quasi-static Load vs. Displacement for IPS 4 SDR 17.

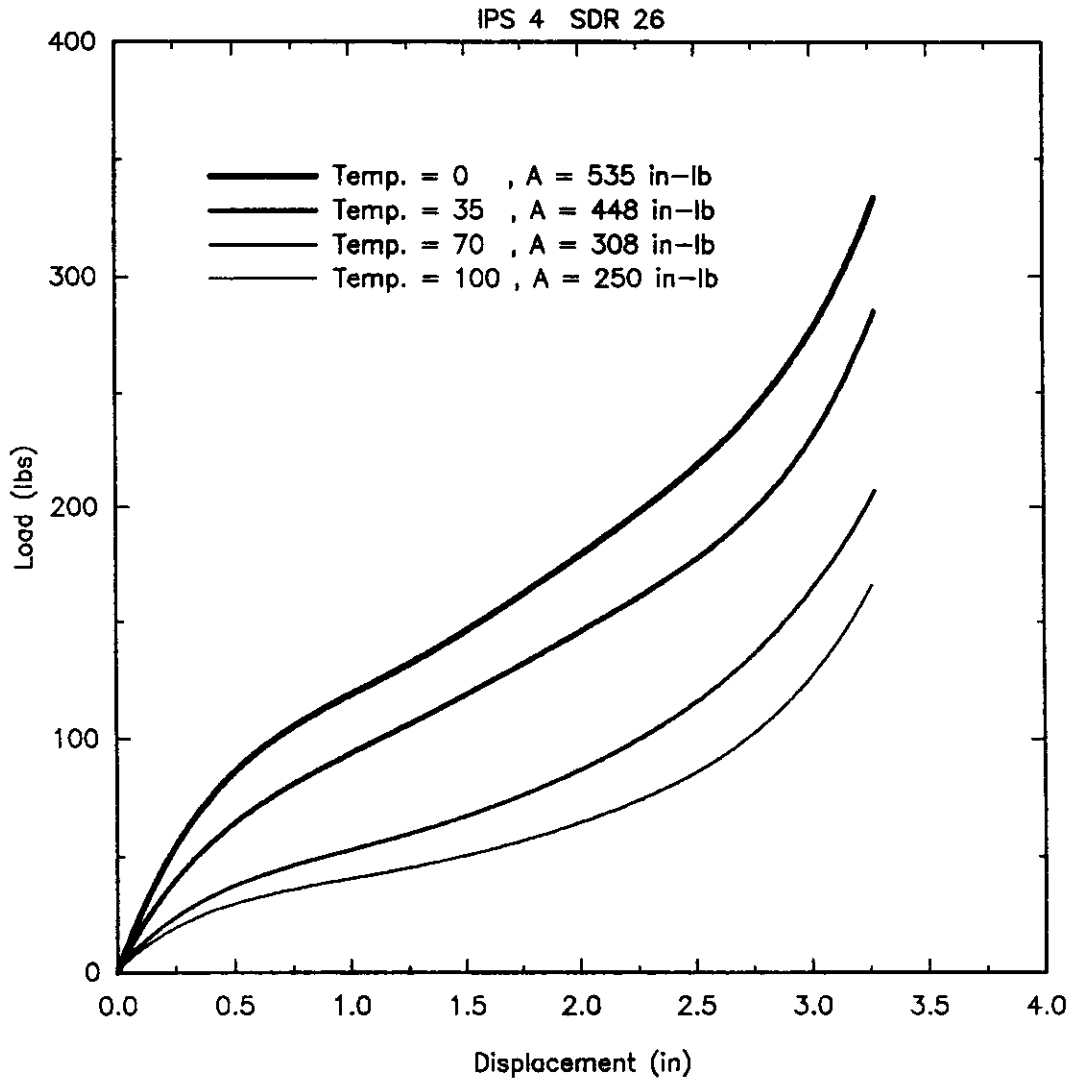


Figure A2. Quasi-static Load vs. Displacement for IPS 4 SDR 26.

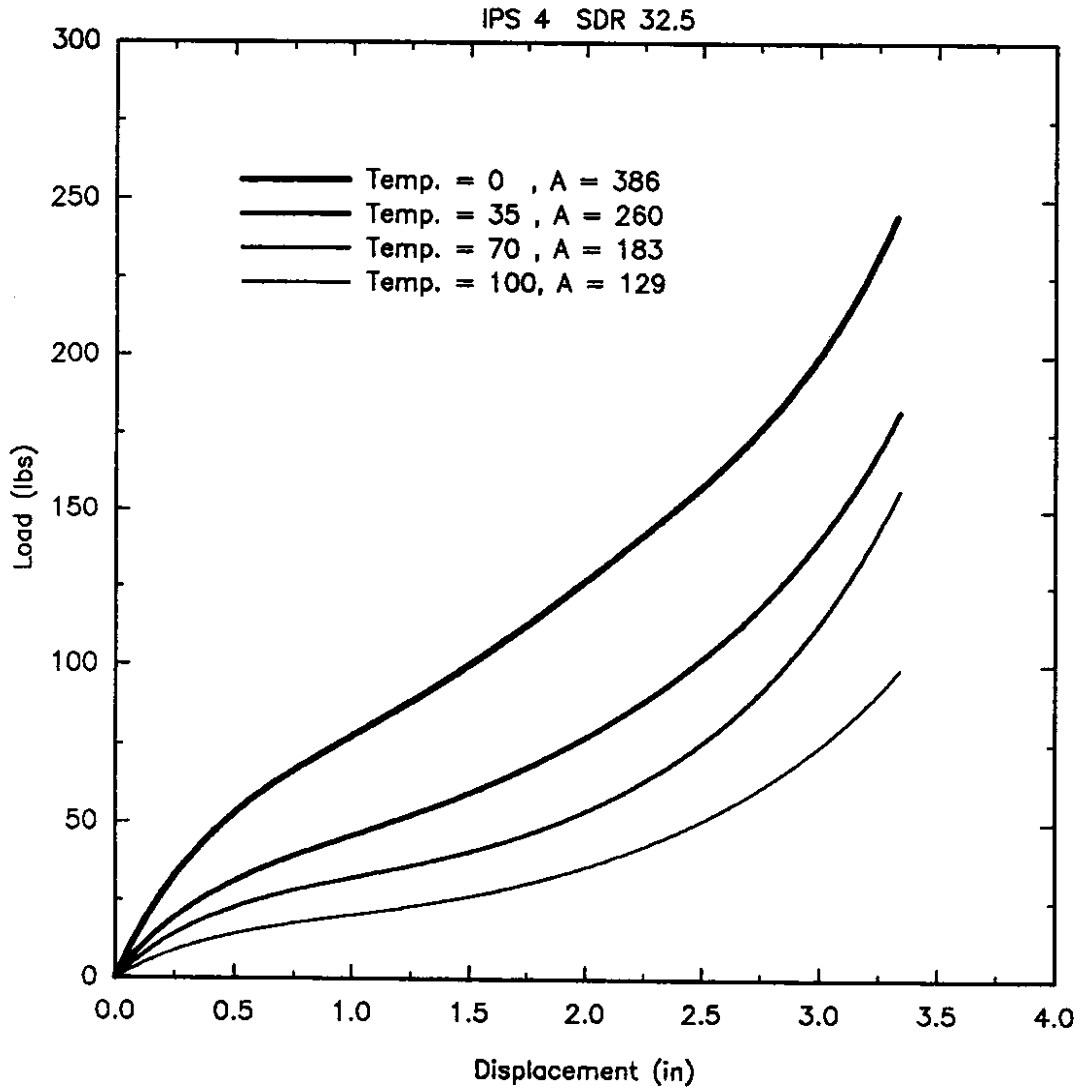


Figure A3. Quasi-static Load vs. Displacement for IPS 4 SDR 32.5.

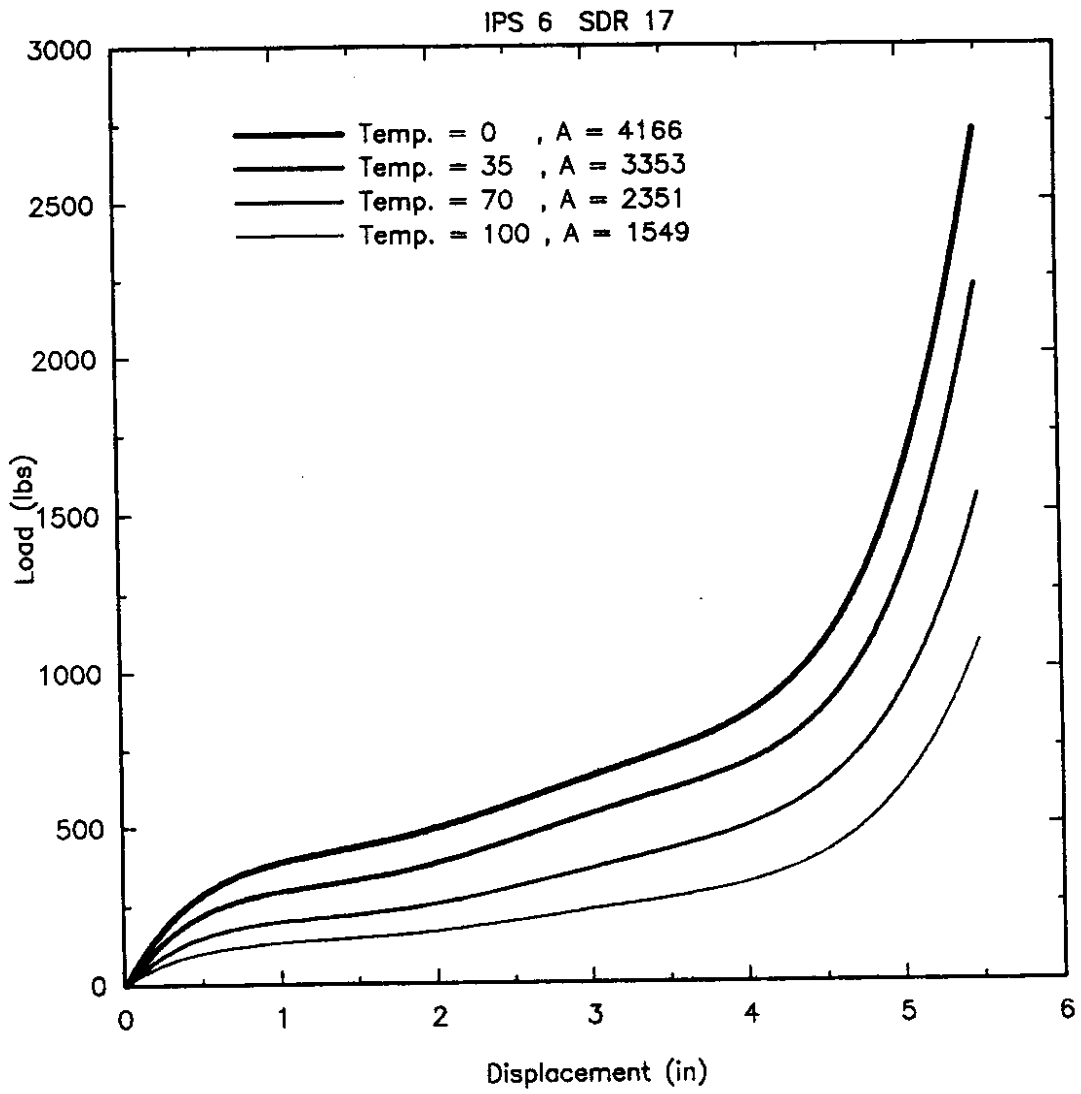


Figure A4. Quasi-static Load vs. Displacement for IPS 6 SDR 17.

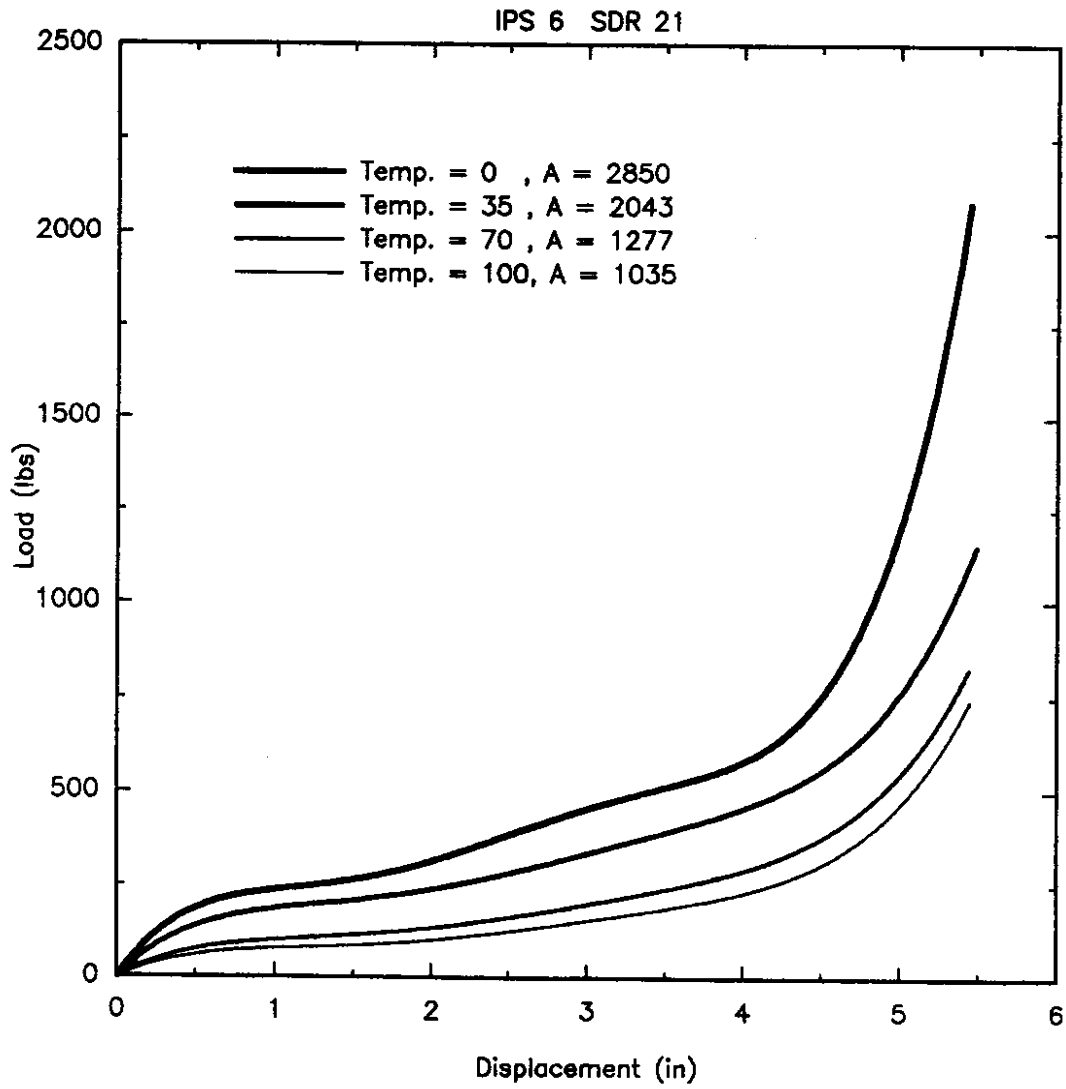


Figure A5. Quasi-static Load vs. Displacement for IPS 6 SDR 21.

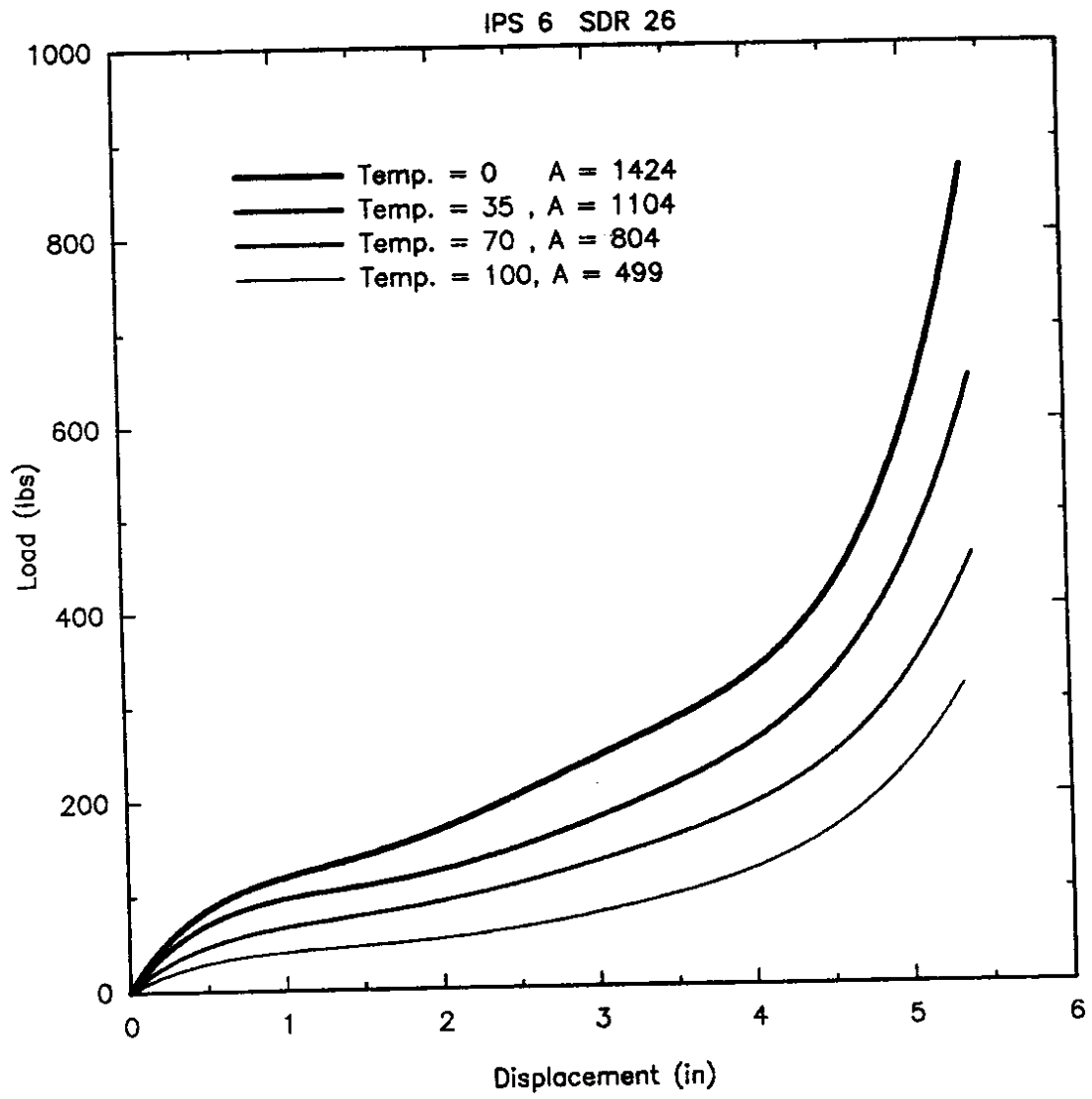


Figure A6. Quasi-static Load vs. Displacement for IPS 6 SDR 26.

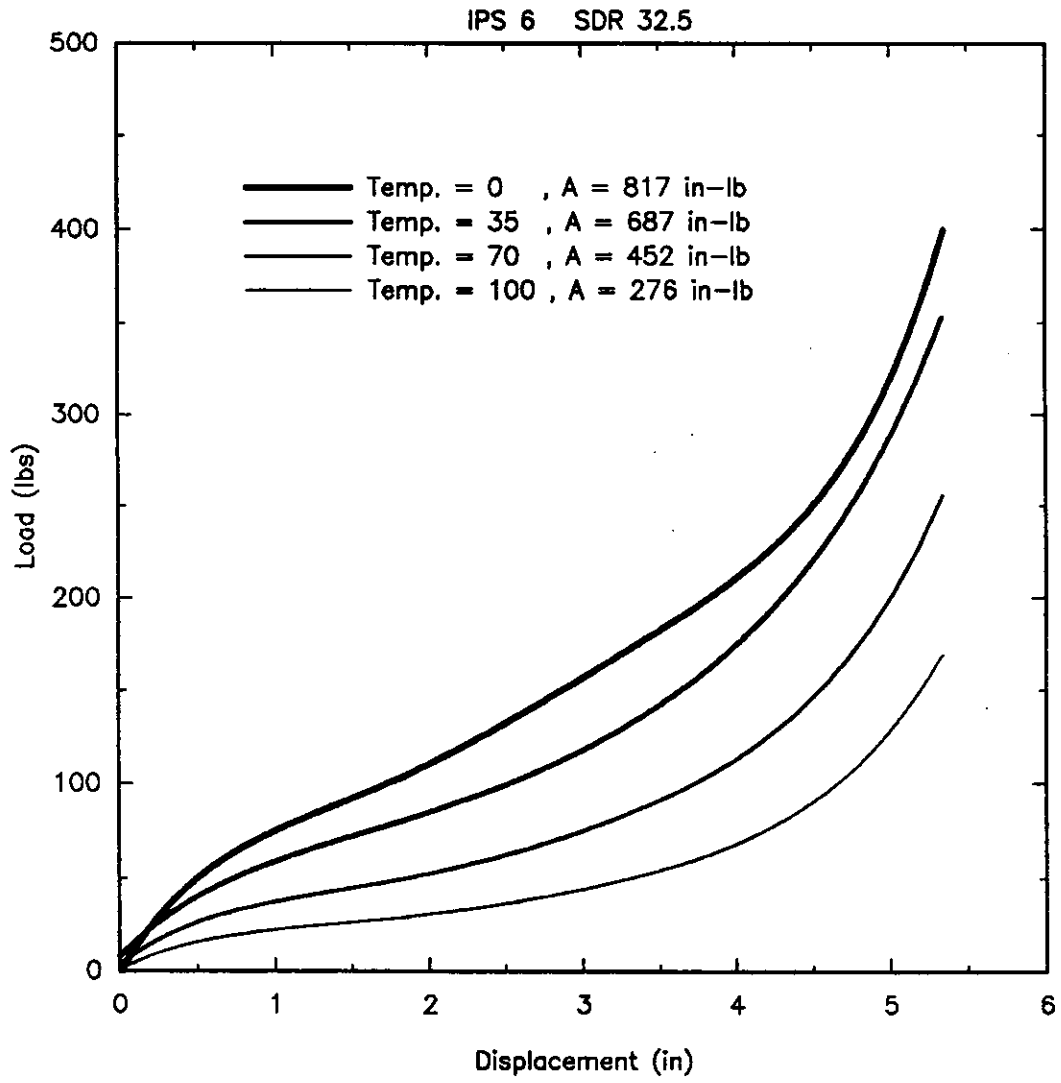


Figure A7. Quasi-static Load vs. Displacement for IPS 6 SDR 32.5.

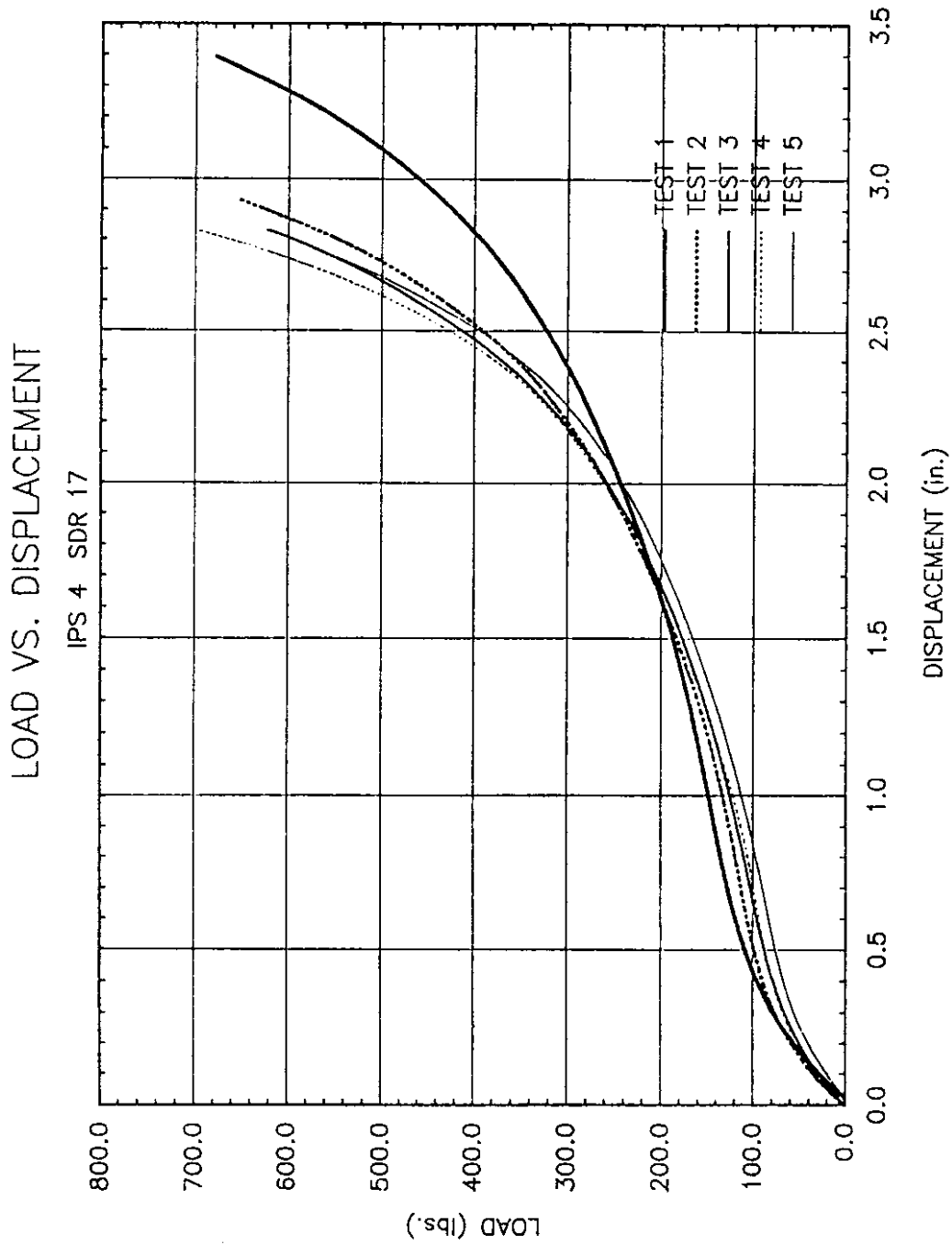


Figure A8. Load vs. Displacement Histories for IPS 4 SDR 17.

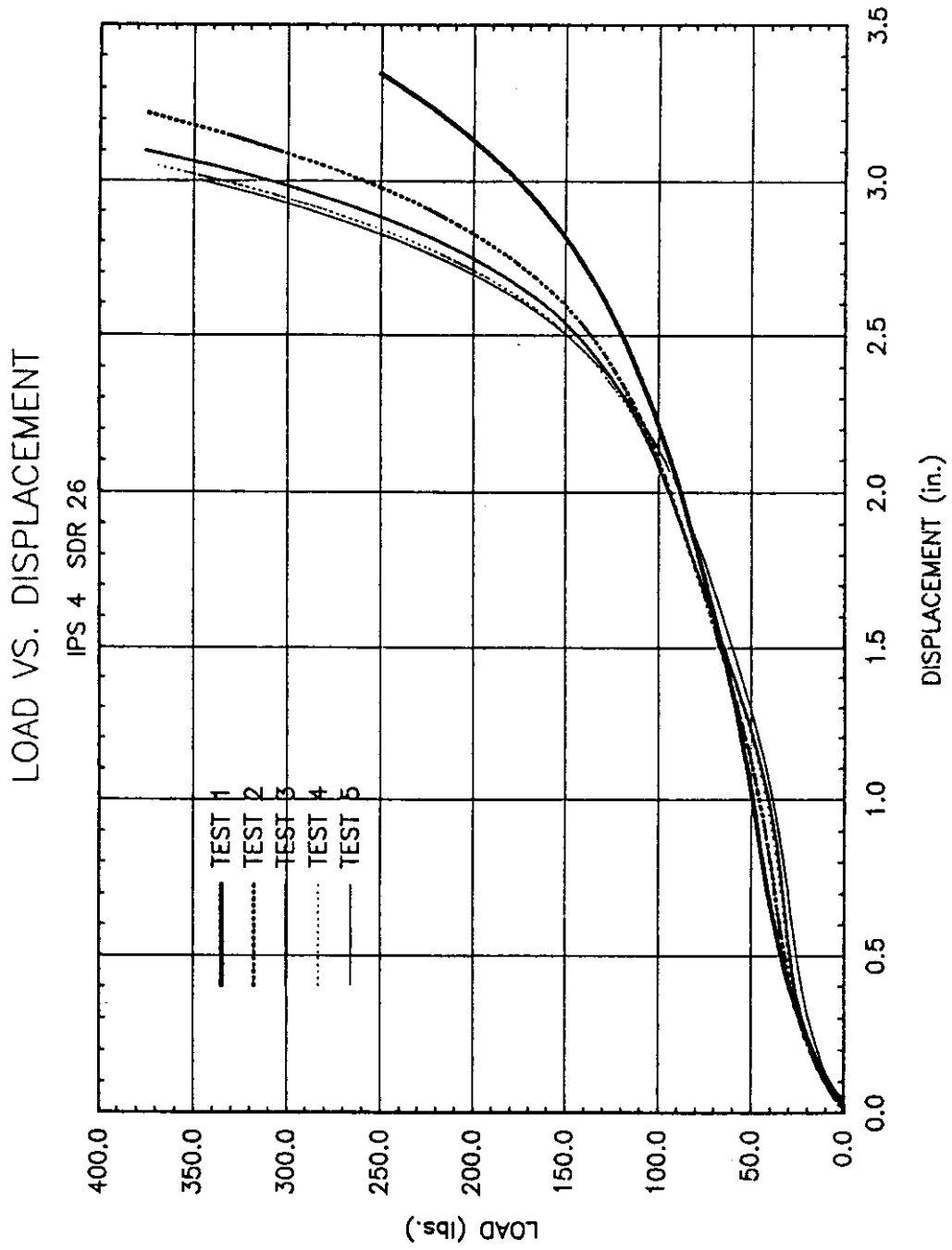


Figure A9. Load vs. Displacement Histories for IPS 4 SDR 26.

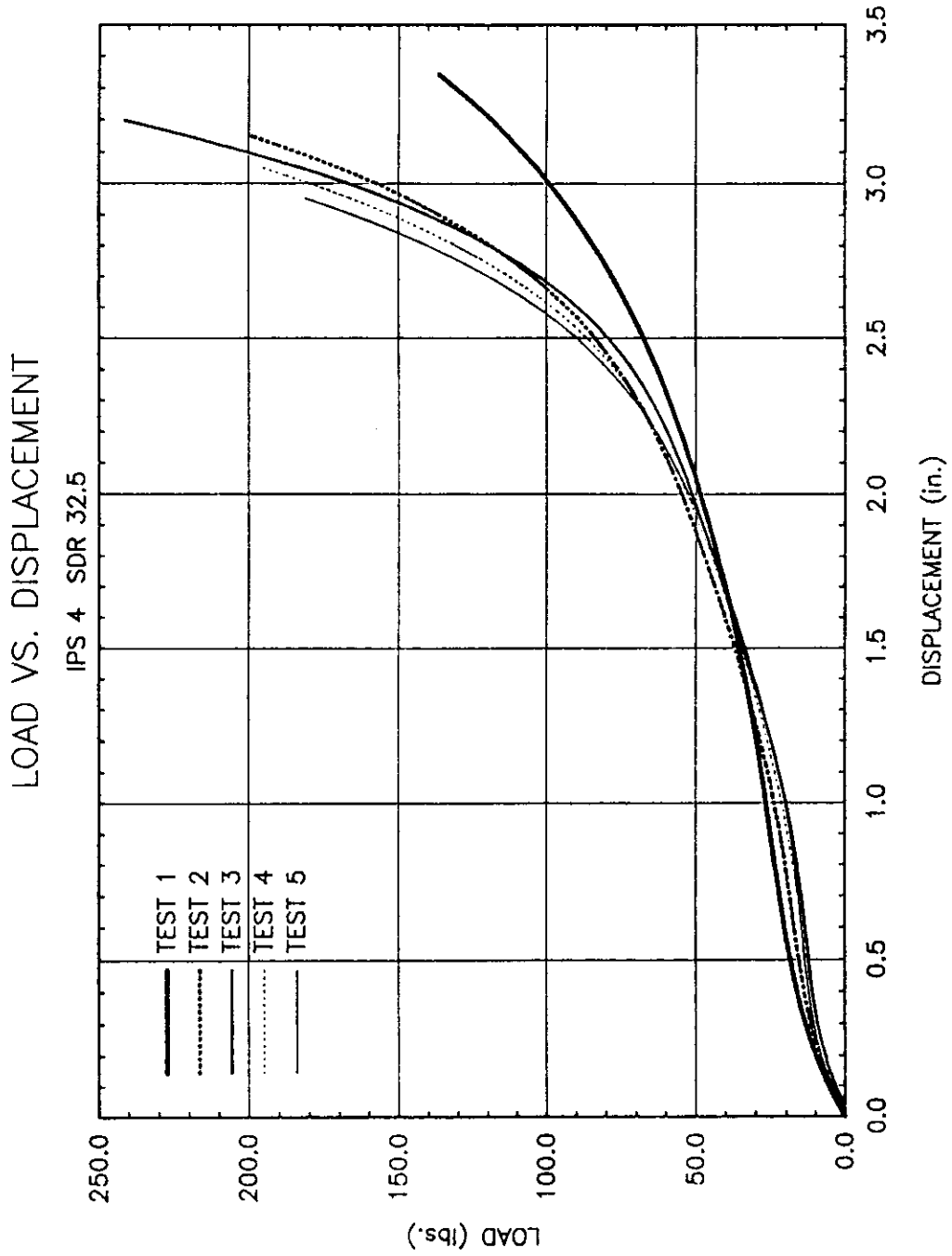


Figure A10. Load vs. Displacement Histories for IPS 4 SDR 32.5.

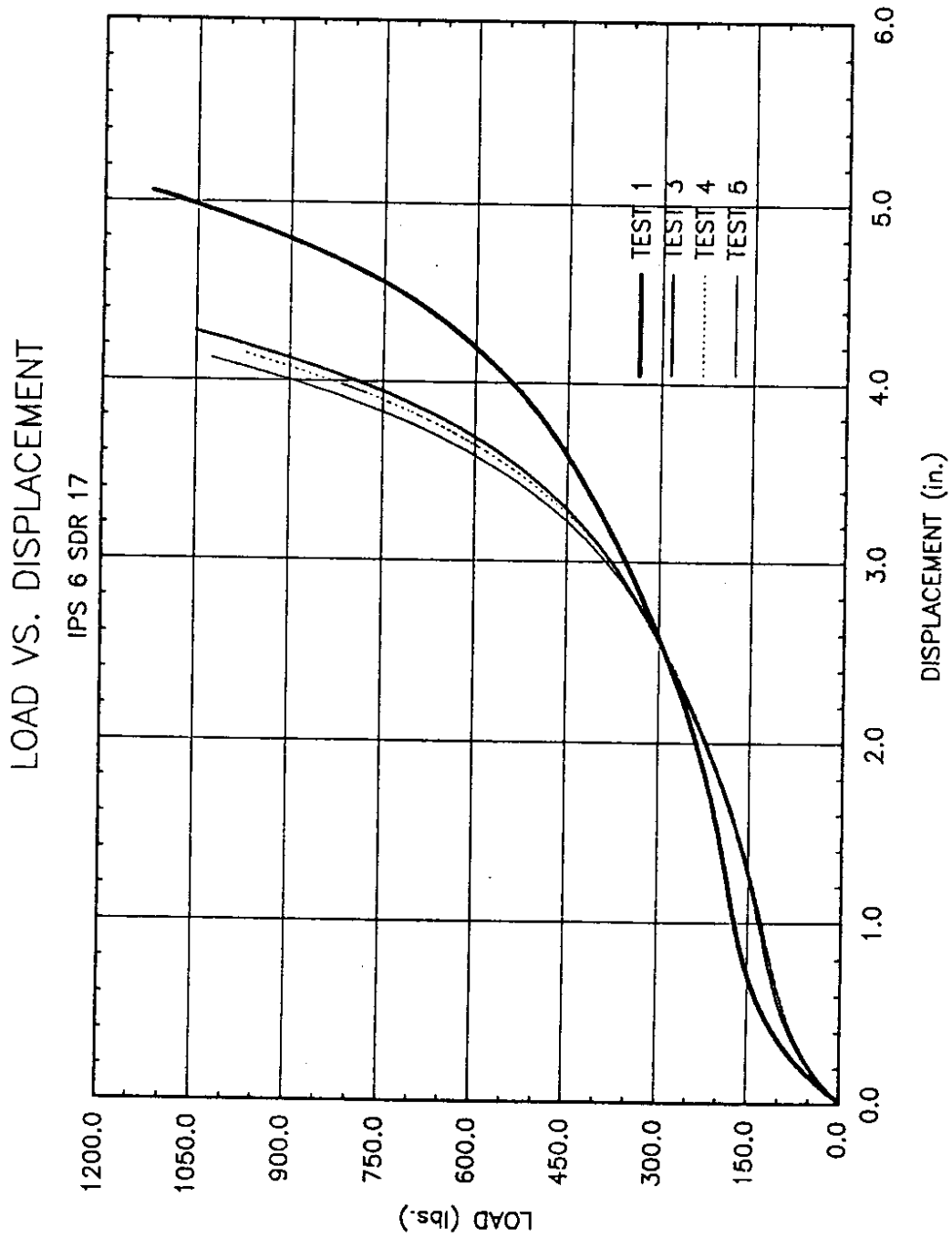


Figure A11. Load vs. Displacement Histories for IPS 6 SDR 17.

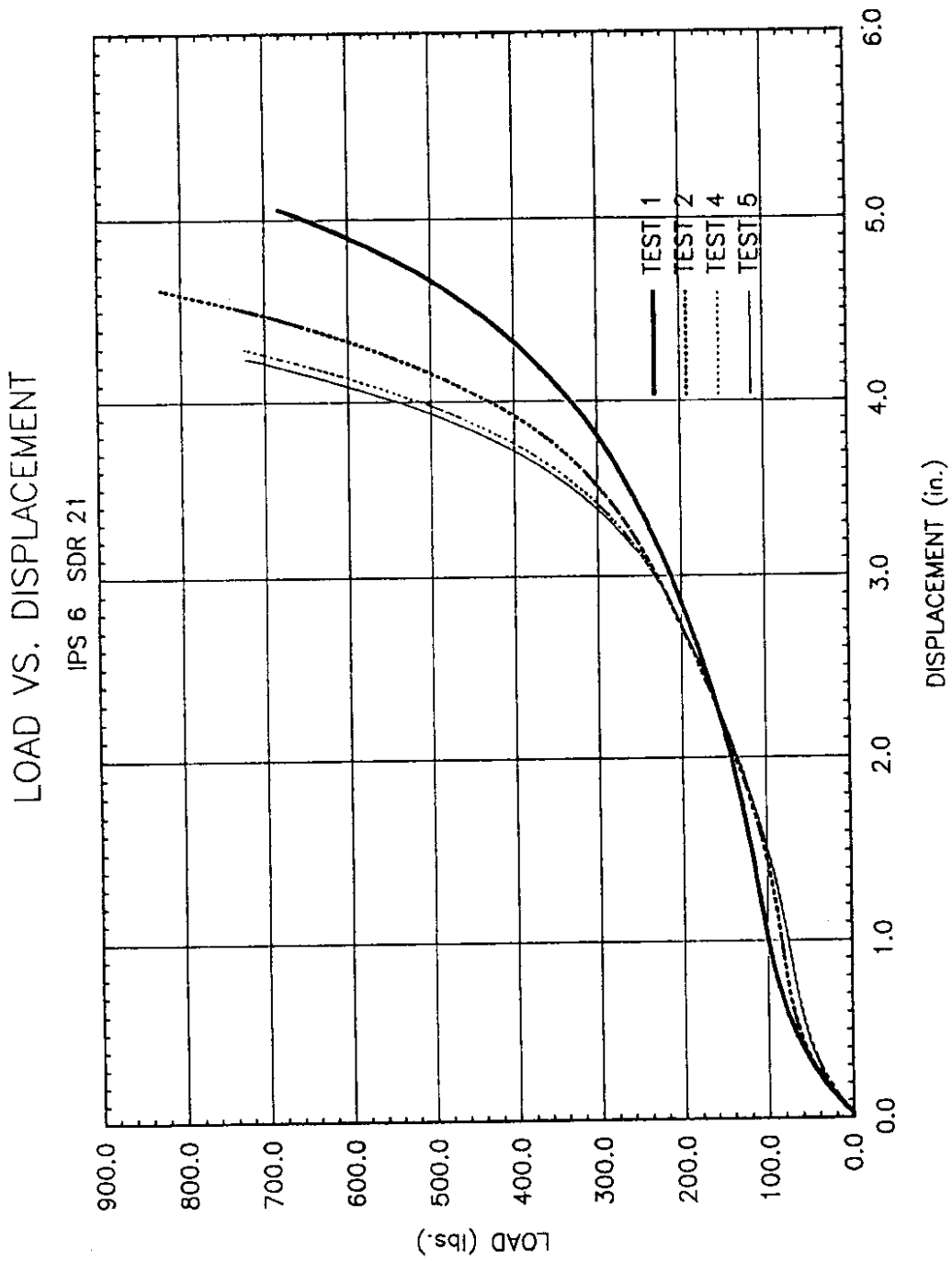


Figure A12. Load vs. Displacement Histories for IPS 6 SDR 21.

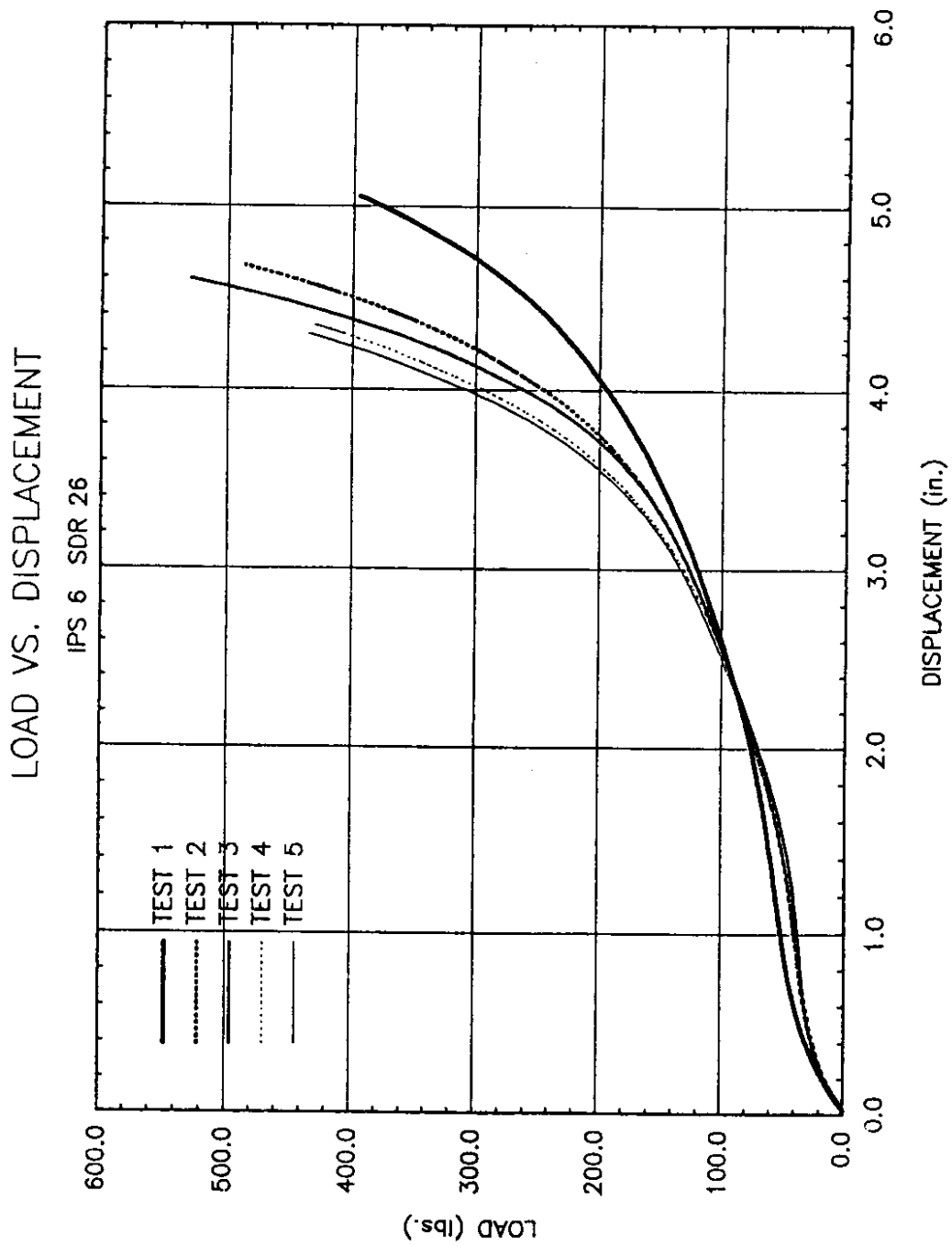


Figure A13. Load vs. Displacement Histories for IPS 6 SDR 26.

LOAD VS. DISPLACEMENT

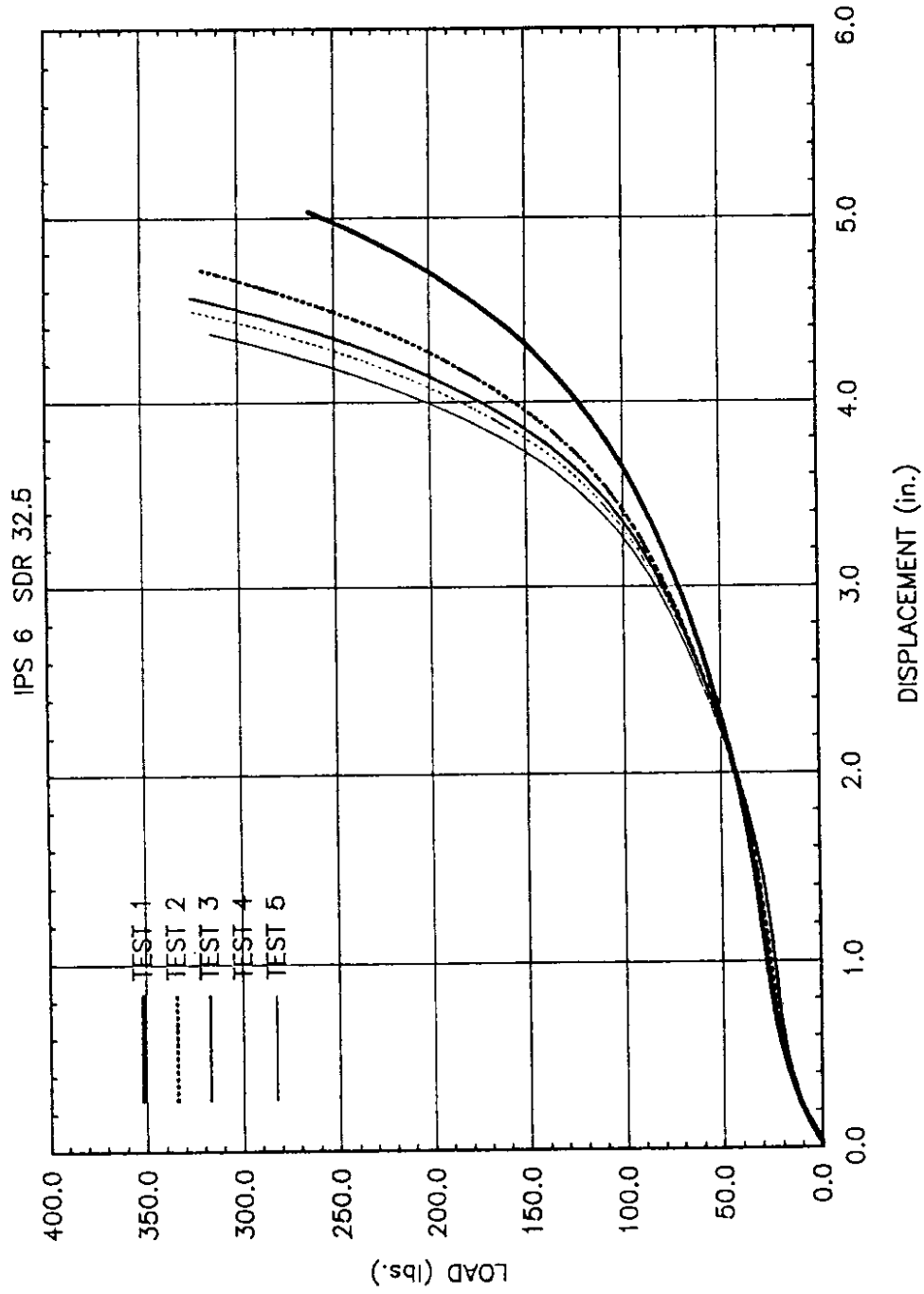


Figure A14. Load vs. Displacement Histories for IPS 6 SDR 32.5.

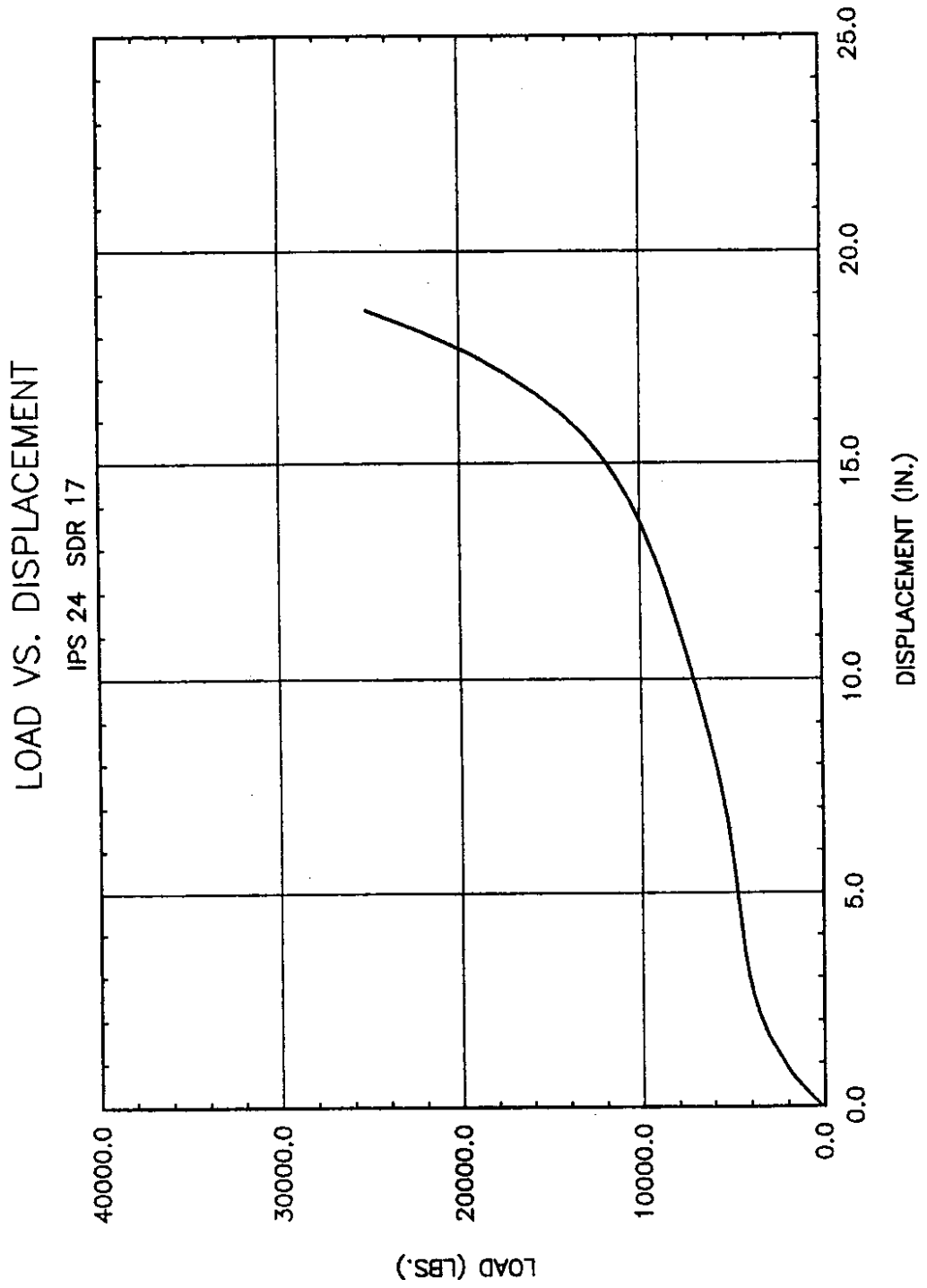


Figure A15. Quasi-static Load vs. Displacement for IPS 24 SDR 17.

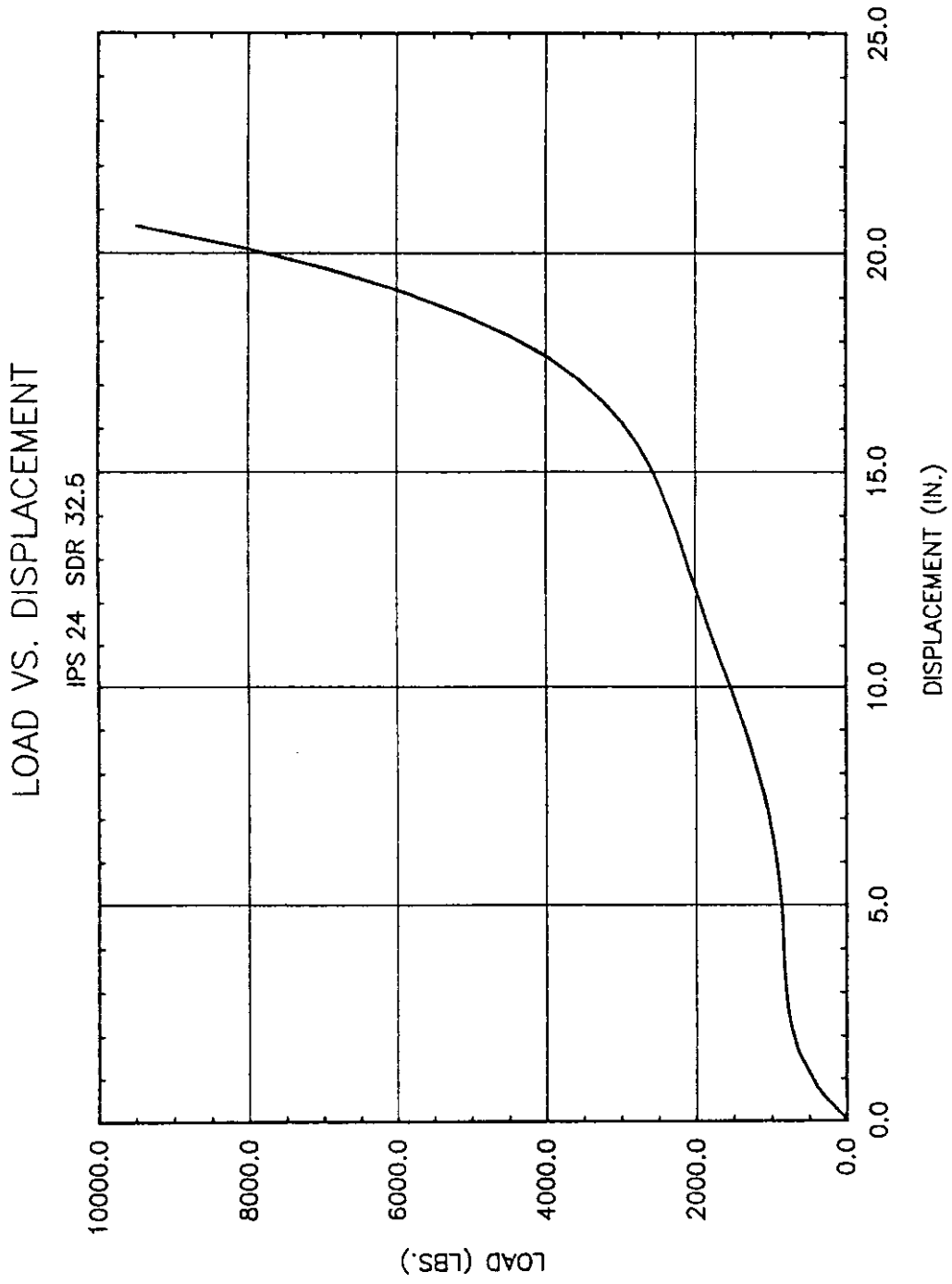


Figure A16. Quasi-static Load vs. Displacement for IPS 24 SDR 32.5.

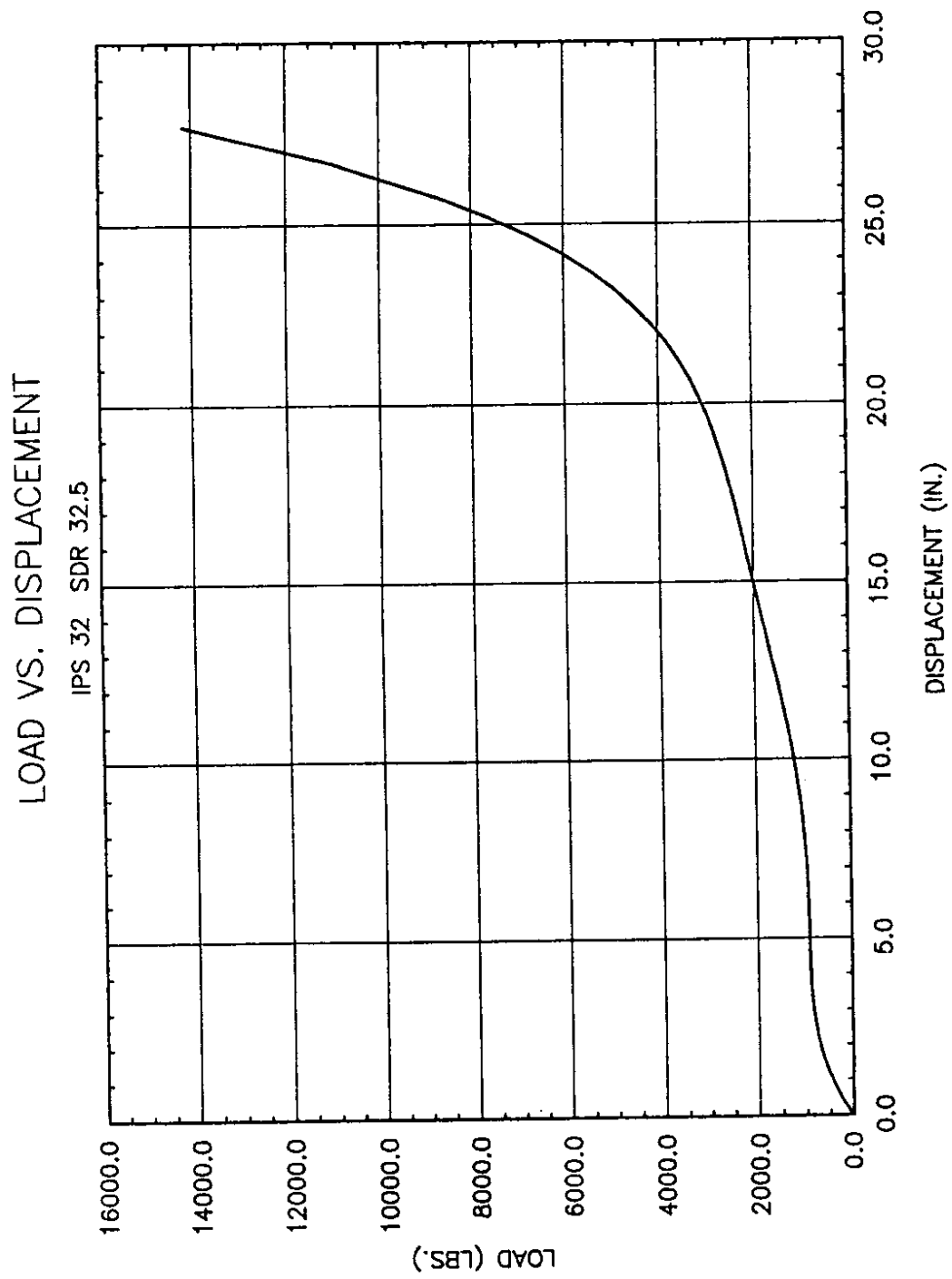


Figure A17. Quasi-static Load vs. Displacement for IPS 32 SDR 32.5.

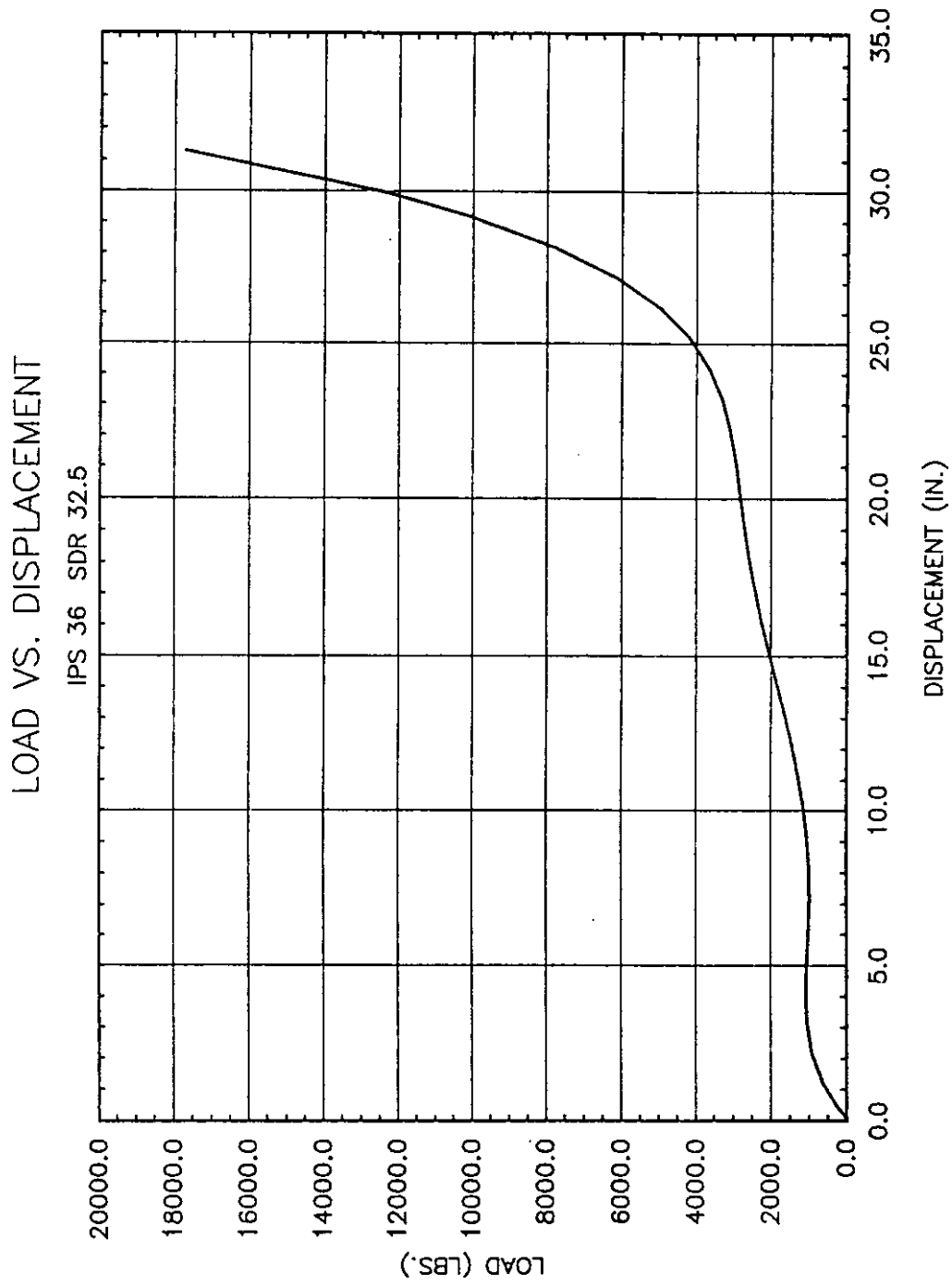


Figure A18. Quasi-static Load vs. Displacement for IPS 36 SDR 32.5.

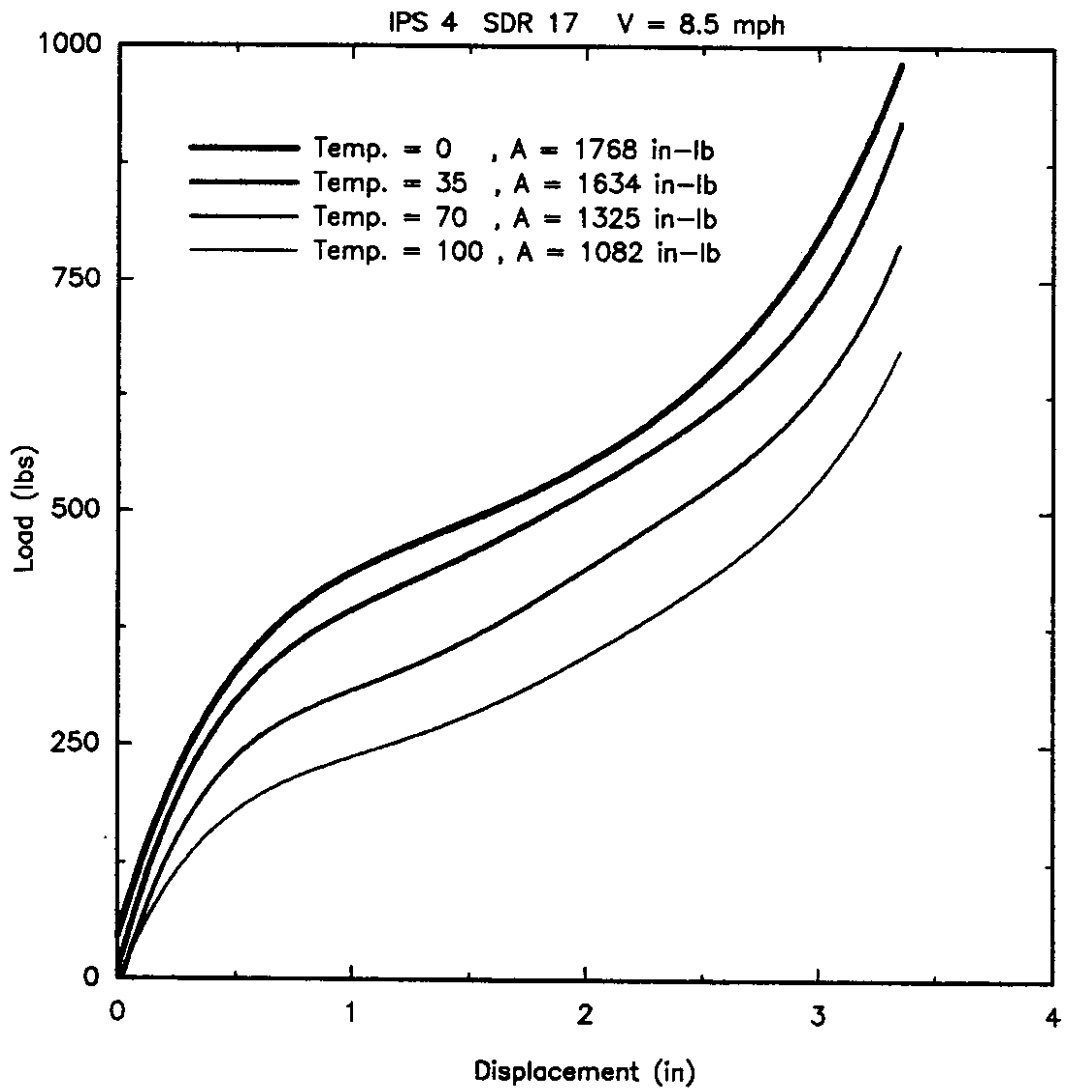


Figure A19. 8.5 mph Impact Test for IPS 4 SDR 17.

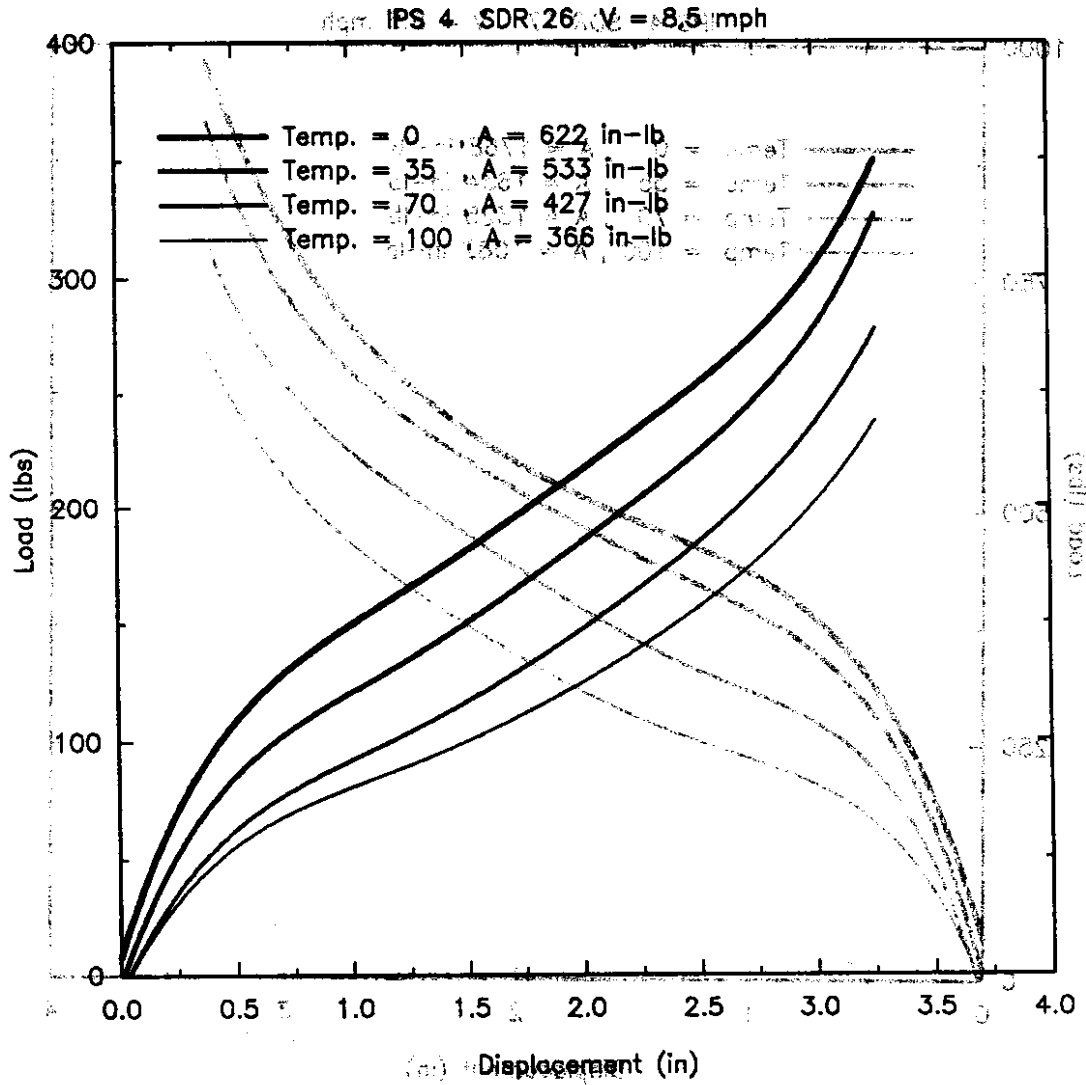


Figure A20. 8.5 mph Impact Test for IPS 4 SDR 26.

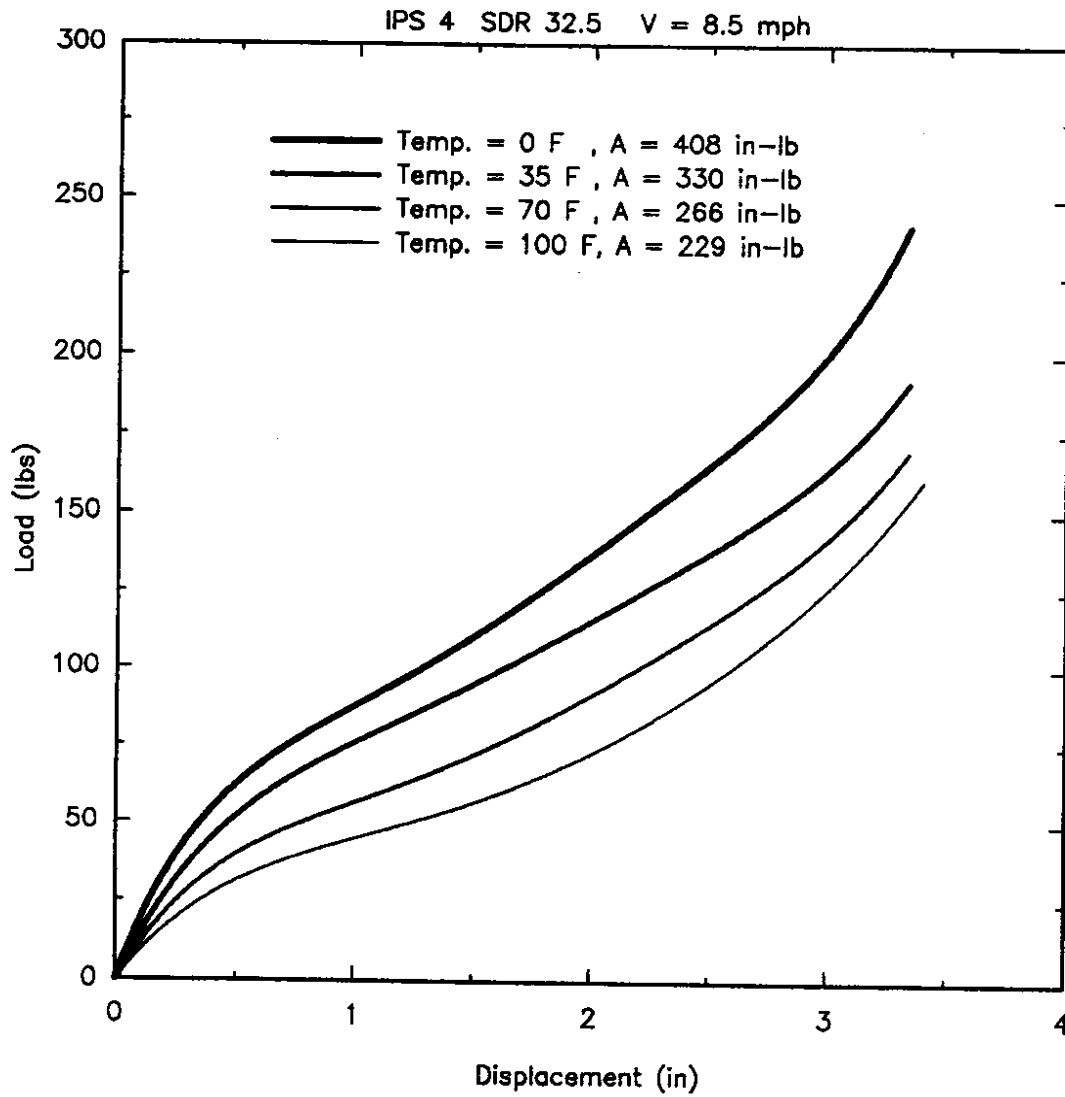


Figure A21. 8.5 mph Impact Test for IPS 4 SDR 32.5.

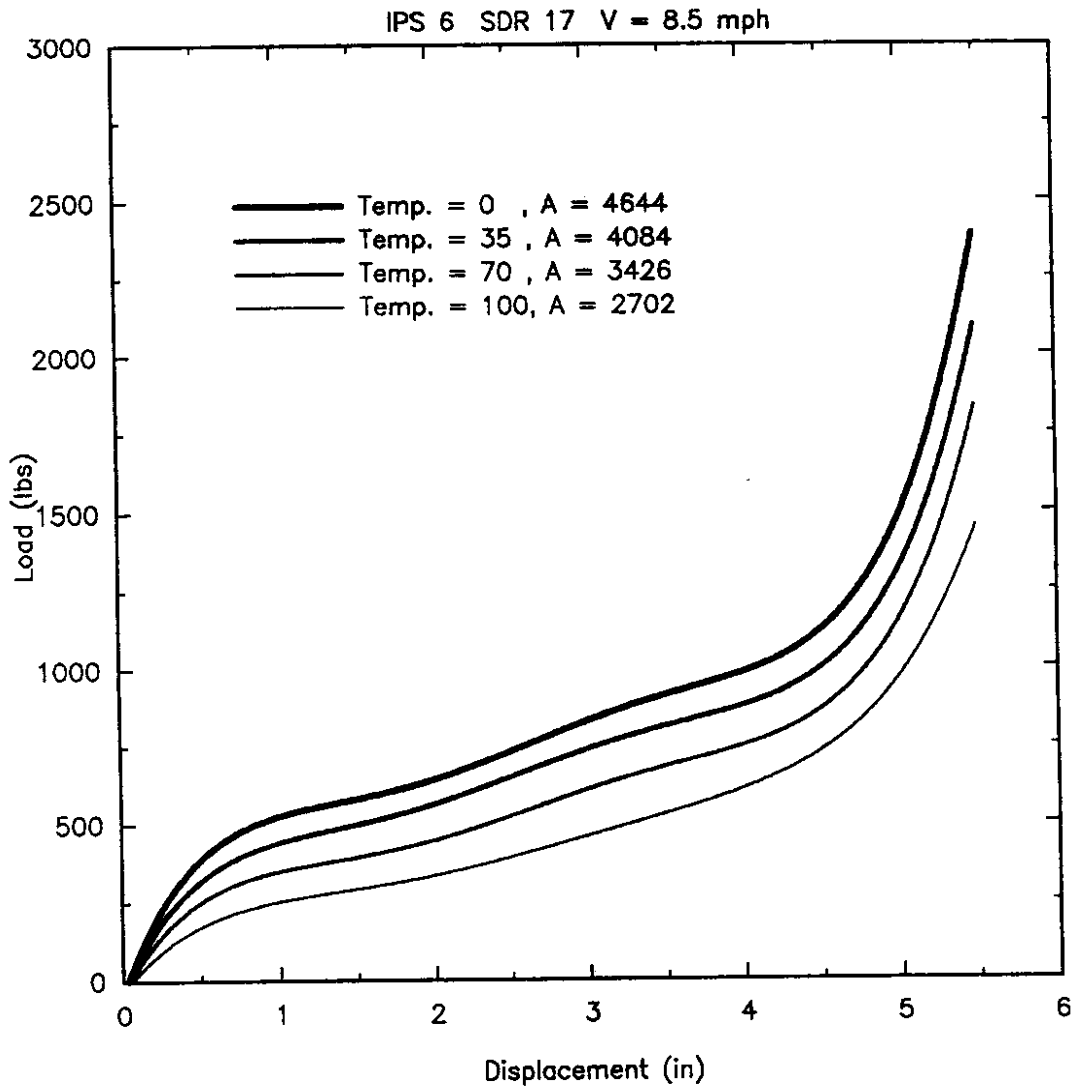


Figure A22. 8.5 mph Impact Test for IPS 6 SDR 17.

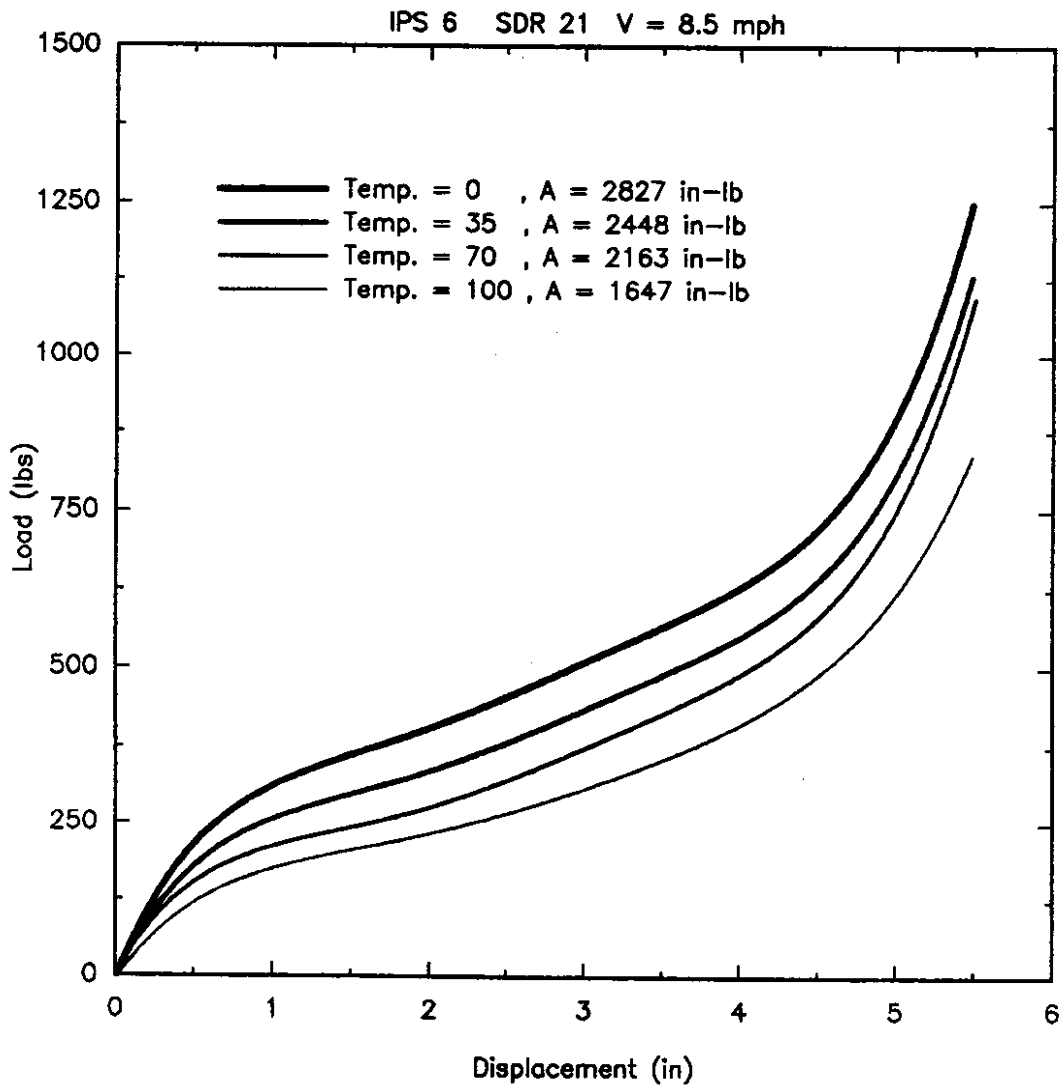


Figure A23. 8.5 mph Impact Test for IPS 6 SDR 21.

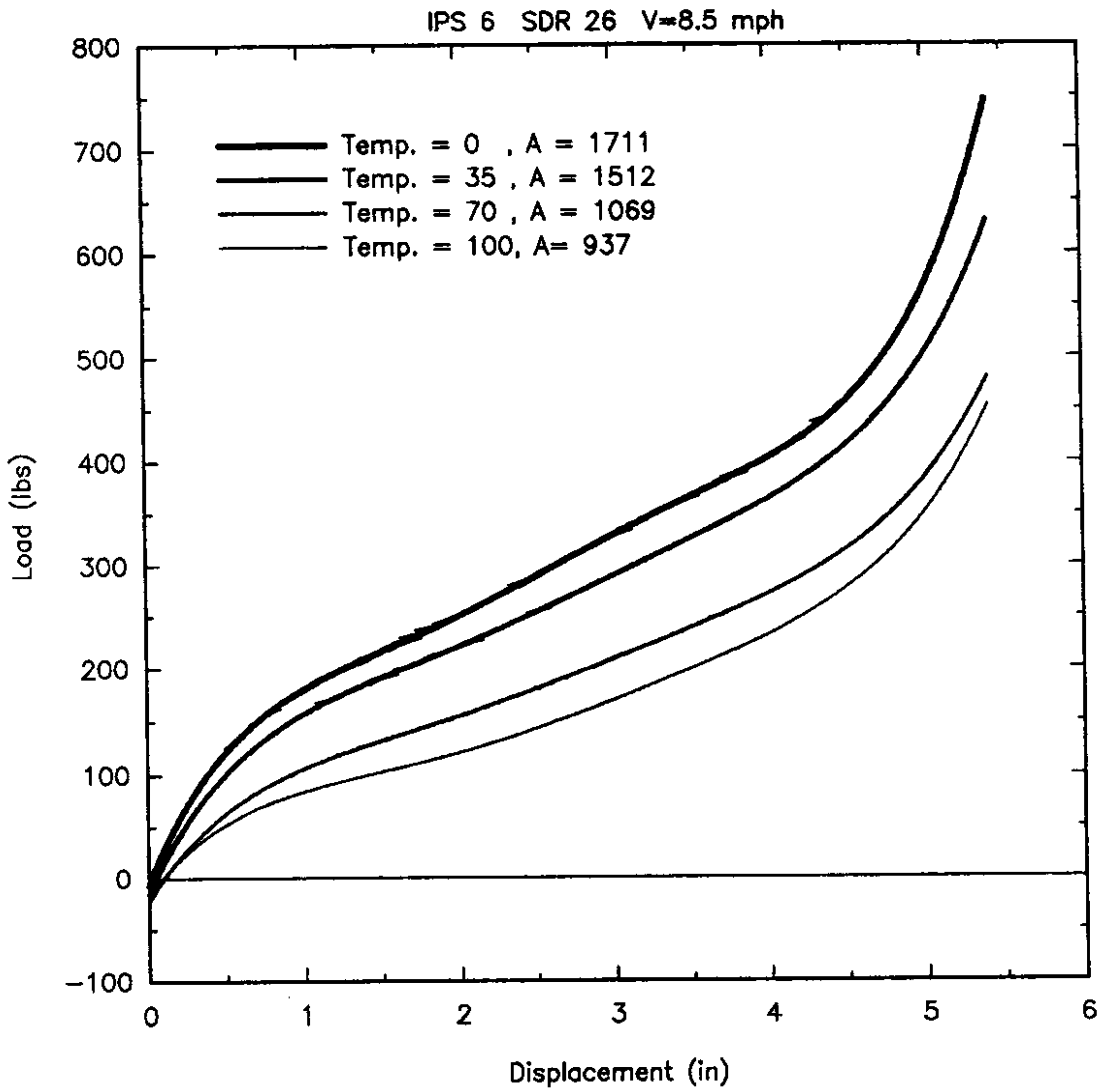


Figure A24. 8.5 mph Impact Test for IPS 6 SDR 26.

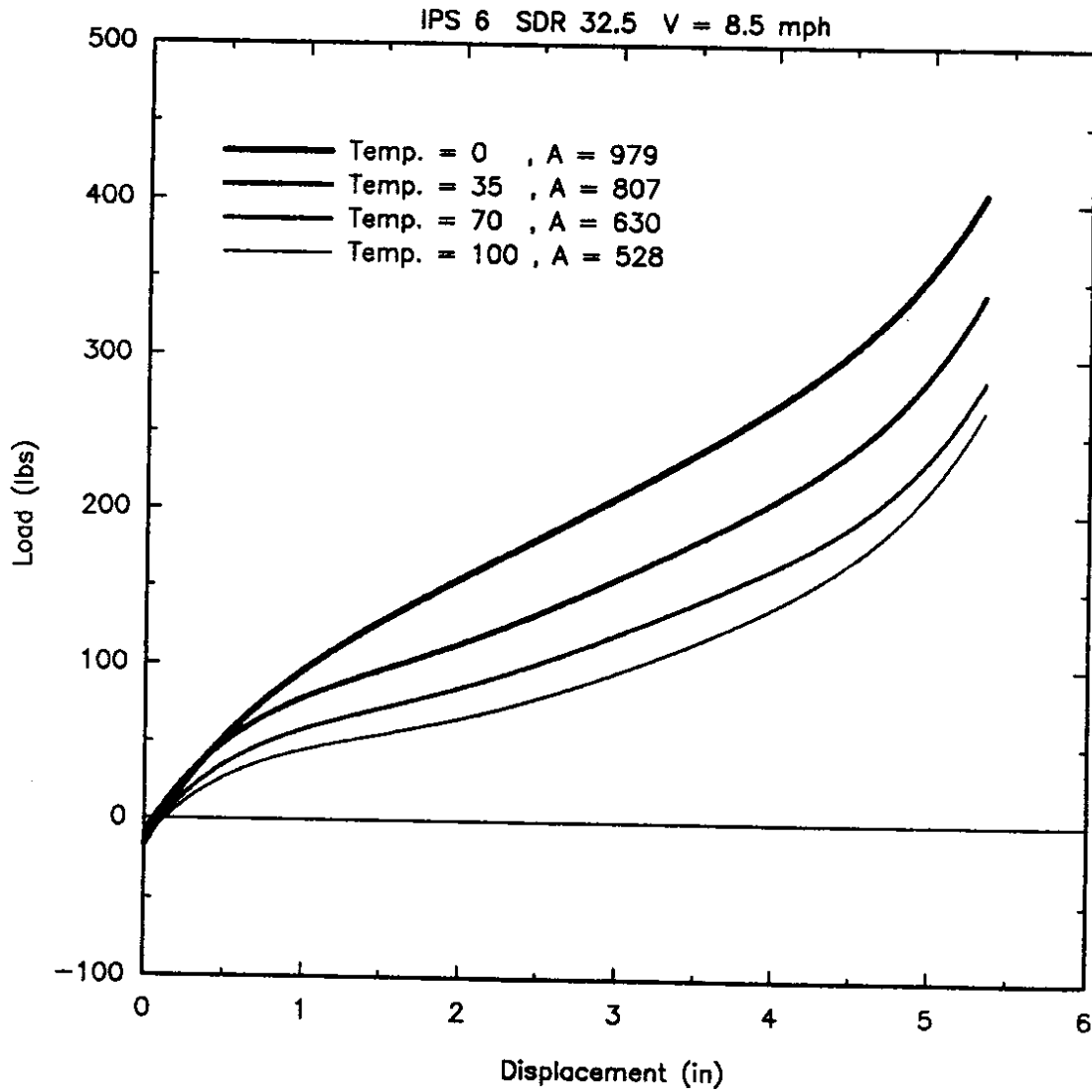


Figure A25. 8.5 mph Impact Test for IPS 6 SDR 32.5.

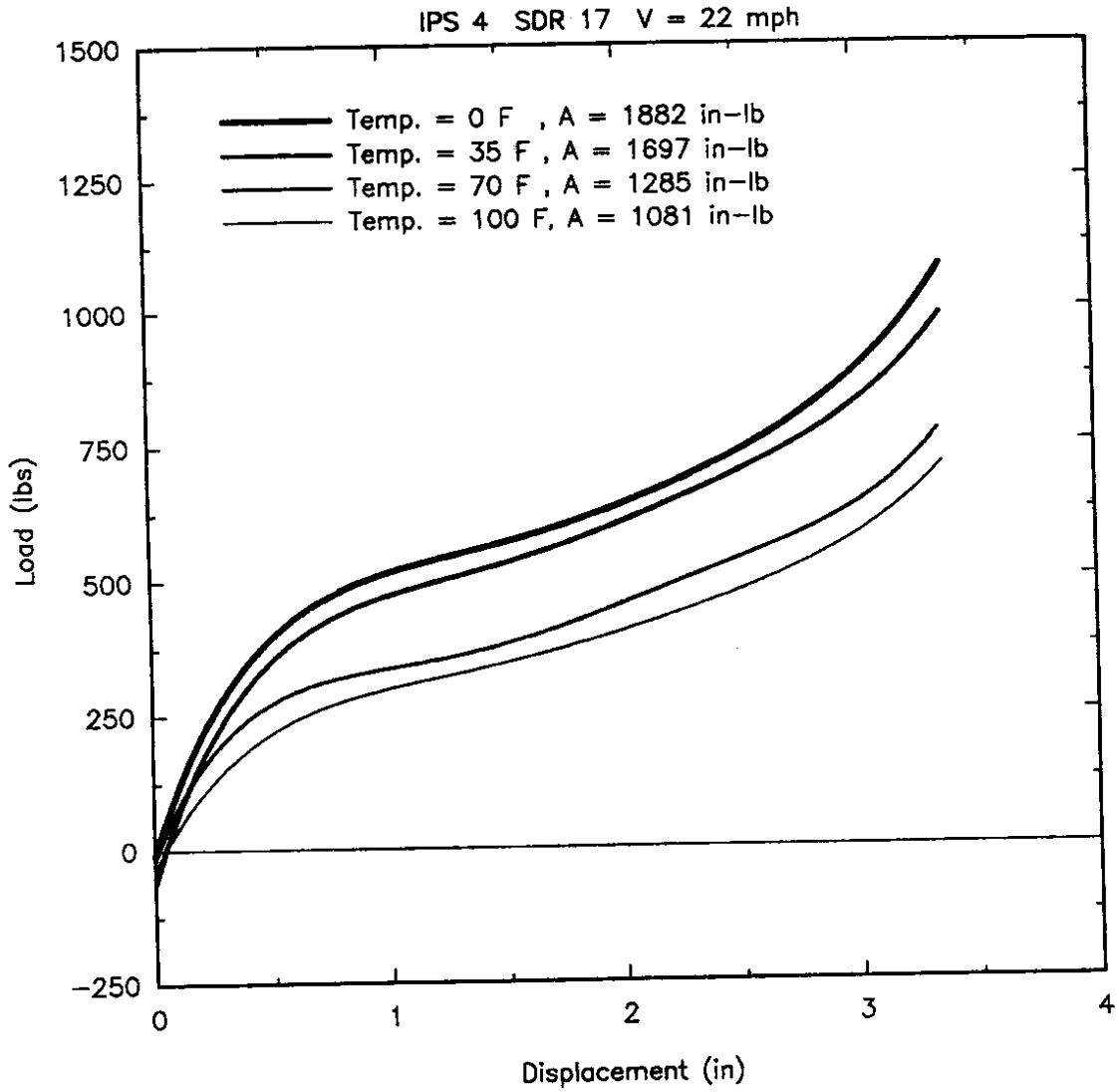


Figure A26. 22 mph Impact Test for IPS 4 SDR 17.

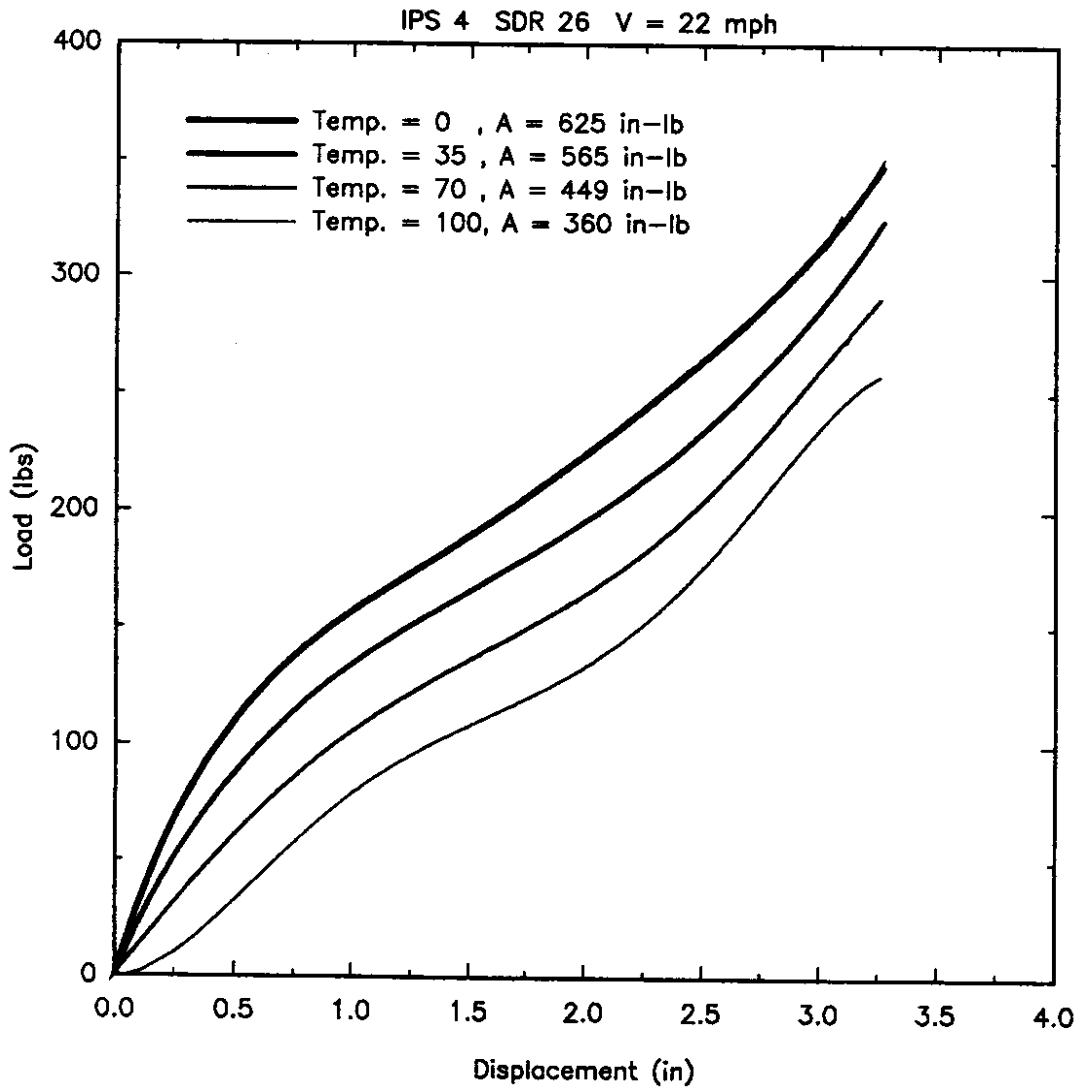


Figure A27. 22 mph Impact Test for IPS 4 SDR 26.

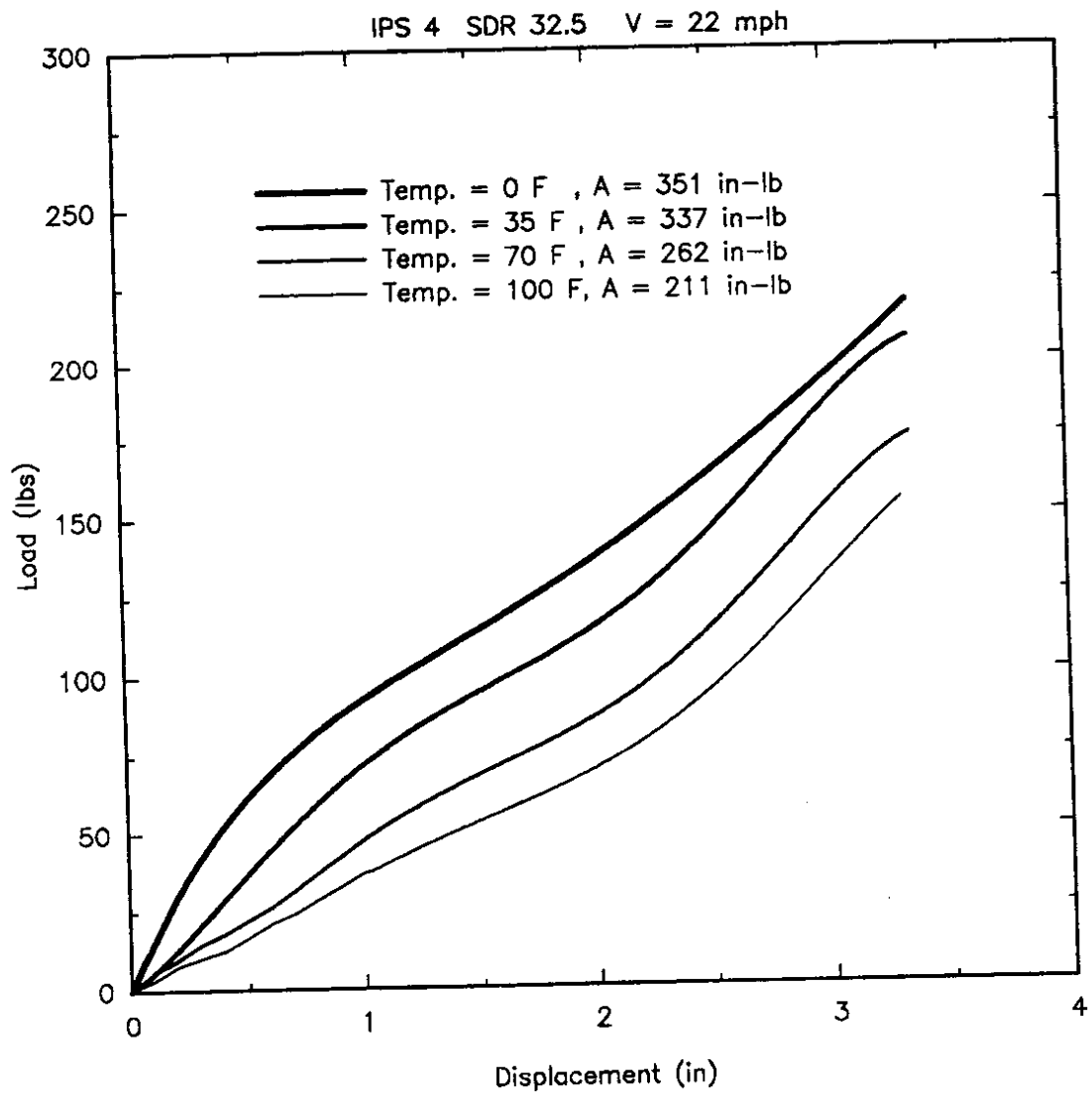


Figure A28. 22 mph Impact Test for IPS 4 SDR 32.5.

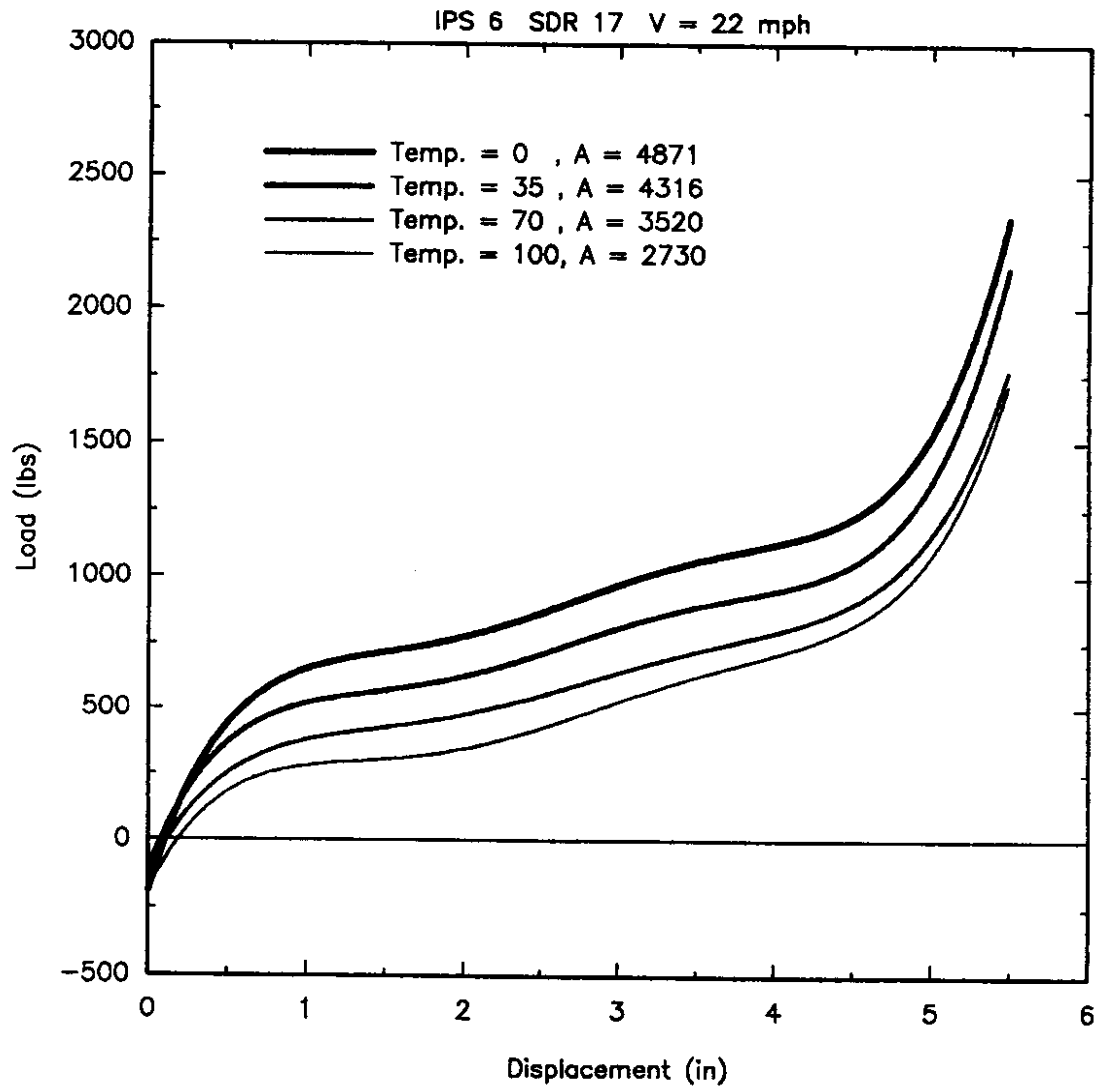


Figure A29. 22 mph Impact Test for IPS 6 SDR 17.

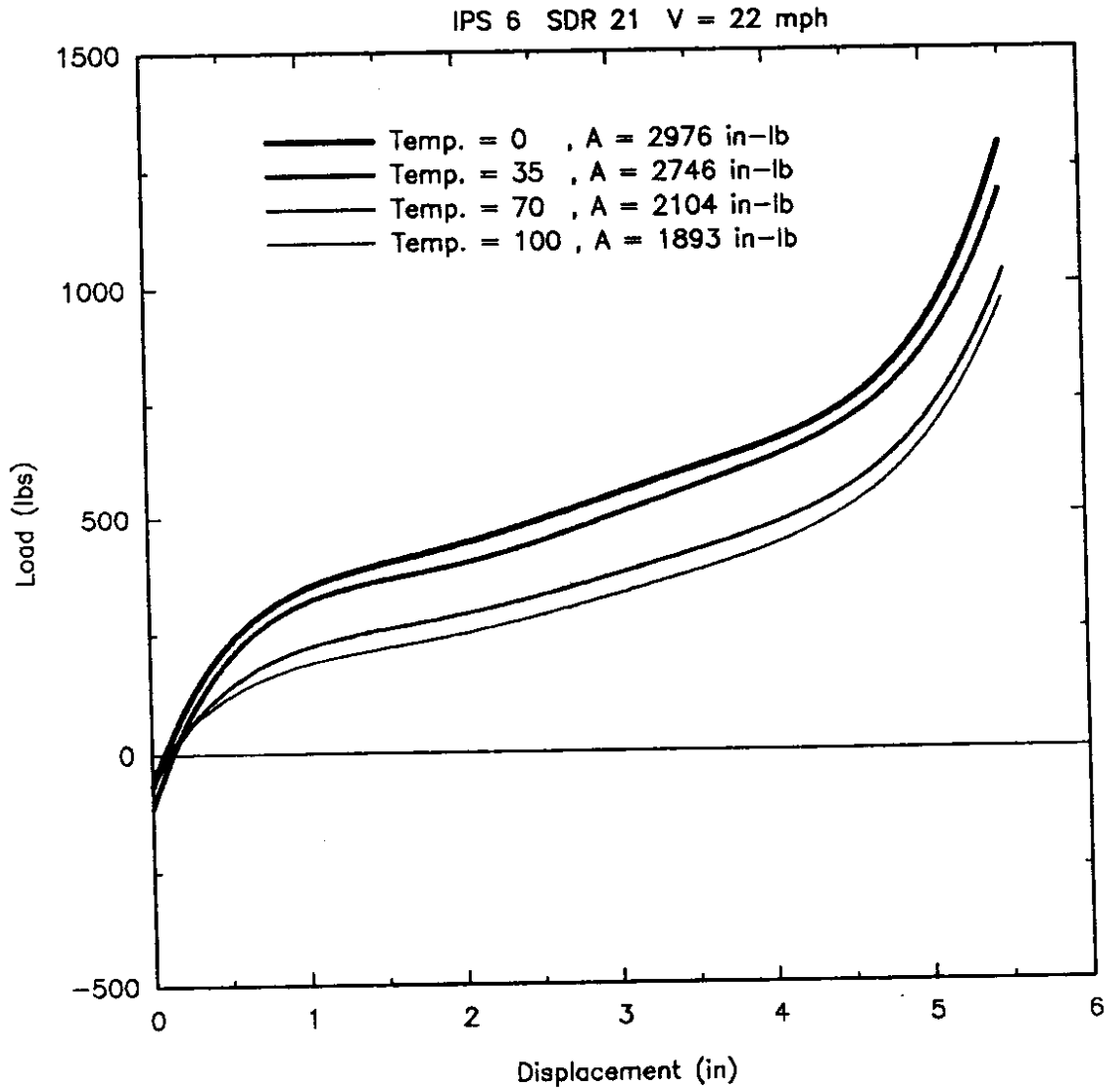


Figure A30. 22 mph Impact Test for IPS 6 SDR 21.

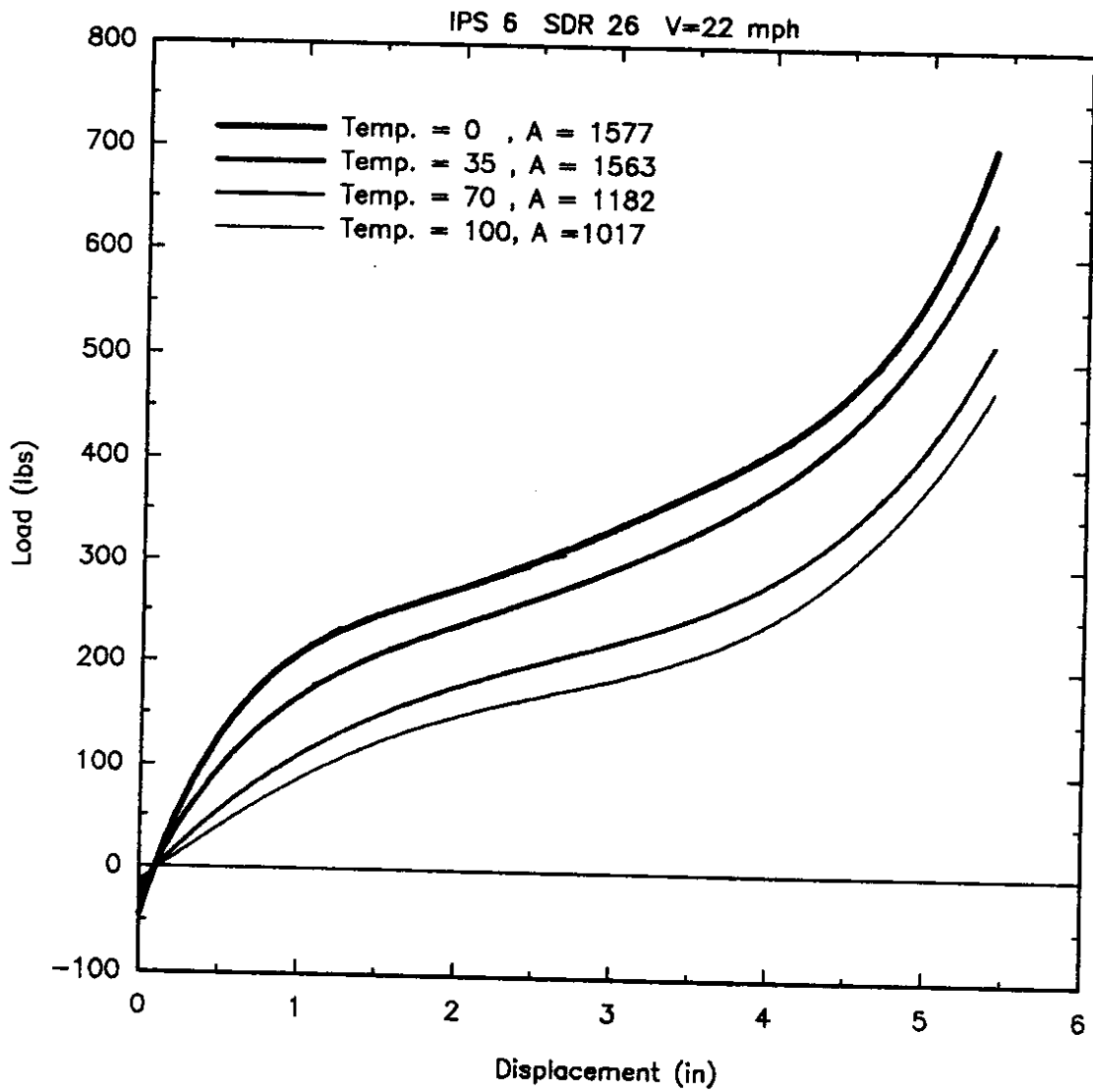


Figure A31. 22 mph Impact Test for IPS 6 SDR 26.

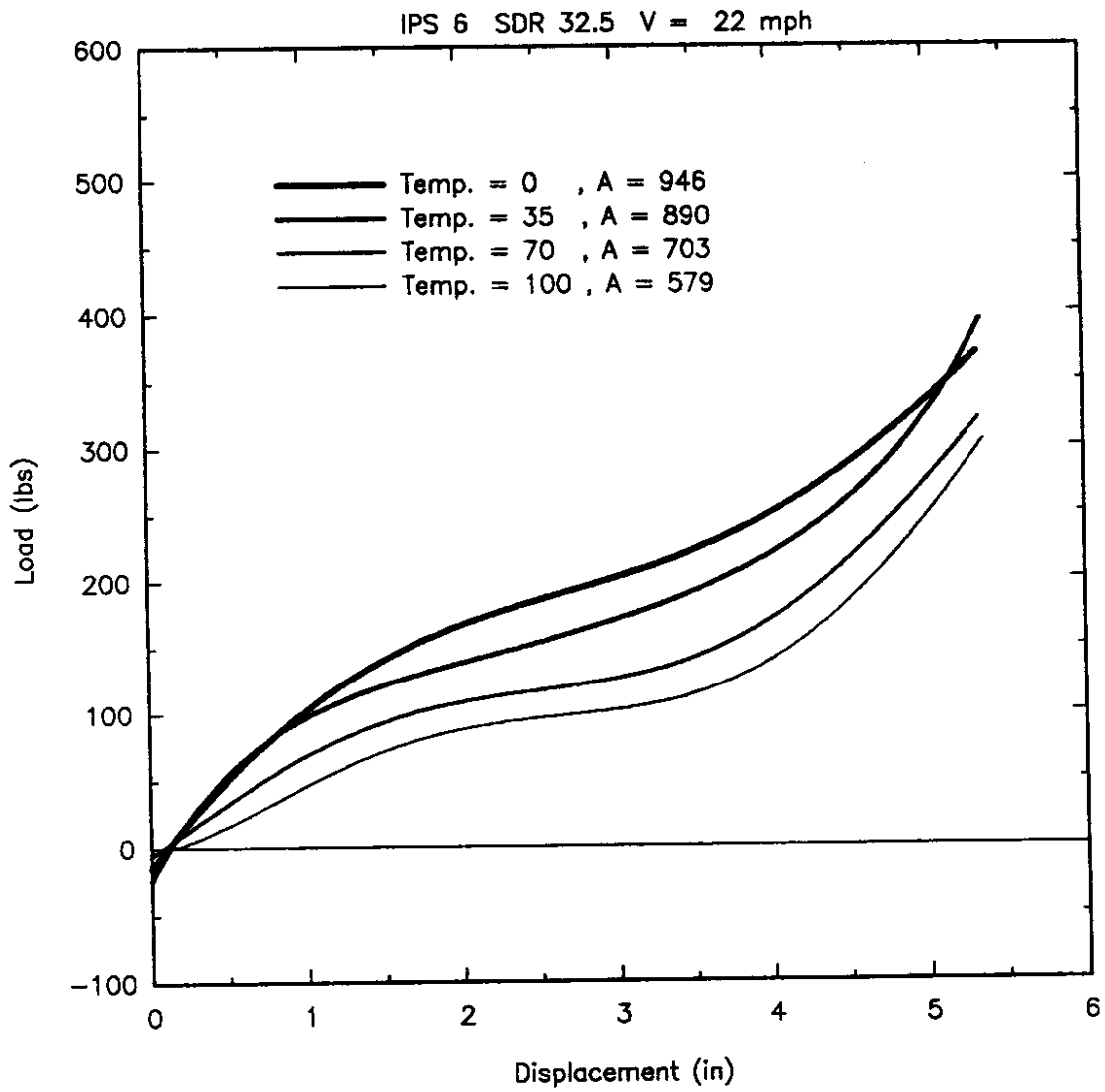


Figure A32. 22 mph Impact Test for IPS 6 SDR 32.5.

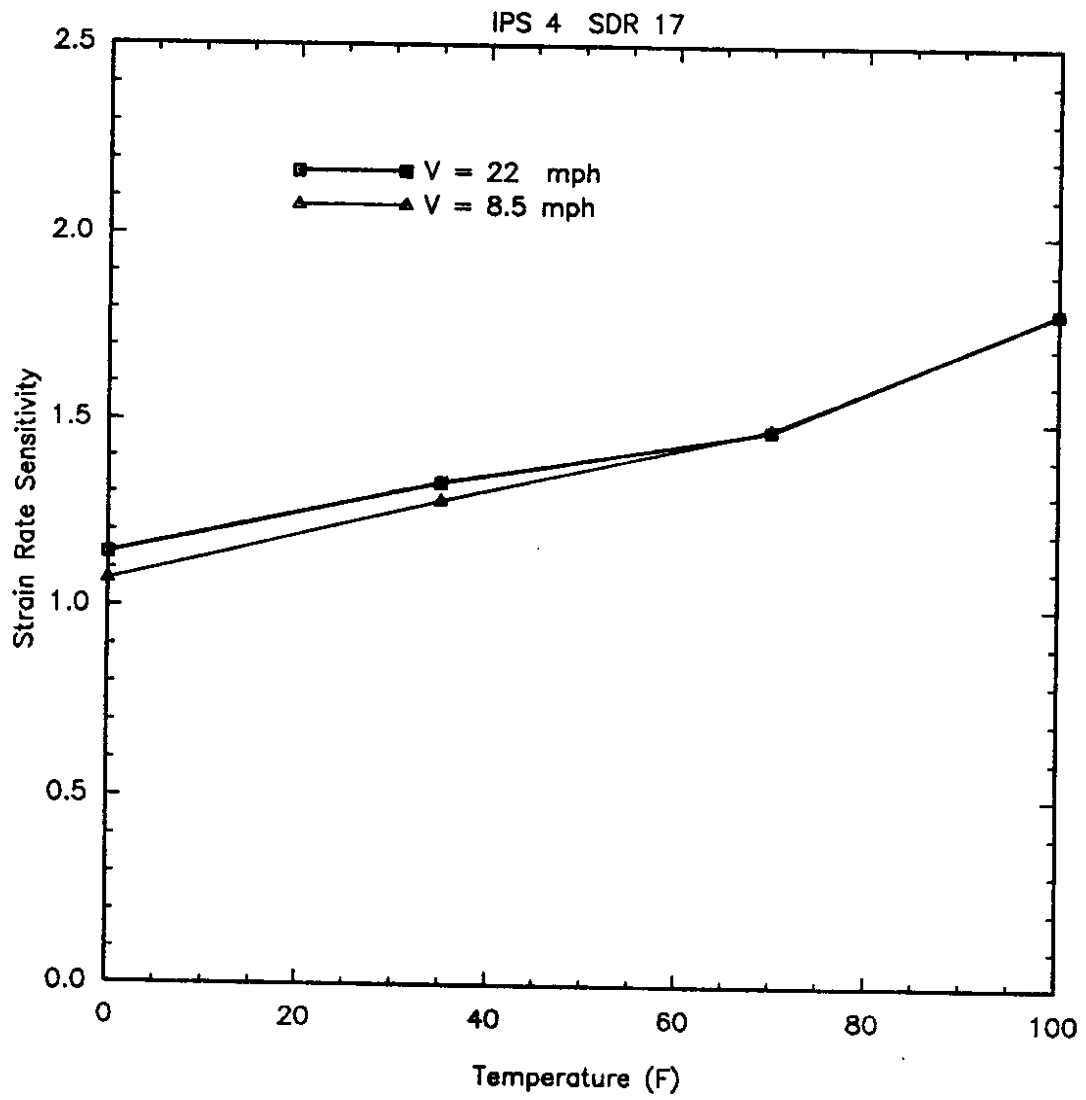


Figure A33. Strain Rate Sensitivity Factors for IPS 4 SDR 17.

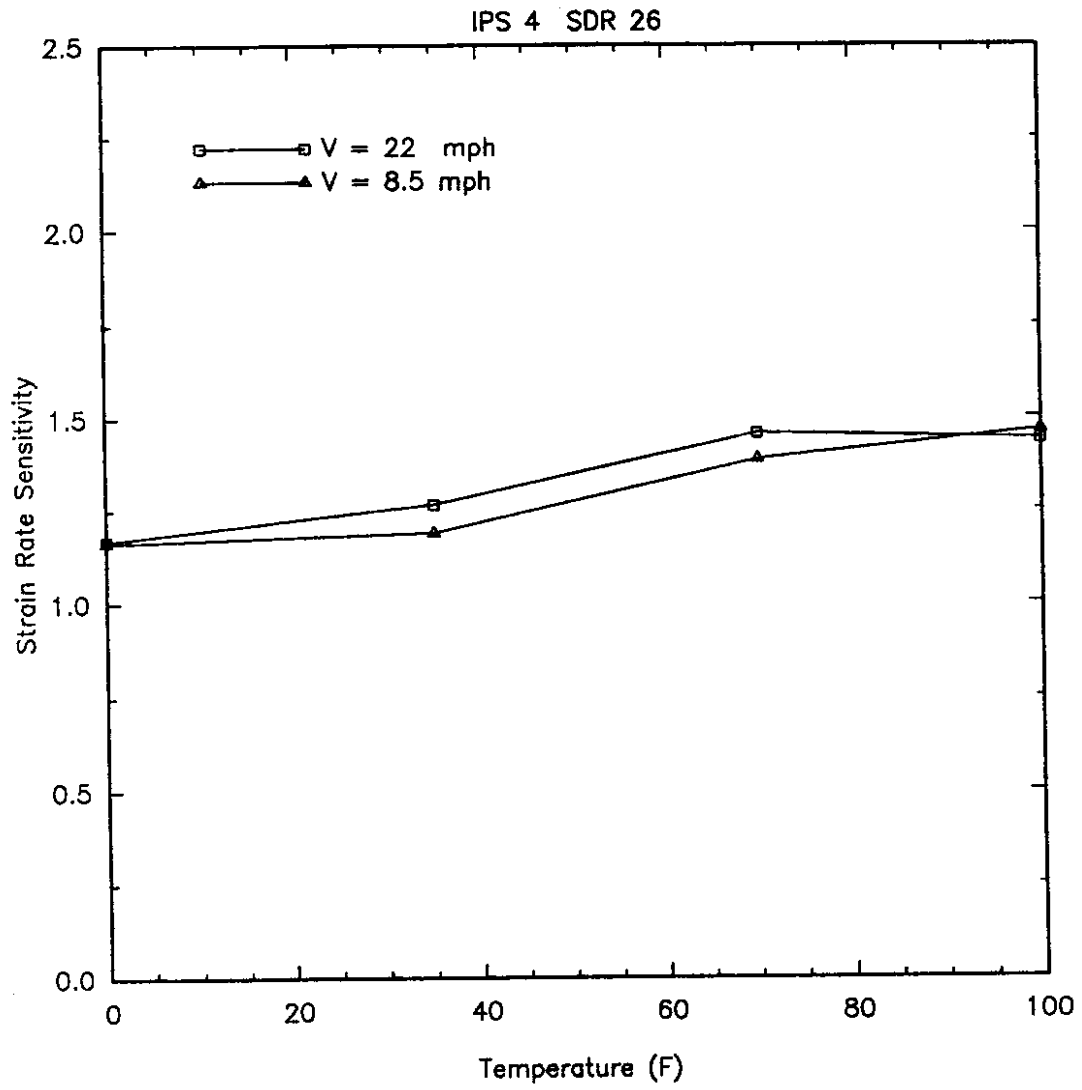


Figure A34. Strain Rate Sensitivity Factors for IPS 4 SDR 26.

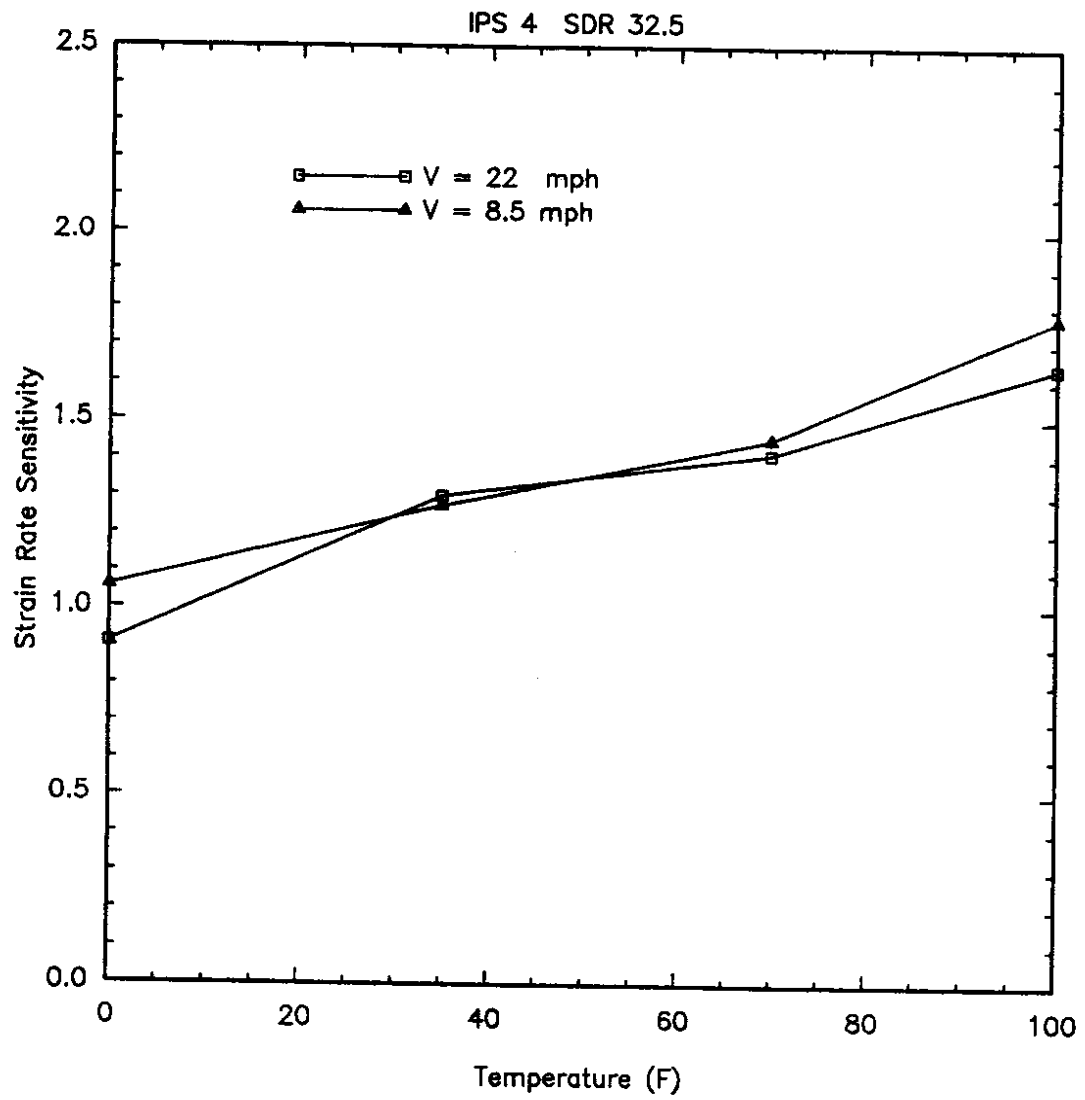


Figure A35. Strain Rate Sensitivity Factors for IPS 4 SDR 32.5.

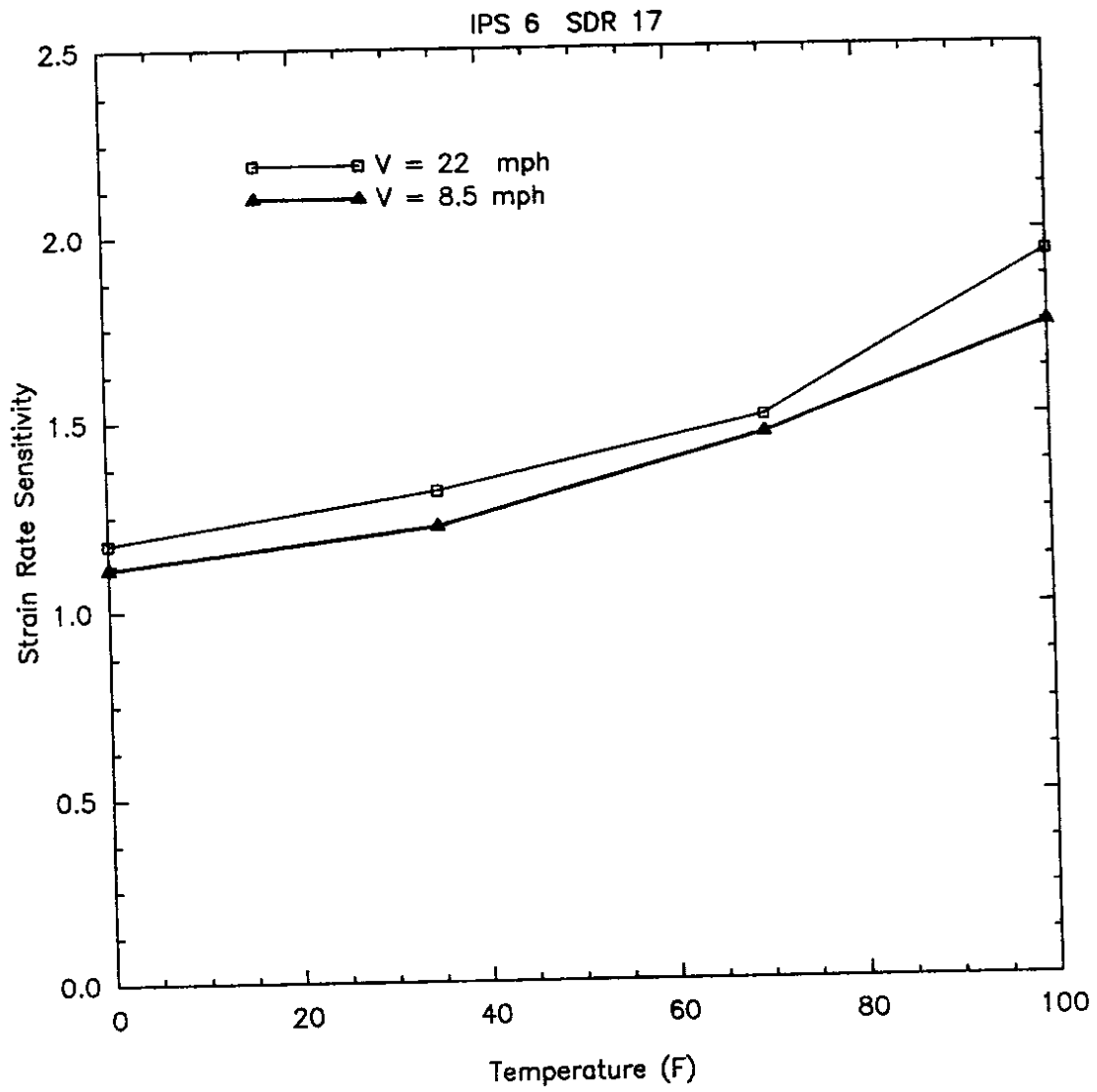


Figure A36: Strain Rate Sensitivity Factors for IPS 6 SDR 17.

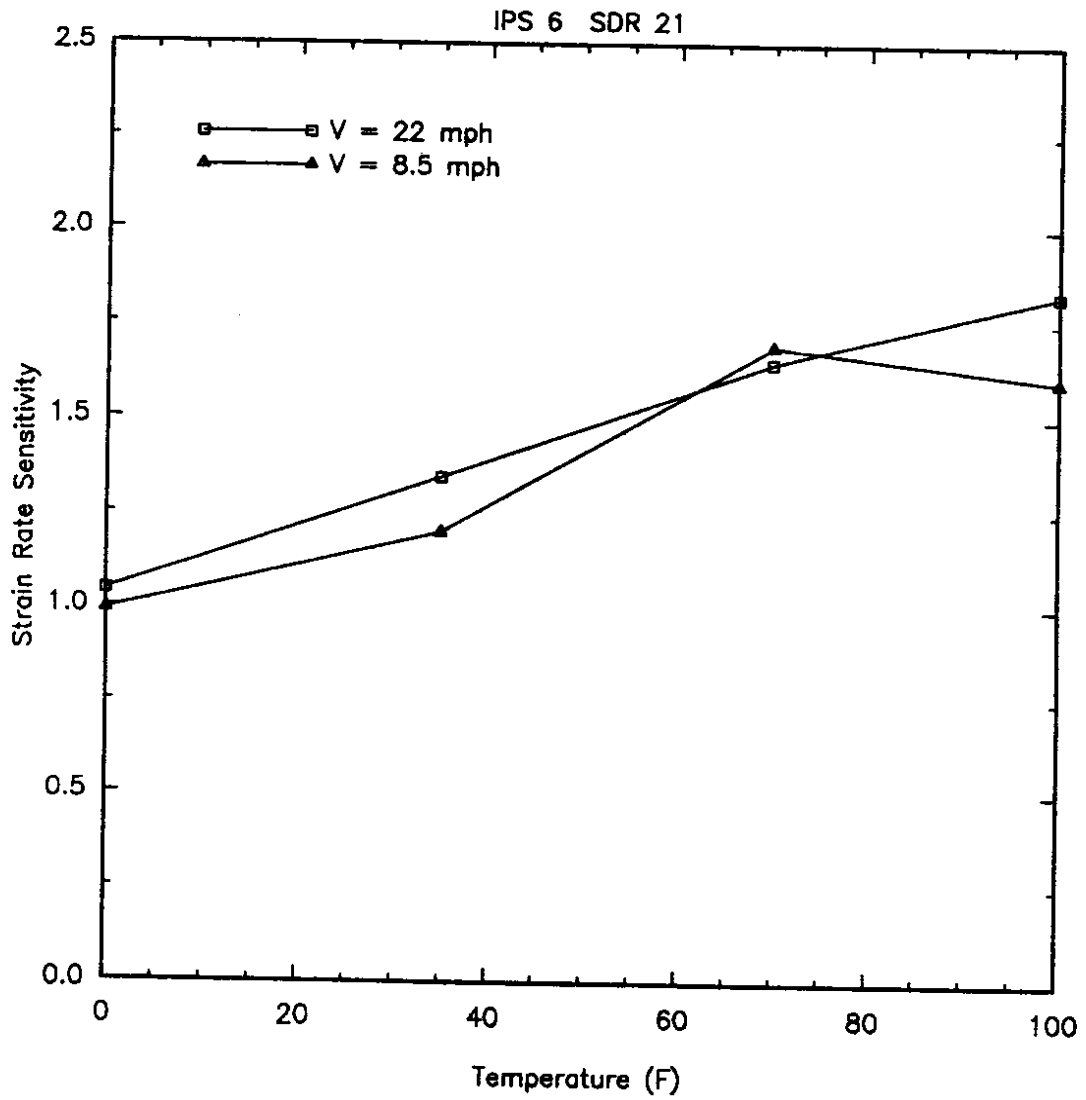


Figure A37. Strain Rate Sensitivity Factors for IPS 6 SDR 21.

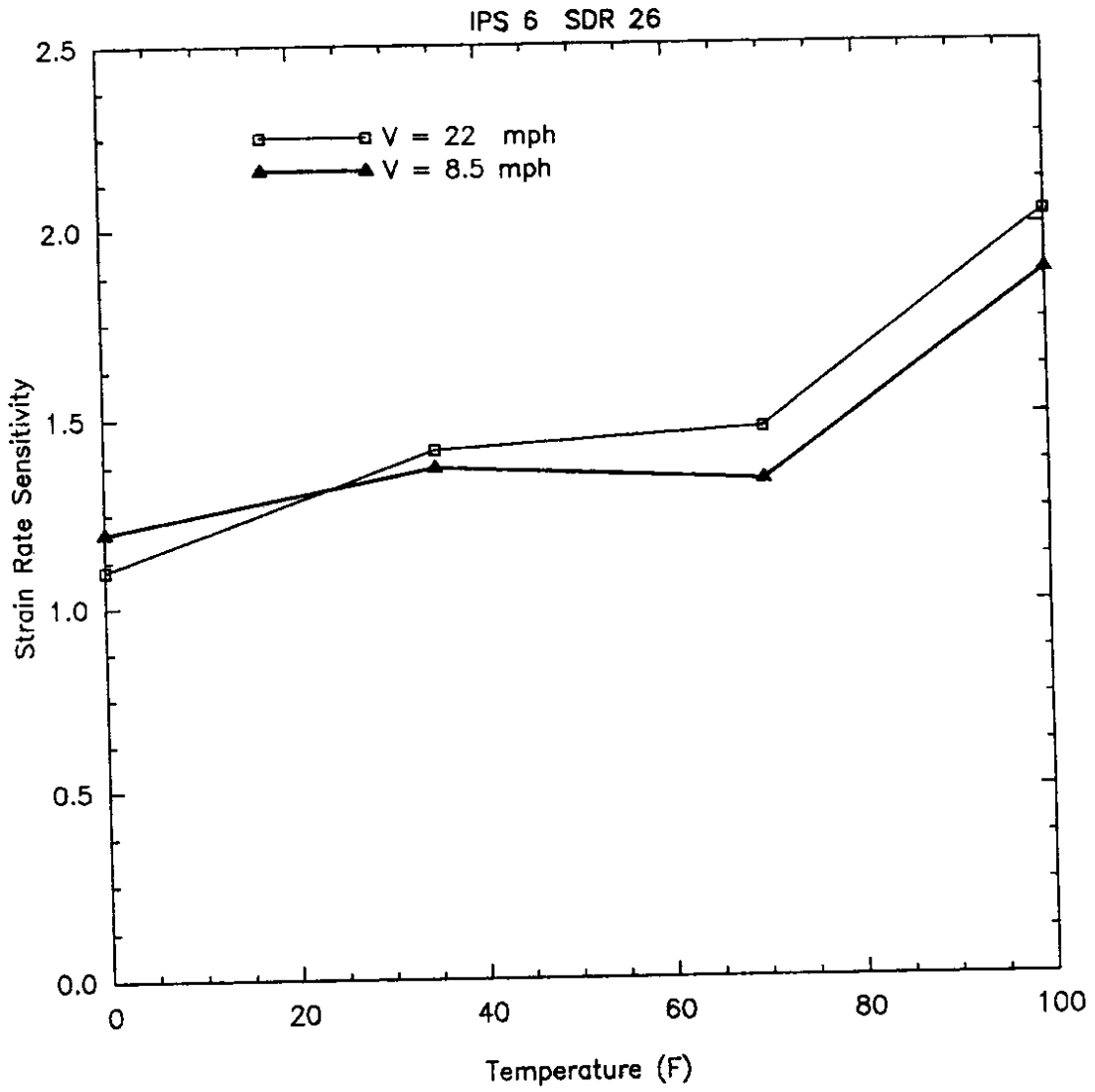


Figure A38. Strain Rate Sensitivity Factors for IPS 6 SDR 26.

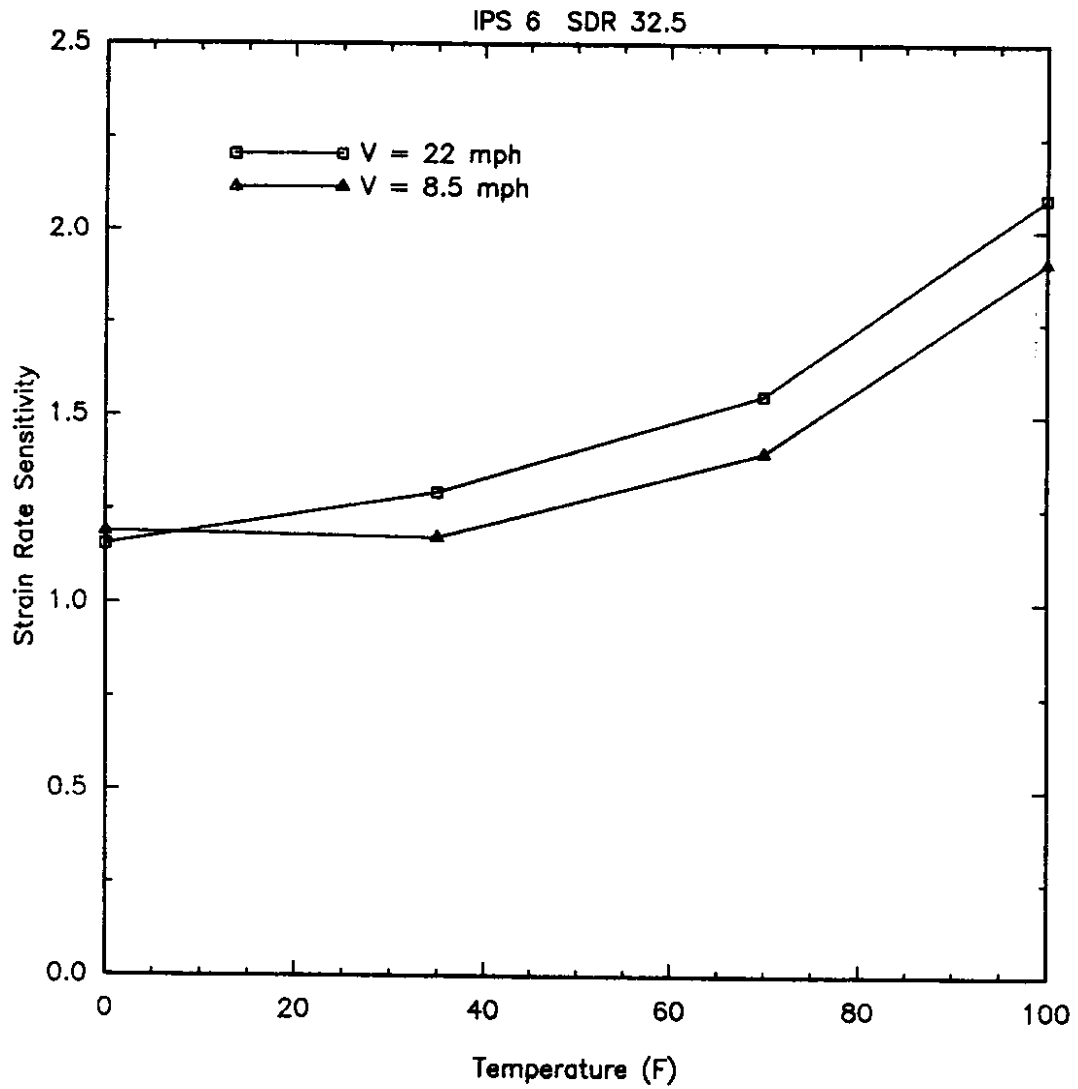


Figure A39. Strain Rate Sensitivity Factors for IPS 6 SDR 32.5.